VAPORIZATION OF BIOLOGICAL MACROMOLECULES USING INTENSE, ULTRAFAST LASERS: MECHANISM AND APPLICATION TO PROTEIN CONFORMATION

A Dissertation
Submitted
to the Temple University Graduate Board

In Partial Fulfillment
of the Requirements for the Degree of
Doctor of Philosophy

By
John J. Brady
January, 2012

Examining Committee Members:

Robert J. Levis, Advisory Chair, Department of Chemistry, Temple University
Spiridoula Matsika, Department of Chemistry, Temple University
Daniel R. Strongin, Department of Chemistry, Temple University
Kevin G. Owens, External Member, Department of Chemistry, Drexel University

ABSTRACT

This dissertation details the design and implementation of a state-of-the-art ambient trace analysis technique known as laser electrospray mass spectrometry. This novel technique utilizes an intense, nonresonant femtosecond laser pulse to transfer nonvolatile, fragile molecules into the gas phase from various substrates. The vaporized analyte is subsequently captured, solvated and ionized in an electrospray plume enabling mass analysis. Laser electrospray mass spectrometry is capable of analyzing samples in the liquid or solid states, mass spectral imaging of adsorbed molecules and detecting low vapor pressure analytes remotely. Experiments with biomolecules and pharmaceuticals, such as vitamin B12 and oxycodone, have demonstrated that the nonresonant femtosecond laser pulse allows for coupling into and vaporization of all molecules. This implies that sample preparation (elution, mixing with matrix and choosing samples with a particular electronic or vibrational transition) is not necessary, thus creating a universal mass analysis technique.

Investigations using low vapor pressure molecules, such as lipids and proteins, led to the discovery that unfragmented molecules are transferred into the gas phase via a nonthermal mechanism. The laser electrospray mass spectrometry technique has allowed for the nonresonant femtosecond laser vaporization and mass analysis of trace amounts of a nitro-based explosive from a metal surface. The vaporization of unfragmented explosive molecules from a surface facilitates the identification of the explosive, reducing the probability of false positives and false negatives. In addition, this “soft”

vaporization of molecules using nonresonant femtosecond laser pulses allows for protein to be transferred from the condensed phase into the gas phase without altering the molecule's structure, enabling *ex vivo* conformational analysis and possible disease typing.

ACKNOWLEDGMENTS

I would like to thank my advisor, Professor Robert Levis, for his mentorship and guidance throughout my graduate career. I thank Temple University's support staff, Ed Kaczanowicz and Matthew McCormick, for all their help with repairs and construction of the mass spectrometer. I would also like to thank all the members of the Levis lab, whose contributions are too numerous to mention here. Special thanks go to Elizabeth Judge for her contributions to the instrument construction and numerous discussions, science and otherwise. Finally I would like to thank all my family and friends for their support over the years.

To my family and friends
for all their support

TABLE OF CONTENTS

PAGE

LIST OF FIGURES

CHAPTER 1

INTRODUCTION

1.1 Desorption ionization mass spectrometry

The analysis of biomolecules is integral to the study of life sciences. Spectroscopic techniques, such as ultra-violet/visible or infrared spectroscopy, provide information regarding a biomolecule's electronic or vibrational structure allowing insight into the molecules identity. A molecule's structure can be determined from techniques such as x-ray diffraction (*1*) or nuclear magnetic resonance (*2*) spectroscopy. In addition to these successful methods, another way to analyze a biomolecule is to determine its molecular weight. Mass analysis of biomolecules is achieved through a variety of methods including, but not limited to: quadrupole (*3*), orbitrap (*4*) and time-of-flight (TOF) (*5*) mass spectrometry. However, these mass analysis techniques require the biomolecule to be a gas phase cationic or anionic species. This requirement initially restricted mass analysis to only high vapor pressure molecules due to their volatility. These gaseous molecules typically underwent ionization via electron impact (*6*) allowing for their mass analysis and detection. However, the detection of biomolecules is a major challenge for such techniques due to the wide variety of chemical structures and vapor pressures.

Other methods have been developed to analyze the large class of low vapor pressure molecules (*e.g.,* proteins). The non-volatile biomolecule must be transferred into the gas phase and ionized to enable mass analysis and detection. Secondary ion mass spectrometry (SIMS) (*7*), fast atom bombardment (*8*) and laser desorption ionization (*9*)

mass spectrometry are common techniques that enable both desorption and ionization of non-volatile biomolecules. Secondary ion mass spectrometry analyzes low vapor pressure molecules adsorbed onto the surface of a substrate by impinging the sample with a focused ion beam. Secondary ions are formed and transferred into the gas phase, which are subsequently mass analyzed typically via TOF mass spectrometry. Fast atom bombardment is similar to SIMS except that high energy atoms, rather than ions, cause desorption and ionization of the analyte. Laser desorption ionization uses a pulsed laser to ionize and transfer non-volatile molecules into the gas phase allowing for mass analysis. However, these particle and photon based methods can lead to extensive fragmentation of larger, non-volatile analytes giving rise to an upper mass limit of ~ 1,500 Da. The extensive fragmentation is commonly to due to excessive energy being deposited into internal modes of the molecule. For example, laser desorption ionization with nanosecond (ns) laser pulses causes rapid heating (10^8 to 10^{13} K/s) of the metallic substrate leading to thermal desorption and fragmentation (*9*) of the molecular species.

Tanaka *et. al.* (*10*) discovered that the ionization and *intact* transfer of large molecules (> 1,500 Da) into the gas phase could be achieved by adding a glycerol and cobalt powder mixture to the analyte prior to irradiation by a pulsed laser. Karas and Hillenkamp (*11*) made a similar discovery that ionization and *intact* transfer of large molecules could also be achieved by the addition of a small organic acid (*e.g.,* nicotinic acid) to the sample. The addition of these "matrices" to the sample has enabled the analysis of non-volatile large molecules in the solid (*12, 13*) or liquid phase (*14*). The technique, known as matrix-assisted laser desorption ionization (MALDI), typically utilizes a ns laser pulse, at a laser intensity of approximately $10^6 – 10^7$ W/cm^2, to couple

into the externally applied matrix through a resonant excitation to a low lying state (*15*) in the organic acid. A resonant absorption of the laser pulse energy occurs when the spacing between energy levels is equal to the energy of one photon, $h\nu$, where h is Planck's constant and ν is the frequency of the photon (*16, 17*). For MALDI, the resonant excitation process allows for the absorption cross section of the matrix to increase approximately six orders of magnitude (*16*) allowing for efficient absorption of the laser pulse's energy. The energy absorbed by the matrix is converted to heat allowing for desorption of both the externally applied matrix and the non-volatile analyte *i.e.,* protein (*15, 18*). Ionization of the desorbed analyte is thought to occur in the gas phase via secondary reactions, such as proton transfer (*18*). Although resonant ns laser desorption has been successful in analyzing a wide variety of low vapor pressure molecules, the number of neutrals transferred into the gas phase from a surface using a laser pulse can exceed the number of ions by several orders of magnitude (*19*), decreasing the techniques overall sensitivity. The ratio of ions to neutrals may further decrease due to ion neutralization (*20, 21*) occurring in the expanding plume. Therefore, it would be advantageous to ionize the desorbed neutrals to increase the sensitivity of the laser desorption technique.

1.2 Post-ionization of desorbed molecules

Post-ionization of the laser desorbed neutral molecules would result in a gain of sensitivity by several orders of magnitude (*22, 23*) over traditional laser desorption techniques. Post-ionization of the vaporized neutral molecules can be achieved through the use of an electron beam (*24*), a pulsed laser (*25*), atmospheric pressure chemical

ionization (APCI) (*22, 23*) or electrospray ionization (ESI) (*26*). Electron beam and pulsed laser ionization have been very successful at post-ionization of desorbed analyte; however, modest gains in sensitivity are usually achieved due to the small interaction volumes with the laser-desorbed sample.

Atmospheric pressure chemical ionization can increase the sensitivity of the laser desorption technique by several orders of magnitude due to its high ionization efficiency and the increased interaction cross-section. In atmospheric pressure chemical post-ionization, a heated vaporizer volatilizes a liquid solvent. The gas phase solvent molecules are subsequently excited/ionized by a corona discharge. The ionized solvent transfers its charge to the laser desorbed analyte through chemical reactions (chemical ionization), thus ionizing the laser-desorbed sample. The APCI process is very efficient for both polar and nonpolar molecules but it is commonly limited to small molecules (< 2, 000 Da) due to in-source decomposition (*27*). Electrospray ionization overcomes the mass limit of APCI allowing for the analysis of large biomolecules (>2,000 Da) and multiple charging of the sample. In addition, electrospray post-ionization of the laser-desorbed material can also allow for a gain in sensitivity by several orders of magnitude, similar to APCI. In electrospray post-ionization, the charged droplets that are formed via electrospray processes (*28, 29*), capture and solvate the neutral molecules, nanoparticles and clusters ejected from the sample. During the final ion formation process within the droplet, charge is transferred to or from the analyte molecule depending on the charge of the droplet (*e.g.,* for a positively charged droplet, a positively charged adduct is transferred onto the analyte), thus softly ionizing the laser-desorbed sample.

1.3 Laser coupling mechanisms of laser-based electrospray post-ionization mass spectrometry methods

Several mass analysis techniques, electrospray-assisted laser desorption ionization (*26*), laser ablation electrospray ionization (LAESI) (*30*) and matrix-assisted laser desorption electrospray ionization (*31*), allow for the electrospray post-ionization of ns laser-desorbed material at atmospheric pressure. These ns laser-based techniques relax sample preparation requirements and allow for *ex vivo* analysis at ambient temperature and pressure, thus avoiding the need for transferring samples into vacuum and reducing the sample preparation that is commonly required for vacuum-based MALDI (*e.g.,* dehydration or flash freezing) (*32*). Electrospray-assisted laser desorption ionization utilizes ns ultraviolet (337 nm) laser pulses to excite electrons in the substrate leading to thermal desorption (*33*) of the adsorbed sample which is subsequently captured, solvated and post-ionized in an electrospray plume allowing for mass analysis. However, desorption of the sample can also be induced when a molecule, such as a matrix (*33, 34*) or the inherent water in tissue samples (*30*), is present to resonantly absorb the ns laser pulse energy. The resonant absorption process increases the absorption cross section of the matrix approximately six orders of magnitude allowing for more energy to be absorbed in the resonant case when laser power densities are of the order of 10^6 - 10^8 W/cm^2. For example, LAESI uses a ns infrared (2.94 μm) laser to resonantly excite the OH asymmetric stretch in the water inherently contained within the tissue. The absorbed energy from the ns infrared laser pulse desorbs molecules from the water rich sample via a phase explosion (*35, 36*), transferring analyte into the gas phase. The ns laser-desorbed

molecules are then subsequently captured, solvated and post-ionized in the electrospray plume allowing for their mass analysis.

These atmospheric pressure, ns laser-based desorption techniques have been successful in analyzing a variety of condensed phase samples, ranging from aqueous protein (*37*), blood (*30, 38*) and tissues (*39*). In addition, these laser-based techniques have been able to produce mass spectral images of tissue as shown by the two dimensional imaging of lipids and metabolites contained within a section of rat brain tissue *(36)*. However, ns laser pulses induce more fragmentation in molecules in the gas phase under vacuum conditions when compared to ultrashort laser pulses at similar intensities (*40, 41*). The additional fragmentation observed with a ns laser pulse under vacuum conditions is due to the ladder switching mechanism in which the gas phase molecule absorbs energy from the laser pulse and dissociates while the laser pulse is still present (*42*). The fragments subsequently absorb additional energy from the laser pulse leading to further fragmentation. Ladder switching occurs with ns laser pulse excitation because the molecular dissociation time is shorter than the laser pulse duration.

In addition, most molecules or samples do not undergo a resonant transition at the wavelengths (*i.e.,* 337 nm, 532 nm, 1064 nm or 2940 nm) commonly used in the ns laser-based desorption techniques, thus restricting the number of samples that can be analyzed. Hence, a particular matrix is used to absorb a specific excitation frequency overcoming this issue of sample restriction. However, the addition of a matrix to a sample inherently prevents the possibility of *ex vivo* analysis due to modification of the sample. This sample restriction problem can be circumvented by the use of a non laser-based desorption method such as desorption electrospray ionization (DESI) (*43*). In DESI, an electrospray

plume impinges on a sample surface transferring analytes into the gas phase using the droplet pick-up mechanism. The analyte contained within the secondary droplets undergo ionization via ESI processes, allowing for their mass analysis (*43, 44*).

The nonresonant absorption of the laser pulse energy, where two or more photons are absorbed through virtual states, would also alleviate the requirement of resonance for laser-based techniques. Nonresonant absorption occurs when the energy difference between the ground and pertinent excited energy levels is not equal to $nh\nu$, where n is the number of photons. Such nonresonant absorption processes typically require high laser intensity and therefore, short laser pulses are commonly used. The use of an ultrashort pulse may provide certain unique advantages as opposed to resonant ns laser pulses.

One of the advantages of femtosecond (fs) laser pulses is that they have different coupling mechanisms than those of ns lasers pulses. For example, fs laser ionization of a molecule under vacuum conditions does not readily cause fragmentation because the pulse duration of the laser is shorter than the molecular rearrangement time of the molecule (ladder climbing) (*45*). Instead, intact molecular ions are commonly observed with fs laser pulses as opposed to ns laser pulses at similar intensities. In addition, nonresonant absorption processes can be enabled using fs laser pulses due to the high intensities that can be reached at the focus ($> 10^{13}$ W/cm^2). This suggests that a nonresonant fs laser pulse can, in principle, couple into all molecules, implying that samples do not have to be chosen to have a particular electronic or vibrational transition.

Nonresonant fs laser pulses have been used previously to transfer material into the gas phase, typically under vacuum conditions, for mass analysis (*46-49*). For example, when an 800 nm, 130 fs laser pulse at 10^{13} W/cm^2 impinged upon cryogenic multilayers

of organic molecules on metallic substrates, vaporization of neutral molecules without fragmentation is observed with translational energy < 1 eV (*48*). Additional investigations of cryogenic multilayer vaporization using fs duration lasers demonstrated that the quantity of neutral molecules vaporized without fragmentation was inversely proportional to the pulse duration of the laser for film thickness exceeding ~ 10 monolayers (*47*). This is consistent with a laser with a long pulse duration (> 1 picosecond) depositing energy into the substrate to enable thermal desorption of the analyte. Thus as the sample thickness increased, a decrease in the number of vaporized neutral molecules was observed with long laser pulses because of the large increase in the degrees of freedom available in the overlayer. On the other hand, the nonresonant fs laser pulse couples directly into the molecular system, depositing its energy into the sample before a thermal response (*i.e.,* surface heating (*50*)) can be achieved. This nonthermal vaporization results in an increase in the number of neutral molecules transferred into the gas phase with increasing sample thickness demonstrating that nonresonant fs lasers will not only increase the number of *intact* molecules transferred into the gas phase, but should also be able to couple into any molecular system.

1.4 Scope of this dissertation

This dissertation explores the use of nonresonant fs laser pulses for use in atmospheric pressure mass spectrometry of non-volatile analyte such as explosives, lipids, biomolecules, complex biological fluids and proteins. The low vapor pressure analyte is transferred into the gas phase using nonresonant fs laser pulses. The vaporized material is post-ionized upon capture, solvation and ionization in an electrospray plume.

The ions are then subsequently mass analyzed using a TOF mass spectrometer. Chapter 2 details the design and implementation of the nonresonant fs laser vaporization ESI-TOF mass spectrometer. In addition, it was found that the limit of detection of the new mass spectrometry technique, known hence forth as laser electrospray mass spectrometry (LEMS), is approximately 280 pg or 600 fmol as determined via comparison to calibrated conventional ESI-TOF mass spectrometry measurements (no laser present) for a small lipid, 1,2-dihexanoyl-*sn*-glycero-3-phosphocholine.

Chapter 3 demonstrates that intact, neutral molecules are transferred into the gas phase using fs laser pulses. In doing so the LEMS analysis of explosives, lipids and complex biological fluids was demonstrated. The production of neutral molecules, from either the solid or liquid state, was determined by the vaporization of sample with and without the electrospray solvent present during irradiation with the fs laser pulse.

It is shown in chapter 3 that a wide range of molecules, varying in size and polarity, can be transferred into the gas phase. Chapter 4 explores and demonstrates that this wide range of molecules being transferred into the gas phase is due to the nonresonant fs laser pulse nonlinearly coupling into the adsorbed molecules. In addition, the use of a fs laser results in more neutral molecules being vaporized than laser pulses with longer duration (*i.e.,* nanoseconds) as determined through comparison of ns and fs MALDI and LEMS measurements. The nonresonant fs laser pulse deposits energy into the molecule before the surface can thermally respond as shown by the vaporization of a lipid and two proteins from substrates of varying composition. It was further demonstrated that the protein adsorbed on dielectric substrates could be transferred into

the gas phase via a nonresonant, nonthermal mechanism and without alteration of the protein's structural conformation.

Chapter 5 details the exploration of the idea that the nonresonant fs laser pulse allows for vaporization without alteration to a protein's primary, secondary or tertiary structure. This chapter demonstrates that the LEMS technique, nonresonant fs laser vaporization with electrospray-post ionization, allows for the *in vitro* measurement of protein conformation. Cytochrome c and lysozyme are vaporized from the condensed phase into the gas phase intact when exposed to the intense, nonresonant, fs laser pulse. Electrospray post-ionization of the vaporized protein reveals that the solution-phase conformation is preserved upon transfer into the gas phase as determined through measurement of the charge state distribution and the collision-induced dissociation channels. The data ultimately suggests that nonresonant, fs laser vaporization with electrospray post-ionization is a softer vaporization/ionization technique than conventional ESI-TOF mass spectrometry.

References

1. K. Palczewski *et al.*, Crystal structure of rhodopsin: A G protein-coupled receptor. *Science* **289**, 739 (2000).
2. N. Tjandra, A. Bax, Direct measurement of distances and angles in biomolecules by NMR in a dilute liquid crystalline medium. *Science* **278**, 1111 (1997).
3. P. H. Dawson, Ed., *Quadrupole mass spectrometry and its applications.*, (Springer-Verlag New York, LLC, New York, 1997).

4. Q. Hu *et al.*, The orbitrap: A new mass spectrometer. *J. Mass Spectrom.* **40**, 430 (2005).

5. R. Cotter, *Time-of-flight mass spectrometry: Instrumentation and applications in biological research.*, (ACS, Washington, D.C., 1997).

6. F. W. McLafferty, F. Turecek, *Interpretation of mass spectra*. (University Science Books, Sausalito, California, ed. Fourth, 1993).

7. A. F. M. Altelaar *et al.*, Gold-enhanced biomolecular surface imaging of cells and tissue by SIMS and MALDI mass spectrometry. *Anal. Chem.* **78**, 734 (2006).

8. M. Barber, R. S. Bordoli, R. D. Sedgwick, A. N. Tyler, Fast atom bombardment of solids (FAB) - A new ion-source for mass-spectrometry. *J. Chem. Soc., Chem. Comm.*, 325 (1981).

9. M. A. Posthumus, P. G. Kistemaker, H. L. C. Meuzelaar, M. C. Ten Noever de Brauw, Laser desorption-mass spectrometry of polar nonvolatile bio-organic molecules. *Anal. Chem.* **50**, 985 (1978).

10. K. Tanaka *et al.*, Protein and polymer analyses up to *m/z* 100, 000 by laser ionization time-of-flight mass spectrometry. *Rapid Commun. Mass Spectrom.* **2**, 151 (1988).

11. M. Karas, F. Hillenkamp, Laser desorption ionization of proteins with molecular masses exceeding 10, 000 Daltons. *Anal. Chem.* **60**, 2299 (1988).

12. F. Hillenkamp, M. Karas, R. C. Beavis, B. T. Chait, Matrix-assisted laser desorption ionization mass-spectrometry of biopolymers. *Anal. Chem.* **63**, A1193 (1991).

13. E. Nordhoff *et al.*, Matrix-assisted laser desorption ionization mass-spectrometry of nucleic-acids with wavelengths in the ultraviolet and infrared. *Rapid Commun. Mass Spectrom.* **6**, 771 (1992).

14. L. Li, A. P. L. Wang, L. D. Coulson, Continuous-flow matrix-assisted laser desorption ionization mass-spectrometry. *Anal. Chem.* **65**, 493 (1993).

15. K. Dreisewerd, M. Schürenberg, M. Karas, F. Hillenkamp, Influence of the laser intensity and spot size on the desorption of molecules and ions in matrix-assisted laser desorption/ionization with a uniform beam profile. *Int. J. Mass Spectrom.* **141**, 127 (1995).

16. N. B. Delone, V. P. Krainov, *Mulitphoton processes in atoms*. (Springer-Verlag Berlin Heidelberg, ed. Second, 1999), pp. 314.

17. J. H. Posthumus, The dynamics of small molecules in intense laser fields. *Rep. Prog. Phys.* **67**, 623 (2004).

18. R. Knochenmuss, Ion formation mechanisms in UV-MALDI. *Analyst* **131**, 966 (2006).

19. C. D. Mowry, M. V. Johnston, Simultaneous detection of ions and neutrals produced by matrix-assisted laser desorption. *Rapid Commun. Mass Spectrom.* **7**, 569 (1993).

20. H. C. Le, D. E. Zeitoun, J. D. Parisse, M. Sentis, W. Marine, Modeling of gas dynamics for a laser-generated plasma: Propagation into low-pressure gases. *Phys. Rev. E* **62**, 4152 (2000).

21. R. Knochenmuss, L. V. Zhigilei, Molecular dynamics model of ultraviolet matrix-assisted laser desorption/ionization including ionization processes. *J. Phys. Chem. B* **109**, 22947 (2005).

22. J. J. Coon, W. W. Harrison, Laser desorption-atmospheric pressure chemical ionization mass spectrometry for the analysis of peptides from aqueous solutions. *Anal. Chem.* **74**, 5600 (2002).

23. J. J. Coon, K. J. McHale, W. W. Harrison, Atmospheric pressure laser desorption/chemical ionization mass spectrometry: A new ionization method based on existing themes. *Rapid Commun. Mass Spectrom.* **16**, 681 (2002).

24. R. B. Van Breemen, M. Snow, R. J. Cotter, Time resolved laser desorption mass spectrometry, I. Desorption of preformed ions. *Int. J. Mass Spectrom. Ion Processes* **49**, 35 (1983).

25. A. Leisner, A. Rohlfing, S. Berkenkamp, F. Hillenkamp, K. Dreisewerd, Infrared laser post-ionization of large biomolecules from an IR-MALD(I) plume. *J. Am. Soc. Mass Spectrom.* **15**, 934 (2004).

26. J. Shiea *et al.*, Electrospray-assisted laser desorption/ionization mass spectrometry for direct ambient analysis of solids. *Rapid Commun. Mass Spectrom.* **19**, 3701 (2005).

27. B. Desmazieres, W. Buchmann, P. Terrier, J. Tortajada, APCI interface for LC- and SEC-MS analysis of synthetic polymers: Advantages and limits. *Anal. Chem.* **80**, 783 (2007).

28. J. B. Fenn, M. Mann, C. K. Meng, S. F. Wong, C. M. Whitehouse, Electrospray ionization - principles and practice. *Mass Spectrom. Rev.* **9**, 37 (1990).

29. J. V. Iribarne, B. A. Thomson, On the evaporation of small ions from charged droplets. *J. Chem. Phys.* **64**, 2287 (1976).

30. P. Nemes, A. Vertes, Laser ablation electrospray ionization for atmospheric pressure, *in vivo*, and imaging mass spectrometry. *Anal. Chem.* **79**, 8098 (2007).

31. J. S. Sampson, A. M. Hawkridge, D. C. Muddiman, Generation and detection of multiply-charged peptides and proteins by matrix-assisted laser desorption electrospray ionization (MALDESI) Fourier transform ion cyclotron resonance mass spectrometry. *J. Am. Soc. Mass Spectrom.* **17**, 1712 (2006).

32. P. J. Todd, T. G. Schaaff, P. Chaurand, R. M. Caprioli, Organic ion imaging of biological tissue with secondary ion mass spectrometry and matrix-assisted laser desorption/ionization. *J. Mass Spectrom.* **36**, 355 (2001).

33. M.-Z. Huang, S.-S. Jhang, C.-N. Cheng, S.-C. Cheng, J. Shiea, Effects of matrix, electrospray solution, and laser light on the desorption and ionization mechanisms in electrospray-assisted laser desorption ionization mass spectrometry. *Analyst* **135**, 759 (2010).

34. J. S. Sampson, A. M. Hawkridge, D. C. Muddiman, Direct characterization of intact polypeptides by matrix-assisted laser desorption electrospray ionization quadrupole Fourier transform ion cyclotron resonance mass spectrometry. *Rapid Commun. Mass Spectrom.* **21**, 1150 (2007).

35. I. Apitz, A. Vogel, Material ejection in nanosecond Er:YAG laser ablation of water, liver, and skin. *Appl. Phys. A - Mater.* **81**, 329 (2005).

36. Z. Chen, A. Vertes, Early plume expansion in atmospheric pressure midinfrared laser ablation of water-rich targets. *Phys. Rev. E* **77**, 036316 (2008).

37. I. X. Peng, J. Shiea, R. R. O. Loo, J. A. Loo, Electrospray-assisted laser desorption/ionization and tandem mass spectrometry of peptides and proteins. *Rapid Commun. Mass Spectrom.* **21**, 2541 (2007).

38. M. Z. Huang, H. J. Hsu, L. Y. Lee, J. Y. Jeng, L. T. Shiea, Direct protein detection from biological media through electrospray-assisted laser desorption ionization/mass spectrometry. *J. Proteome Res.* **5**, 1107 (2006).

39. P. Nemes, A. S. Woods, A. Vertes, Simultaneous imaging of small metabolites and lipids in rat brain tissues at atmospheric pressure by laser ablation electrospray ionization mass spectrometry. *Anal. Chem.* **82**, 982 (2010).

40. M. J. Dewitt, R. J. Levis, Near-infrared femtosecond photoionization dissociation of cyclic aromatic-hydrocarbons. *J. Chem. Phys.* **102**, 8670 (1995).

41. R. Weinkauf, P. Aicher, G. Wesley, J. Grotemeyer, E. W. Schlag, Femtosecond versus nanosecond multiphoton ionization and dissociation of large molecules. *J. Phys. Chem.* **98**, 8381 (1994).

42. K. W. D. Ledingham *et al.*, Multiply charged ions from aromatic molecules following irradiation in intense laser fields. *J. Phys. Chem. A* **103**, 2952 (1999).

43. Z. Takats, J. M. Wiseman, B. Gologan, R. G. Cooks, Mass spectrometry sampling under ambient conditions with desorption electrospray ionization. *Science* **306**, 471 (2004).

44. Z. Takats, J. M. Wiseman, R. G. Cooks, Ambient mass spectrometry using desorption electrospray ionization (DESI): Instrumentation, mechanisms and applications in forensics, chemistry, and biology. *J. Mass Spectrom.* **40**, 1261 (2005).

45. J. J. Yang, D. A. Gobeli, M. A. El-Sayed, Change in the mechanism of laser multiphoton ionization-dissociation in benzaldehyde by changing the laser pulse width. *J. Phys. Chem.* **89**, 3426 (1985).

46. H. Arnolds, R. J. Levis, D. A. King, Vibrationally assisted DIET through transient temperature rise: The case of benzene on Pt{111}. *Chem. Phys. Lett.* **380**, 444 (2003).

47. H. Arnolds, C. Rehbein, G. Roberts, R. J. Levis, D. A. King, Femtosecond near-infrared laser desorption of multilayer benzene on Pt{111}: A molecular Newton's cradle? *J. Phys. Chem. B* **104**, 3375 (2000).

48. H. Arnolds, C. E. M. Rehbein, G. Roberts, R. J. Levis, D. A. King, Femtosecond near-infrared laser desorption of multilayer benzene on Pt{111}: Spatial origin of hyperthermal desorption. *Chem. Phys. Lett.* **314**, 389 (1999).

49. J. M. Wichmann, C. Lupulescu, L. Wöste, A. Lindinger, Matrix-assisted laser desorption/ionization by using femtosecond laser pulses in the near-infrared wavelength regime. *Rapid Commun. Mass Spectrom.* **23**, 1105 (2009).

50. J. M. Hicks, L. E. Urbach, E. W. Plummer, H.-L. Dai, Can pulsed laser excitation of surfaces be described by a thermal model? *Phys. Rev. Lett.* **61**, 2588 (1988).

CHAPTER 2

DESIGN AND CONSTRUCTION OF THE NONRESONANT FEMTOSECOND LASER VAPORIZATION WITH ELECTROSPRAY POST-IONIZATION MASS SPECTROMETER

2.1 Overview

Typical laser-based desorption techniques transfer molecules into the gas phase via a first order resonant absorption process (*1*). However, most molecules do not have a resonant transition at a particular laser wavelength and thus necessitates the addition of a matrix to the sample to enable absorption of the laser pulse energy. Nonresonant absorption reduces sample compatibility restrictions and allows a variety of molecules to be studied, but this process requires high laser intensities. The use of femtosecond (fs) laser pulses facilitates such nonlinear (nonresonant) processes. The laser pulse energy is rapidly absorbed via mulitphoton processes allowing for intact neutral molecules to be observed due to the ultrashort pulse duration. This and other advantages of femtosecond laser vaporization will be further discussed in Chapters 3, 4 and 5.

Once vaporized, the neutral unfragmented molecules must be characterized. Mass spectrometry is one such method to characterize samples but requires ionization of the neutral molecules. To enable mass analysis, electrospray post-ionization was chosen to solvate and ionize the vaporized molecules and clusters. The newly formed ions are then mass analyzed. Mass analysis of ions can be achieved through a variety of techniques including but not limited to: quadrupole (*2*), orbitrap (*3*) and time-of-flight (TOF) (*4*) mass spectrometry. Each have their own unique advantages and disadvantages. The TOF

is the most versatile and cheapest of the mass analysis techniques and separates ions based on their velocity without scanning of an electric field. The TOF mass spectrometer provides high mass resolution when using a reflection configuration (m/Δm ~40,000) and is technically unlimited in the *m/z* value that can be analyzed. Therefore, based on cost, ease of use and the unlimited *m/z* range, the TOF was selected to analyze the positive ions formed via the electrospray post-ionization of the fs laser vaporized molecules. This chapter concerns the design, construction and implementation of the nonresonant fs laser vaporization with electrospray post-ionization TOF mass spectrometer.

2.2 Equipment

2.2.1 Oscillator and regenerative amplifier

The high energy, fs laser pulses used in the experiments described in Chapters 3, 4 and 5, were produced by amplifying low energy, fs laser pulses created by an oscillator (purchased as a kit, Kapteyn-Murnane Laboratories Inc., Boulder, Co, USA, Model: TS Ti:Sapphire Kit). In the oscillator, a doubled (532 nm), 4 W, continuous wave (CW), neodymium-doped vanadate ($Nd:YVO_4$) pump laser (Coherent Inc., Santa Clara, CA, USA, Model: VERDI 5W) is used to irradiate a large gain bandwidth crystal (titanium-doped sapphire ($Ti:Al_2O_3$)). The large gain bandwidth of the titanium-doped sapphire crystal (*5*) allows for ultrashort pulses to be produced upon mode locking via the Kerr lens effect (*6*). In this manner, a coherent superposition of frequencies creates a 3.5 nJ, 10 fs laser pulse (full width half maximum) at a repetition rate of 86.3 MHz in the oscillator which is in a folded configuration. However, due to dispersion, the pulse width increases to ~30 fs.

The fs laser pulses produced by the oscillator do not have sufficient energy to induce the nonlinear absorption required to enable vaporization of the molecules described in Chapters 3-5. Therefore, the low energy fs laser pulses are amplified using a regenerative amplifier (Coherent Inc., Model: L-USP-1K-HE). However, prior to amplification the low energy fs laser pulse must first be stretched since direct amplification would lead to higher order nonlinear effects that could lead to subsequent damage of optical materials (*7*). The low energy fs laser pulse is stretched to be ~100 picoseconds in length by chirping (*i.e.*, the instantaneous frequency rises or decreases with time) the pulse via a dispersion delay line composed of a diffraction grating, a spherical mirror and high reflectors (*8*). The stretched laser pulse (known as the seed pulse) is subsequently amplified.

In the amplification process, a second Ti:Al_2O_3 crystal is pumped by a doubled (527 nm), 30 W, < 250 ns, Q-switched (500 Hz), neodymium-doped yttrium lithium fluoride (Nd:YLF) pump laser (Coherent Inc., Model: Evolution-30). A synchronization delay generator (SDG, Coherent Inc., Model: 200-9295) is used to control the input of the stretched laser pulse into the laser cavity for amplification. The injected seed pulse passes through the gain medium several times (approximately 20x) allowing for an amplification of the pulse energy by several orders of magnitude (~10^6). The resulting amplified pulse has a similar pulse duration to that of the seed pulse (approximately 100 ps) and must undergo compression. The short pulse duration of the laser can be regained by compensating for the chirp that was applied in the stretching region (*9*). This is done through the use of a grating, a horizontal mirror set and a vertical retro mirror set, which negates the chirp of the amplified pulse by applying chirp opposite in sign. In this

manner, a 3 mJ, 70 fs laser pulse centered at 800 nm is produced. The amplified fs laser pulses can now be used to enable the nonlinear absorption processes, which will induce vaporization of biomolecules. A schematic view of the fs laser system and its components is shown in Figure 2.1.

2.2.2 Atmospheric pressure electrospray ionization TOF mass spectrometry

2.2.2.1 Electrospray ionization source

The electrospray ionization (ESI) TOF mass spectrometer (Figure 2.2) was built in house and was composed of an ESI source (Analytica of Branford, Branford, CT, USA, Model: 107649), ion optics and a TOF mass spectrometer (Jordan TOF Products Inc., Grass Valley, CA, USA). To enable ESI (*10*) in our system, an analyte is dissolved in solution (commonly 1:1 (v:v) water mixed with a volatile organic compound, *e.g.,* methanol) and pumped through a grounded hypodermic needle (with an inner diameter ~140 μm) at a rate of 0.6 to 3.0 μl/min as set by a syringe pump (Harvard Apparatus, Holliston, MA, USA, Model: 11 Plus). The solution exits the needle in the presence of an electric field (> 300 V/m) where a droplet forms. In the presence of the electric field, the positive charges within the solvent droplet migrate to the solution/air interface, causing the formation of a cone (the Taylor cone) (*11*). Charge repulsion begins to overcome the surface tension (the Rayleigh limit), causing instability in the cone which leads to the formation of daughter droplets via Coulomb fission (*12*). It should be noted that the surface tension of the droplet/cone can be reduced by the use of a nebulization gas, facilitating Coulomb fission.

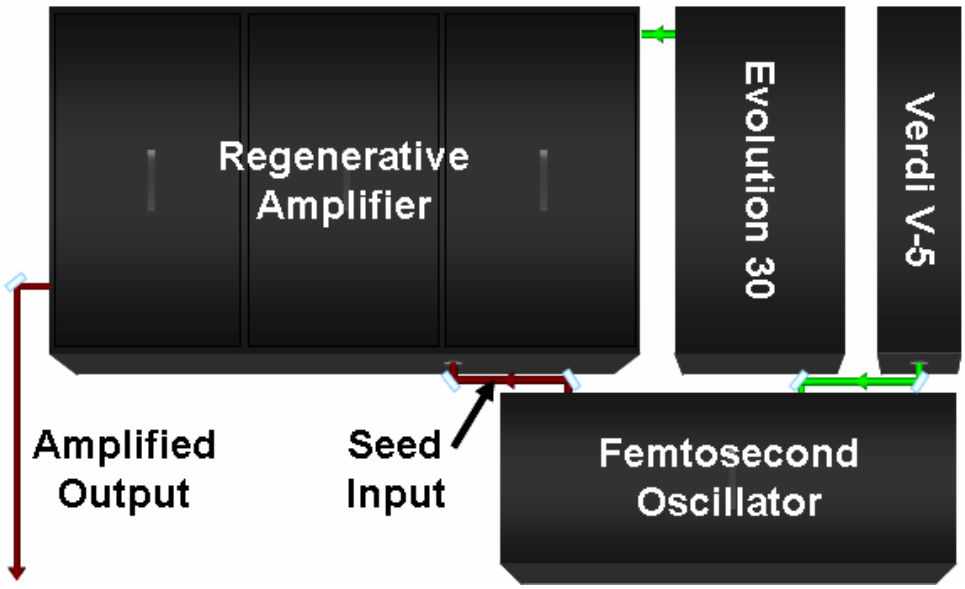

Figure 2.1. Schematic view of the femtosecond laser system.

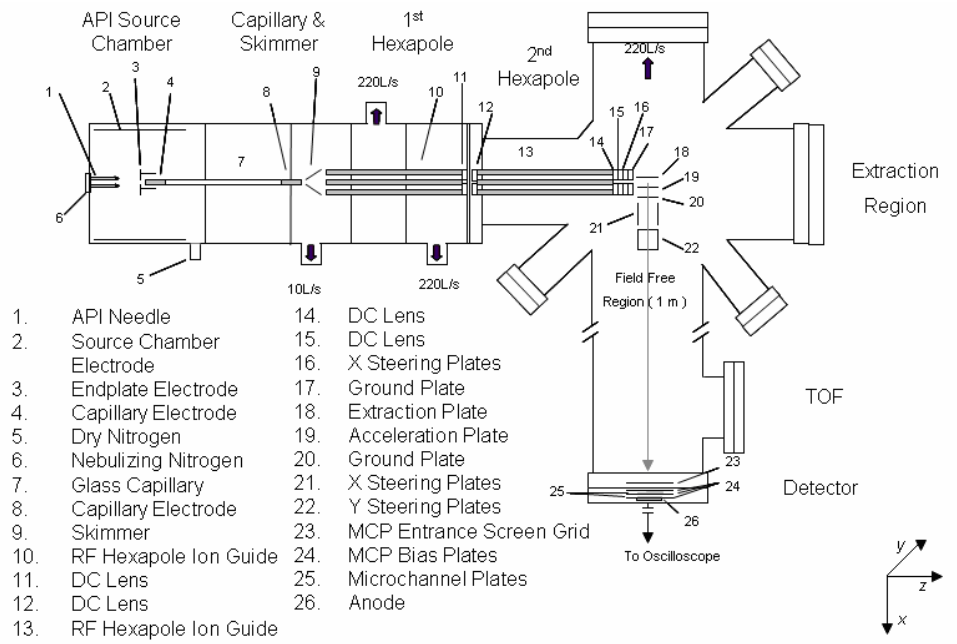

Figure 2.2. Schematic view of the atmospheric pressure ESI-TOF mass spectrometer.

The resulting plume of droplets is dried by the counter-propagating nitrogen gas at 180°C and a flow rate of approximately 12.2 L/min, causing a reduction in the size of the droplets via evaporation. As the size of the droplet decreases, the field strength increases until Coulomb fission results again. As additional daughter droplets are formed from secondary Coulomb fissions, the final analyte ions are desolvated by one of two models. The first model, ion evaporation (*13*), suggests that as the droplet size decreases due to evaporation a critical radius is reached. At the critical radius, the field strength from within the droplet becomes large enough to field desorb the analyte ion. In the second model, charge residue (*14*), solvent free analyte ions are formed after undergoing several evaporation and Coulomb fissions cycles. However, the exact mechanism for transferring the analyte ion into the gas phase is still debated and under investigation.

The ions formed in the experiments described herein are positive ions due to the negative voltage differential between the grounded needle and the mass inlet (-5.3 kV applied to inlet capillary). The desolvated positive ions, regardless of how they are transferred into the gas phase (ion evaporation or charge residue), are typically the result of adduct formation with a cationic species. Some common adduct ions are $[M+H]^+$, $[M+Na]^+$, $[M+K]^+$ and $[M+NH_4]^+$, where *M* is the molecule of interest. The addition of the adduct ion to the molecule typically depends on the solution-phase and/or gas-phase basicity of the molecule (*15*). For large molecules, such as proteins, the formation of multiply charged ions is quite common (*16*) and results from several cations attaching to the molecule forming the $[M+nC]^{n+}$ ion where *C* is the bound cation (*i.e.,* H^+, Na^+, K^+, NH_4^+, etc.) and *n* is the number of bound cations.

After electrospray ionization, the ions enter a dielectric capillary (18 cm in length, 6.4 mm outer diameter and 500 μm inner diameter) which is coated at both ends with metal. The positive ions are transferred to the exit end of the capillary (biased to +130 V) despite the positive bias. The transfer of the positive ions in the presence of the bias is due to the high linear velocity of the nitrogen gas dragging the positive ions to the capillary exit (*17*).

Upon exiting the dielectric capillary, the ions undergo a supersonic expansion in which collisions with background nitrogen gas (~1.2 Torr) occur, rapidly decreasing the internal energy of the ions (*18, 19*). In addition to cooling the ions, "in source" collision induced dissociation (CID) can be performed (*20*) in this region and is dependent on the collisional cross section of the ion, the activation barrier for fragmentation and the kinetic energy of the ion as determined by the voltage difference between the exit capillary and the skimmer. One advantage to CID is that noncovalent bonds in the solvent-analyte clusters can be broken, enhancing the analyte ion yield (*17*).

After the free-jet expansion, the positive ions and any related fragments are transferred to a skimmer (a 1.2 mm circular aperture, 3.5 mm from the exit capillary, typically biased to +50.0 V) via Laminar flow, the directional effect of the free-jet expansion process and the direction of the electric field. The ions and residual gas pass through the skimmer which serves to sample the central portion of the free jet expansion and as a collimating ion lens.

Upon passing through the skimmer, the ions enter a hexapole ion guide (125 mm in length, ~1 mm inscribed diameter, with typical voltages of 650 V for the radio frequency (RF) amplitude and +13.0 V for the DC bias). When RF and DC biases are

applied to the hexapole ion guide (mass filtering mode), only a specific range of *m/z* values are transmitted though the hexapole as determined by their trajectory (*21*). However, the mass filtering mode is only applicable for low pressure conditions (< 1 x 10^{-4} Torr) (*22*) due to a decrease in sensitivity and resolution (*23*) at higher pressures. However, the hexapole in our system is not operated at low pressure, and there are three regions of differential pumping leading to three regions of high pressure (~1.2, ~10^{-2} and ~10^{-4} Torr). The high pressure regions allow for better transmission due to collisions occurring with the analyte ions and background gas, focusing the ions (*24*) into the center of the hexapole as they travel to the exit lens. This collisional focusing, similar to that observed in quadrupole ion traps (*24*), prevents the ions from escaping the hexapole ion guide, allowing for more efficient ion transmission.

In addition, the hexapole can be operated in continuous ion mode, which allows for steady transmission of the electrosprayed ions through the hexapole to the exit lens (biased to +0.5 V) where they are focused prior to entering the ion transfer optics. However, the ion abundance that results is typically lower than when operated in trapping mode. In trapping mode, the transmission of the ions is stopped by raising the voltage on the exit lens (from +0.5 V to +30.0 V). This prevents ions from exiting the ESI source since the ions do not have enough kinetic energy to overcome the applied potential. In this manner, the ions are trapped for approximately 250 μs before the voltage on the exit lens is decreased to +0.5 V allowing for the trapped ions to exit the source and enter the ion transfer optics. The timing for the trapping pulse was set by a transistor–transistor logic pulse (TTL) which was created using a digital delay generator (DDG, Stanford Research Systems, Sunnyvale, Ca, USA, Model: DG 535). The DDG was internally

triggered at a repetition rate of 10 Hz. The timing diagram for the trapping pulse is shown in Figure 2.3.

2.2.2.2 Ion transfer optics

After trapping in the ESI source, the positive ions are transferred from the ESI source hexapole into the ion transfer hexapole (Ardara Technologies, North Huntingdon, PA, USA) via a focusing lens (stainless steel plate with a ~4 mm circular aperture biased to approximately +2 V). The focusing lens ensures that ions do not gain any additional energy in the *z* direction and minimizes space charge expansion effects. The ions are then transferred to another set of ion optics via the ion transfer hexapole (125 mm in length, ~4 mm inscribed diameter, with typical voltages of 300 V for the RF amplitude and 0 V for the DC bias), which was operated in a continuous ion transfer mode (RF only, DC bias 0 V).

After exiting the hexapole, the ions pass through several sets of ion optics (Ardara Technologies) allowing transfer of the ions to the extraction region of the TOF. The first two ion optics, each with a 4 mm circular aperture and biased to approximately +2 V, serve as collimating lenses. The second set consists of split lenses (each lens is biased to approximately 0 V and +8 V, respectively) which allow for translation of the positive ions in the *x* direction. The ions are translated along the *x* axis to pre-compensate for a small DC bias that is present on the acceleration plate in the extraction region. The final lens is grounded and serves as a shield for any electric field present in the extraction and acceleration region preventing alteration of the ion's kinetic energy in the *x* or *z* directions.

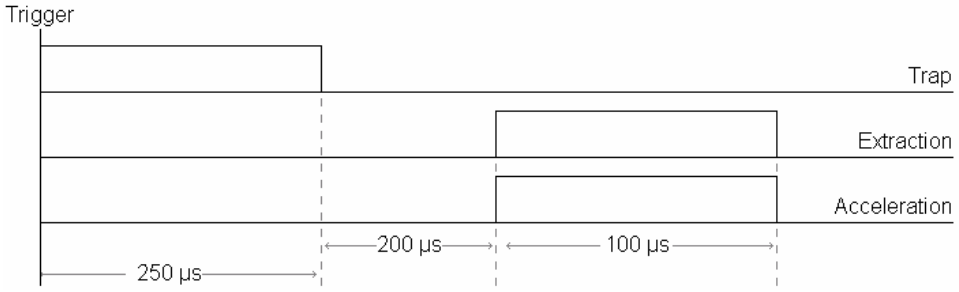

Figure 2.3. Timing diagram for the atmospheric pressure ESI-TOF mass spectrometer.

2.2.2.3 TOF mass spectrometry

In our system (Figure 2.2), the positive ions have kinetic energy in the *z* direction. If the TOF ion optics and TOF mass analyzer were along the same axis, low resolution mass spectra would be obtained due to the initial velocity of the ions (*25*). To enable acquisition of higher resolution mass spectra, the TOF ion optics and the TOF analyzer were positioned to be orthogonal to the ion propagation axis (*z* direction) (*25, 26*). The ion optics (Jordan TOF Products Inc.) of the TOF analyzer consists of three stainless steel plates, a repeller plate, an acceleration plate and a grounded plate (each with a 1 cm aperture in the center, covered with a fine metal mesh (70 lines per inch)). The three plates form two regions, extraction and acceleration, in the ion optics. Once the ions enter the extraction region, two high voltage pulser generators are triggered simultaneously via a TTL pulse from the DDG (the timing diagram for the extraction and acceleration pulses are shown in Figure 2.3). The maximum voltage of the pulse applied to the repeller plate is approximately +3.5 kV (via a high voltage pulse generator from Directed Energy Inc., Fort Collins, CO, USA, Model: PVX-4140) while the maximum voltage of the pulse applied to the acceleration plate is approximately +3.0 kV (via a high voltage pulse generator from Quantum Technologies Inc., Lake Mary, FL, USA, Model: HVP-5LP). The ions are then injected into the acceleration region of the ion optics due to the charge of the ion and the voltage differential between the two plates (+500 V). After entering the acceleration region, the ions are then injected into the field free drift region (~1 m, Jordan TOF Products Inc.) of the TOF mass spectrometer, which is held at a pressure of ~10^{-6} Torr through the use of a turbo pump (Varian Vacuum Technologies, Lexington, MA, USA, Model: V301) and a dual stage rotary vane vacuum pump (Varian Inc., Model: DS

602). It is important to note that all the ions are given the same amount of kinetic energy in the direction of the flight tube. Since the ions have the same kinetic energy in the direction of the flight tube but have different masses, the ions will reach the microchannel plate (MCP) detector (Jordan TOF Products Inc.) at different times (*27*). The "light" ions, low *m/z*, reach the detector first because they have a greater velocity than the heavy ions, high *m/z*. Once the ions reach the MCP detector they collide with the first MCP (40 mm active diameter with a channel diameter of 25 μm, center-center spacing of 32 μm and bias angle of 8 μm) producing electrons, which are subsequently amplified by a second MCP to provide gain on the ion signal. The detector gain is governed by the potential applied to the plates and is approximately 10^6 for the applied potential of -3 kV.

2.2.2.4 Signal processing

The resulting TOF spectra are collected for a specified number of trapping pulses and averaged using a digital oscilloscope (LeCroy Corporation, Chestnut Ridge, NY, USA, Model: WaveSurfer 422) displaying a particular signal-to-noise (S/N).

To enable mass calibration of the ESI-TOF system in positive ion mode, an electrospray tuning solution (Agilent Technologies Inc., Santa Clara, CA, USA, Part: G2421A) containing molecules that produce ions ranging in *m/z* from 100 to 3,000 was analyzed. A quadratic calibration was performed using software (Labview 8.5) written in house to ensure *m/z* accuracy. The mass calibrated spectra were produced in Origin 7.5. A typical mass spectrum obtained for the Agilent electrospray tuning solution using the above mass spectrometer configuration is shown in Figure 2.4. The mass resolution was determined to be m/Δm ~320 at *m/z* 1522 as shown in Figure 2.5.

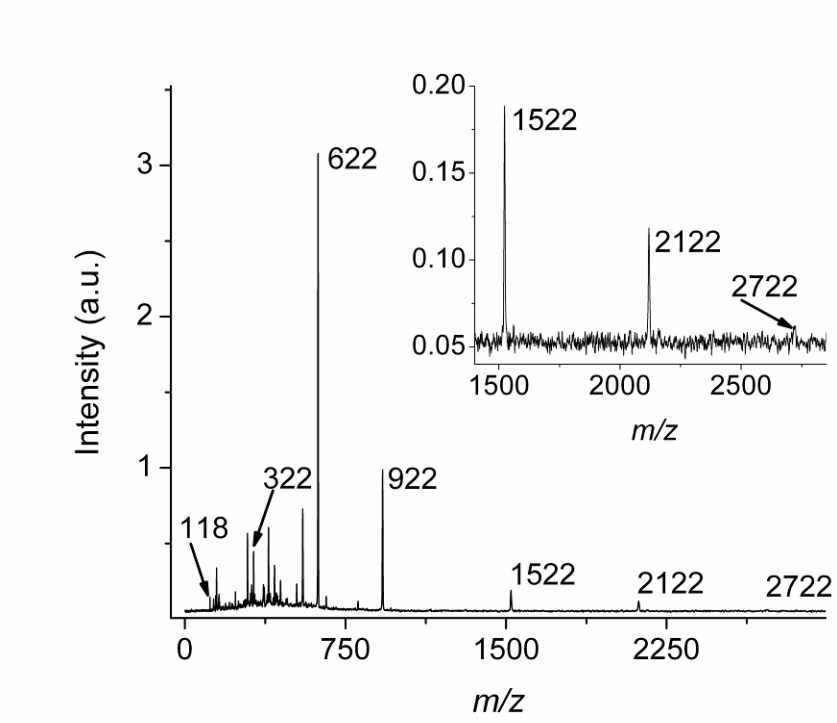

Figure 2.4. A typical mass spectrum obtained for the Agilent electrospray tuning solution, displaying the peaks at *m/z* 118, 322, 622, 922, 1522, 2122, and 2722 used for calibration.

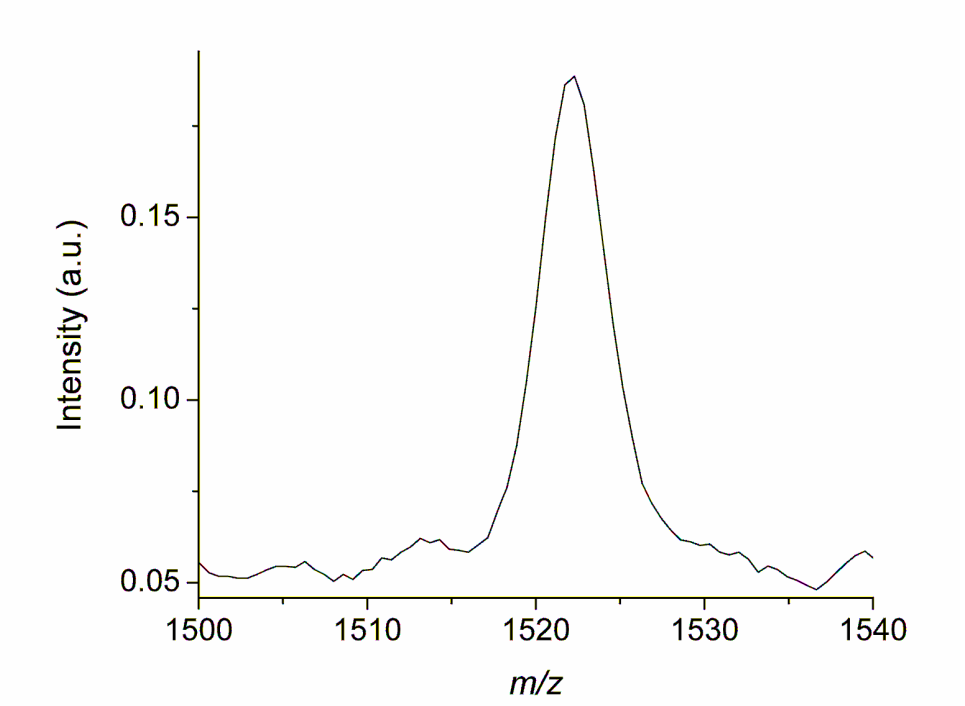

Figure 2.5. An expansion of the peak at *m/z* 1522. The mass resolution was determined to be m/Δm ~320 at *m/z* 1522.

2.2.2.5 Limit of detection

The lipid, 1,2-dihexanoyl-*sn*-glycero-3-phosphocholine (DHPC, Avanti Polar Lipids Inc., Alabaster, AL, USA), was chosen to determine the limit of detection (LOD) for the ESI-TOF system due to its amphiphilic nature. The LOD was determined by electrospraying a solution of DHPC of varying sample molarity (5×10^{-6} to 5×10^{-8} M) dissolved in 1:1 (v:v) methanol:water acidified with 1.0% glacial acetic acid (Figure 2.6). Upon inspection of the mass spectrum resulting from the electrosprayed 5×10^{-8} M solution (Figure 2.7), it was found the LOD was approximately 1 pg or 2.5 fmol of DHPC since the resulting $[M+H]^+$ peak yielded a S/N ratio of 4.4, where the S/N threshold is greater than three.

2.3 Nonresonant femtosecond laser vaporization coupled to the ESI-TOF mass spectrometer

2.3.1 Coupling of the nonresonant femtosecond laser to the ESI-TOF mass spectrometer

To enable nonresonant absorption processes for the transfer of molecules into the gas phase, the fs laser system's repetition rate was reduced to 10 Hz to couple to the ESI-TOF mass spectrometer. The amplified fs laser beam is split by a 80/20 beam splitter (CVI-Melles Griot Inc., Albuquerque, NM, USA) after exiting the regenerative amplifier. The portion of the beam containing 20% of the laser pulse energy is directed to a beam dump and not utilized in the experiments. The second beam, containing 80% of the energy from the regeneratively amplified laser pulse, is directed to the atmospheric

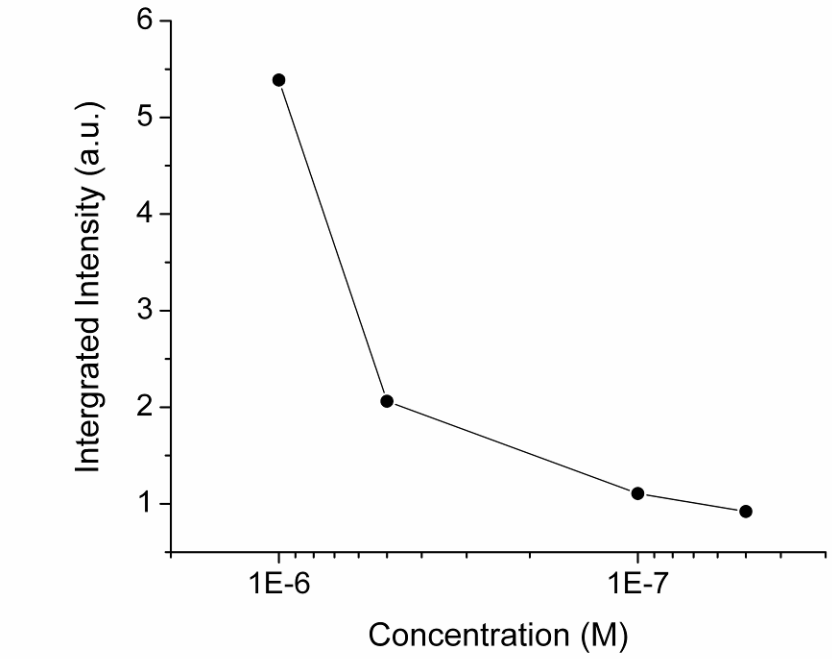

Figure 2.6. A plot of the integrated ion abundance for the $[M+H]^+$ peak of DHPC as a function (log scale) of concentration for electrospray solutions of varying sample molarity (5×10^{-6} to 5×10^{-8} M) dissolved in 1:1 (v:v) methanol:water acidified with 1.0% glacial acetic acid.

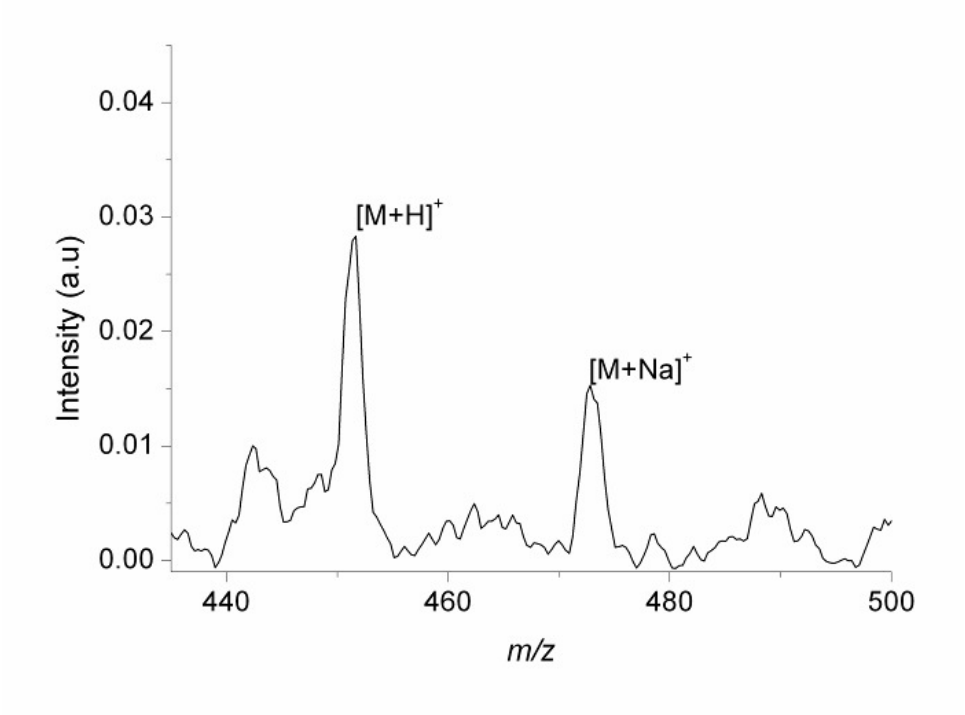

Figure 2.7. The conventional ESI-MS of a 5 x 10^{-8} M solution of DHPC dissolved in 1:1 (v:v) methanol:water containing 1.0% acetic acid. The signal-to-noise for the $[M+H]^+$ ion was 3.3.

pressure ESI-TOF mass spectrometer using dielectric broadband mirrors (CVI-Melles Griot Inc.) coated for 800 nm. The laser beam passes through a 17.5 cm focal length lens (CVI-Melles Griot Inc.) mounted on a translational stage which allows for adjustment of the focusing conditions. The beam is directed through the glass shield in the ESI source assembly via a dielectric broadband mirror. A circular hole, one inch in diameter, was removed from the glass shield to ensure that the beam profile, energy and duration of the propagating laser pulse were not altered. The laser was focused to a spot size of approximately 250 μm in diameter, with an incident angle of 45° with respect to the sample. The intensity of the laser pulse on the sample was approximately 10^{13} W/cm^2.

The laser beam was positioned along the axis of the electrospray needle and inlet capillary so that the area sampled was approximately 6 mm below the electrospray needle and ~1 mm in front of the electrospray needle (Figure 2.8). The sample was supported by a three-dimensional translation stage which permitted the analysis of fresh sample. The three-dimensional translation stage was inserted into the ESI source assembly approximately 6 mm below the electrospray needle and was biased to -2 kV to correct for the distortion in the electric field between the needle and capillary inlet caused by the sample plate. This bias optimizes the entrance current of the ions, formed via ESI, into the dielectric capillary. It should be noted that in order to introduce the stage, the door to the source assembly of the atmospheric pressure ESI-TOF mass spectrometer was removed and the high-voltage interlocks were overridden. In addition, to position the electrospray needle to be on axis with the ion optics, the needle was removed from the source assembly door and mounted on a separate three dimensional translational stage.

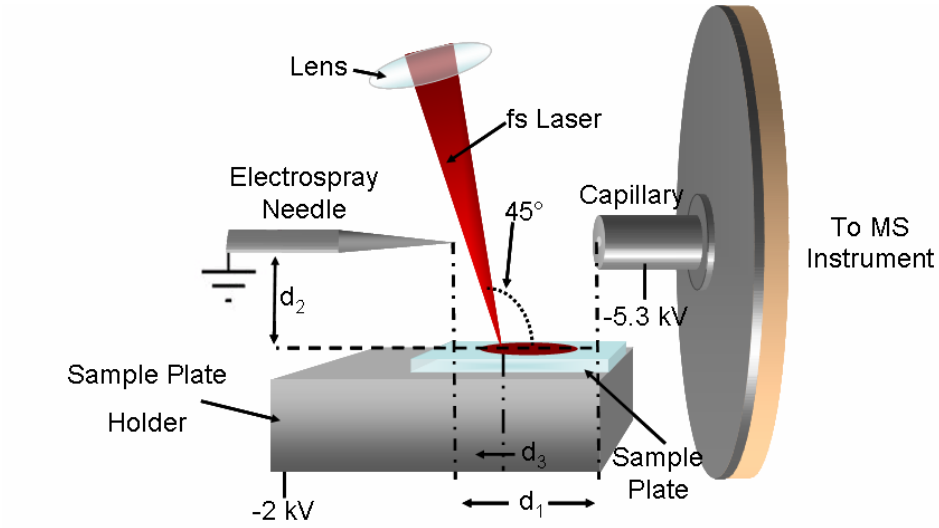

Figure 2.8. A schematic representation of the vaporization and ionization apparatus. The needle to capillary distance, d_1, is ~6 mm. The distance from the bottom of the capillary to the sample, d_2, was maintained at ~6 mm. The sample was placed on a three dimensional stage to allow for easy translation. The laser had an angle of incidence of 45° with respect to the sample plate. The distance from the electrospray needle to the laser ablation spot, d_3, was ~1 mm.

The solvent, typically composed of 1:1 (v:v) methanol:water acidified with 1.0% glacial acetic acid, is electrosprayed perpendicular to the laser-vaporized material. The vaporized neutral molecules were captured, solvated and ionized by the electrospray plume. The electrospray droplets, containing the solvated and ionized analyte, were then dried by counter propagating nitrogen gas at 180°C (flow rate 12.2 L/min) before entering the inlet capillary where they are mass analyzed using the modified ESI-TOF mass spectrometer. Appropriate laser eye protection was worn by all personel and the high voltage area was enclosed in plexiglass to prevent accidental contact with the biased electrodes. A schematic view of the nonresonant fs laser coupled to the modified atmospheric pressure ESI-TOF mass spectrometer is shown in Figure 2.9 and the timing diagram for the laser, trapping, extraction and acceleration pulses is shown in Figure 2.10. The DDG was not internally triggered as with the atmospheric pressure ESI-TOF mass spectrometer, instead the sync pulse from the SDG box was used to externally trigger the DDG at a 10 Hz repetition rate.

2.3.2 Signal processing

The resulting mass spectra are collected for a specified number of laser pulses and averaged using a digital oscilloscope displaying a particular S/N. An electrospray solvent background mass spectrum (no laser present) was acquired before each experiment and subtracted from the laser vaporization measurement to produce the spectra shown. Significant differences in the ion abundance of the solvent mass spectrum were caused by the presence of the laser-vaporized molecules. The vaporized molecules compete for the charge in the electrosprayed solvent cluster, causing a change in the observed ion

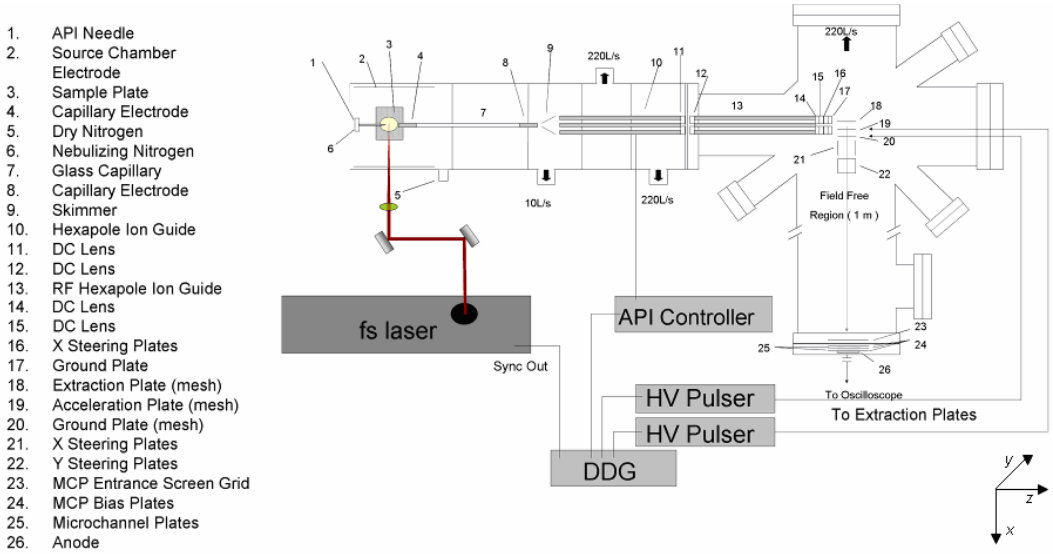

Figure 2.9. Schematic view of the nonresonant femtosecond laser coupled to the atmospheric pressure ESI-TOF mass spectrometer.

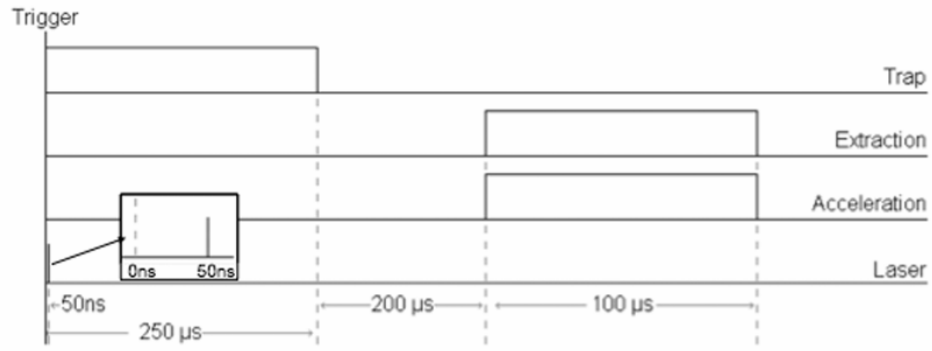

Figure 2.10. Timing diagram of the laser, trapping, extraction and acceleration pulses.

abundance for the solvent related features. This leads to the formation of negative and positive solvent features seen in the subtracted mass spectra.

2.3.3 Limit of detection

The LOD was determined through comparison of LEMS and conventional ESI-MS data (see 2.2.2.5) for the molecule DHPC. The LEMS data was acquired by vaporizing the dried lipid from a metal slide after deposition of a 30 μL aliquot of a solution with varying molarity (1×10^{-4} to 5×10^{-6} M, Figure 2.11). The vaporized sample was captured, solvated and ionized by an electrospray plume composed of 1:1 (v:v) methanol:water acidified with 1.0% glacial acetic acid. Each laser shot resulted in the complete vaporization of lipid in the area investigated. Routinely five averaged mass spectra, consisting of fifty laser shots each, would be acquired per sample prepared. Therefore, approximately one-fifth of the sample is vaporized from the metal slide during the acquisition of a single mass spectrum. When an aliquot of a 5×10^{-6} M solution of DHPC was deposited and dried on the metal surface, ~14 ng of DHPC was vaporized upon analysis. Therefore, the quantity of DHPC consumed from the sample per laser shot was < 280 pg (600 fmol). This suggests that for lipid analysis, the sensitivity per laser shot is approximately 600 fmol. It was found that the signal-to-noise for the $[M+H]^+$ ion for such a LEMS measurement was 6.3 (Figure 2.12).

This is not the LOD for the fs laser vaporization technique. The LOD of the mass spectral system depends on multiple factors including: laser parameters (wavelength, pulse duration, intensity, etc.), ionization parameters (solvent system), mass analysis technique (linear TOF, reflectron TOF, orbitrap, etc.), amount of material deposited, film

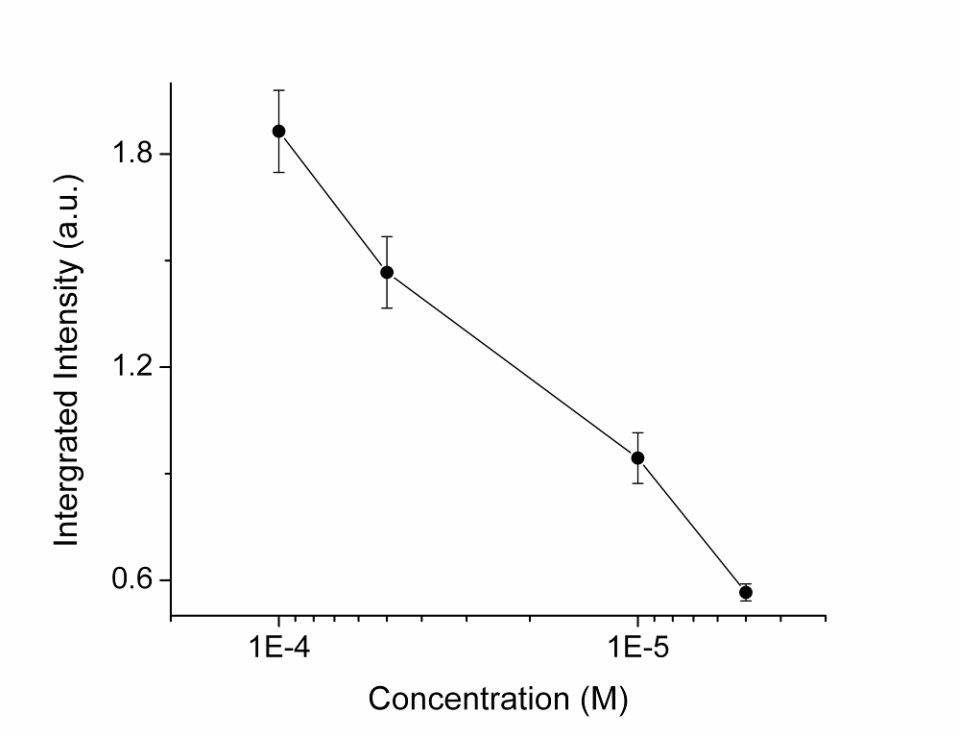

Figure 2.11. A plot of the integrated ion abundance for the $[M+H]^+$ peak of DHPC as a function (log scale) of concentration for the vaporized solution of varying sample molarity (5×10^{-6} to 5×10^{-8} M).

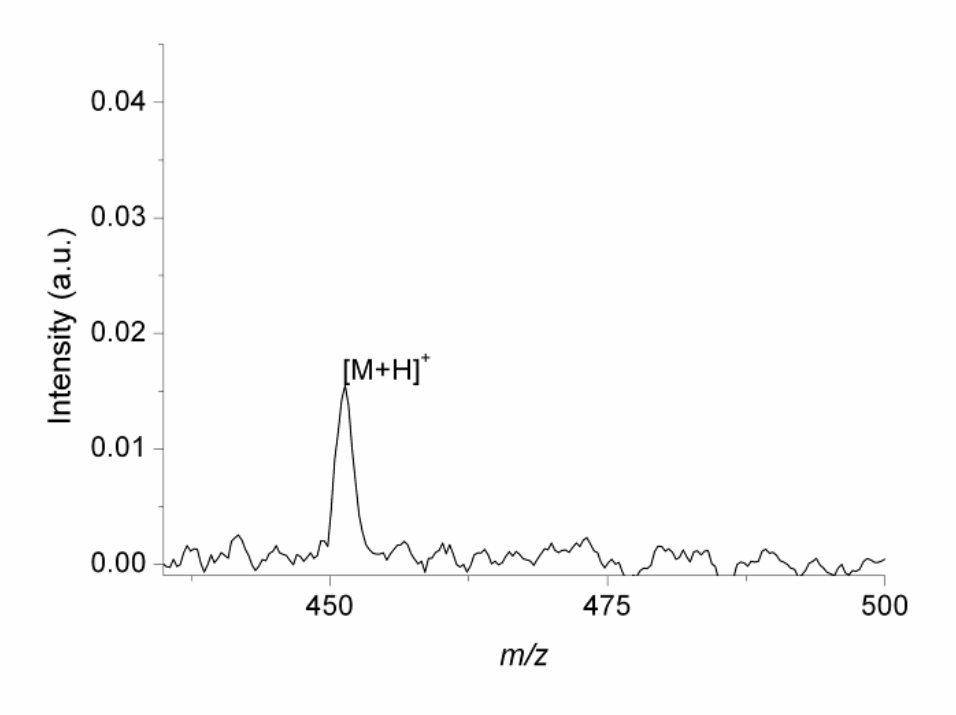

Figure 2.12. The background subtracted mass spectrum of an aliquot of 5 x 10^{-6} M DHPC deposited on a metal plate vaporized and post-ionized in the electrospray plume (1:1 (v:v) methanol:water with 1.0% glacial acetic). The signal-to-noise for the $[M+H]^+$ ion was 6.3.

morphology and chemical noise due to interferents. By determining the quantity of sample consumed during the conventional ESI-MS analysis (~1 pg or 2.5 fmol) to the quantity consumed per laser shot for the LEMS, a better quantification of the LOD can be determined irrespective of mass spectral system used. A comparison of the LOD for the two techniques yields that LEMS is ~240x less sensitive for the analysis of DHPC. The decrease in sensitivity for LEMS, in comparison to conventional ESI-MS, is due to the neutral capture efficiency which has been determined to range from 2.4 ± 1.5% to 0.25 ± 0.18% (*28*). Nevertheless, the LEMS technique would be capable of detecting <10 fmol of material from a surface if current high sensitivity mass spectrometers (orbitrap ~50 attomol for ESI-MS) were implemented.

2.3.4 Femtosecond laser vaporization of mixtures

To address whether the fs laser vaporization signal response is linear with concentration, we measured the mass spectra for binary mixtures of varying composition. A 30 μL aliquot of a mixture made from 10^{-4} M DHPC and 10^{-4} M 1-monooleoyl-*rac*-glycerol (monoolein, MP Biomedicals Solon, OH, USA) was deposited onto a stainless steel slide, vaporized and captured by an electrospray solution composed of 1:1 (v:v) methanol:water with 1.0% acetic acid. The molar ratio of DHPC:monoolein was varied between 1:0 and 0:1. The measurements shown in Figure 2.13 reveal a linear relationship between the amount of monoolein applied to the surface and the average integrated signal for the sum of the $[M\text{-}H_2O+H]^+$, $[M+H]^+$ and $[M+Na]^+$ ions resulting from fifty laser shots. Similarly, there is a linear relationship between the amount of DHPC applied to the stainless steel slide and the average integrated signal abundance for the $[M+H]^+$ and

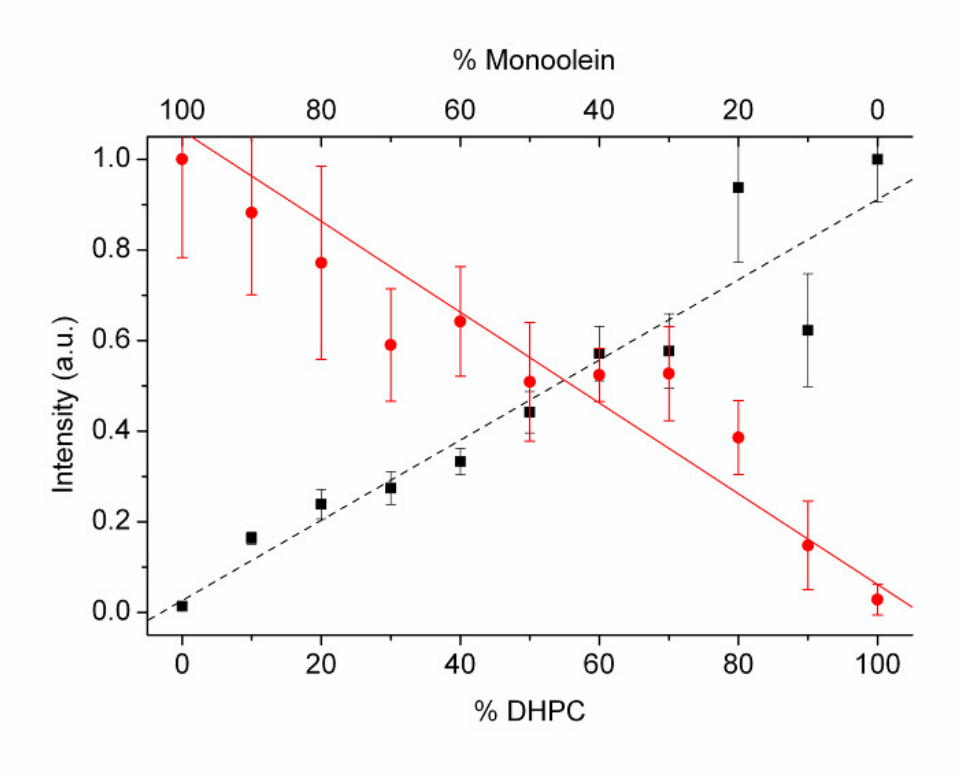

Figure 2.13. Plot of the average total integrated ion signal from the $[M\text{-}H_2O+H]^+$, $[M+H]^+$ and $[M+Na]^+$ ions of monoolein (●, solid red line) and $[M+H]^+$ and $[M+Na]^+$ ions of DHPC (■, dashed black line) as a function of mixture composition.

$[M+Na]^+$ ion channels. These trends suggest that the signal response in LEMS is linear with lipid concentration.

The error bars reported for the measurements in Figure 2.13 do not arise from fluctuations in laser intensity, or voltage fluctuations in the ESI source or mass spectrometer ion optics. The dry drop deposition method of sample preparation prepares a spatially inhomogeneous distribution of sample on the steel surface. The variance is most likely due to vaporization of an inconsistent amount of sample as a function of position on the stainless steel slide. A similar situation was observed for quantitative MALDI analysis prior to electrospray deposition of sample (*29*). Despite the differences in size and polarity of the lipids applied to the surface, both can be detected and discriminated as a function of concentration.

References

1. F. Hillenkamp, M. Karas, R. C. Beavis, B. T. Chait, Matrix-assisted laser desorption ionization mass-spectrometry of biopolymers. *Anal. Chem.* **63**, A1193 (1991).
2. W. Paul, Electromagnetic traps for charged and neutral particles. *Rev. Mod. Phys.* **62**, 531 (1990).
3. Q. Hu *et al.*, The orbitrap: A new mass spectrometer. *J. Mass Spectrom.* **40**, 430 (2005).
4. R. Cotter, *Time-of-flight mass spectrometry: Instrumentation and applications in biological research.*, (ACS, Washington, D.C., 1997).

5. J. H. Posthumus, The dynamics of small molecules in intense laser fields. *Rep. Prog. Phys.* **67**, 623 (2004).

6. M. Piché, F. Salin, Self-mode locking of solid-state lasers without apertures. *Opt. Lett.* **18**, 1041 (1993).

7. D. Strickland, G. Mourou, Compression of amplified chirped optical pulses. *Opt. Commun.* **56**, 219 (1985).

8. S. Backus, C. G. Durfee III, M. M. Murnane, H. C. Kapteyn, High power ultrafast lasers. *Rev. Sci. Instrum.* **69**, 1207 (1998).

9. M. Pessot, P. Maine, G. Mourou, 1000 times expansion/compression of optical pulses for chirped pulse amplification. *Opt. Commun.* **62**, 419 (1987).

10. J. B. Fenn, M. Mann, C. K. Meng, S. F. Wong, C. M. Whitehouse, Electrospray ionization for mass-spectrometry of large biomolecules. *Science* **246**, 64 (1989).

11. G. Taylor, Disintegration of water drops in an electric field. *Proc. R. Soc. Edin. A-Ma.* **280**, 383 (1964).

12. P. Kebarle, L. Tang, From ions in solution to ions in the gas phase - the mechanism of electrospray mass spectrometry. *Anal. Chem.* **65**, 972A (1993).

13. J. V. Iribarne, B. A. Thomson, On the evaporation of small ions from charged droplets. *J. Chem. Phys.* **64**, 2287 (1976).

14. M. Dole *et al.*, Molecular beams of macroions. *J. Chem. Phys.* **49**, 2240 (1968).

15. R. B. Cole, Some tenets pertaining to electrospray ionization mass spectrometry. *J. Mass Spectrom.* **35**, 763 (2000).

16. J. B. Fenn, M. Mann, C. K. Meng, S. F. Wong, C. M. Whitehouse, Electrospray ionization-principles and practice. *Mass Spectrom. Rev.* **9**, 37 (1990).

17. R. B. Cole, *Electrospray and MALDI mass spectrometry: Fundamentals, instrumentation, practicalities, and biological applications*. (John Wiley & Sons, 2009).

18. V. Gabelica, E. D. Pauw, Internal energy and fragmentation of ions produced in electrospray sources. *Mass Spectrom. Rev.* **24**, 566 (2005).

19. J. M. Hayes, G. J. Small, Supersonic jets, rotational cooling, and analytical-chemistry. *Anal. Chem.* **55**, A565 (1983).

20. S. A. McLuckey, Principles of collisional activation in analytical mass spectrometry. *J. Am. Soc. Mass Spectrom.* **3**, 599 (1992).

21. P. E. Miller, M. B. Denton, The quadruple mass filter: Basic operating concepts. *J. Chem. Educ.* **63**, 617 (1986).

22. P. H. Dawson, Ed., *Quadrupole mass spectrometry and its applications.*, (Springer-Verlag New York, LLC, New York, 1997).

23. J. Visser, Mass spectrometric analysis of the sputter gas atmosphere without pressure reduction system. *J. Vac. Sci. Technol.* **10**, 464 (1973).

24. D. J. Douglas, J. B. French, Collisional focusing effects in radio frequency quadrupoles. *J. Am. Soc. Mass Spectrom.* **3**, 398 (1992).

25. J. H. J. Dawson, M. Guilhaus, Orthogonal-acceleration time-of-flight mass spectrometer. *Rapid Commun. Mass Spectrom.* **3**, 155 (1989).

26. A. N. Verentchikov, W. Ens, K. G. Standing, Reflecting time-of-flight mass spectrometer with an electrospray ion source and orthogonal extraction. *Anal. Chem.* **66**, 126 (1994).

27. M. Guilhaus, Special feature: Tutorial. Principles and instrumentation in time-of-flight mass spectrometry. Physical and instrumental concepts. *J. Mass Spectrom.* **30**, 1519 (1995).

28. E. J. Judge, J. J. Brady, D. R. Dalton, R. J. Levis, Mass analysis of pharmaceutical compounds from glass, cloth, steel and wood surfaces at atmospheric pressure using non-resonant femtosecond laser vaporization and electrospray ionization *Anal. Chem.* **82**, 3231 (2010).

29. R. R. Hensel, R. C. King, K. G. Owens, Electrospray sample preparation for improved quantitation in matrix-assisted laser desorption/ionization time-of-flight mass spectrometry. *Rapid Commun. Mass Spectrom.* **11**, 1785 (1997).

CHAPTER 3

LASER ELECTROSPRAY MASS SPECTROMETRY OF EXPLOSIVES, LIPIDS AND BIOMOLECULES

3.1 Overview

In this chapter, the transfer of intact, non-volatile, biological macromolecules from the condensed phase into the gas phase using intense femtosecond laser pulses is explored. Electrospray post-ionization of the vaporized material allows for mass spectral measurements to be made for the various samples, including explosives, lipids, biomolecules and protein adsorbed on stainless steel surfaces. No appreciable signal was detected when femtosecond laser vaporization was performed without the electrospray plume present, indicating that molecules, rather than ions, are transferred into the gas phase. Finally, the vaporization of aqueous protein indicates that large molecules can be transferred into the gas phase, ionized and analyzed using electrospray ionization mass spectrometry.

3.2 Introduction

The universal detection of analytes is a major challenge for any single analytical technique due to the wide variety of chemical structures and the enormous range of vapor pressures (ranging from Torr to picoTorr at room temperature). One common soft vaporization/ionization technique for analyzing non-volatile molecules is electrospray ionization (ESI) (*1, 2*), in which molecules with low vapor pressure are transferred from the solution phase into the gas phase via a charged droplet formed in the presence of an

electric field. The charged droplet undergoes several cycles of solvent evaporation and Coulomb fission leaving an unsolvated analyte ion in the gas phase to undergo subsequent mass analysis (*3*). Although conventional ESI mass spectrometry is very effective for analyzing molecules in the aqueous state, the technique can not directly analyze samples in the solid state or adhered to a surface. For example, a solid sample containing explosives can be detected using conventional ESI mass spectrometry (*4, 5*) but requires the sample to be transferred using a swab (*6*) followed by elution with solvent.

Secondary ion mass spectrometry (SIMS) (*7, 8*) is a mass analysis technique that allows for the analysis of low vapor pressure molecules adsorbed onto the surface of a substrate by impinging the sample with a focused ion beam (*e.g.*, C_{60}^+). Secondary ions are formed and transferred into the gas phase, which are subsequently mass analyzed, typically via time-of-flight (TOF) mass spectrometry. Secondary ion mass spectrometry has been extremely successful, allowing for the analysis of a variety of molecules, such as peptides (*9*) and lipids (*10*), and the mass spectral imaging of highly curved membranes during *Tetrahymena* mating (*11*). Although a successful technique, it has its limitations. The first limitation is that SIMS is strictly a vacuum based technique, thus preventing the analysis of tissue in its native state. The second drawback is that fragmentation readily occurs due to the energy deposited into the internal modes of the adhered molecules upon interaction with the primary ion. The dissociation of the analyte limits the size of molecules available for analysis to < 1,500 Da.

A mass spectrometry technique that can overcome the solution phase requirement of ESI and desorb intact molecules/ions is matrix-assisted laser desorption ionization

(MALDI) (*12, 13*). Matrix-assisted laser desorption ionization mass spectrometry can analyze large biological molecules (> 1,500 Da) in the solid (*12, 13*) or liquid states (*14*). In addition, MALDI can also be performed at atmospheric pressure (*15, 16*) reducing time constraints associated with analysis performed under vacuum conditions. During MALDI analysis, a nanosecond (ns) laser excites the matrix molecules, which are co-crystallized with the analyte, to a low lying excited state via resonant absorption process. The laser pulse energy, which is absorbed by the matrix, is converted to heat enabling desorption of both the matrix and the analyte (*17*). Although ns laser desorption has been successful in analyzing a wide variety of molecules, the coupling mechanisms are markedly different for femtosecond (fs) laser pulses and these differences suggest that ultrafast excitation may be useful.

One such case illustrating the difference in coupling mechanisms is shown when ns and fs laser pulses are used for the ionization of a gas phase biomolecule under vacuum conditions. Upon examination of the obtained mass spectra, the ns laser pulse yields more fragmentation than a fs laser pulse (*18*). The additional fragmentation observed with ns laser ionization is due to the ladder switching mechanism in which the molecule absorbs energy from the laser pulse and dissociates while the laser pulse is still present. This allows for the fragments to subsequently absorb additional energy from the laser pulse, leading to further fragmentation (*19*). Ladder switching occurs with ns laser pulse excitation because the molecular dissociation time is shorter than the laser pulse duration. During fs excitation, the molecule does not readily undergo fragmentation during excitation because the pulse duration of the laser is shorter than the molecular

rearrangement time of the molecule (ladder climbing) (*20*). Therefore, intact molecular ions are commonly observed with fs laser pulses.

Femtosecond laser pulses have been used in MALDI schemes and typically result in a lower yield of ions (*21, 22*) when compared to MALDI using ns laser pulses. However, the number of neutrals transferred into the gas phase from a surface using a laser pulse can exceed the number of ions by several orders of magnitude as shown by laser desorption experiments with electron beam post-ionization (*23*). Thus, the use fs laser pulses for vaporization most likely results in the production of an abundant amount of neutral molecules rather than ions. Post-ionization of the vaporized neutral molecules would result in a gain of sensitivity by several orders of magnitude (*24, 25*) over traditional ns-laser based desorption/ionization techniques.

Post-ionization of laser-desorbed material can be achieved via an electron beam (*23*), a pulsed laser (*26*), atmospheric pressure chemical ionization (APCI) (*24, 25*) or ESI (*27*). Electron beam and pulsed laser ionization have been very successful at post-ionization of desorbed analyte under vacuum conditions; however, modest gains in sensitivity are usually achieved due to the small interaction volumes with the laser-desorbed sample. An atmospheric based post-ionization technique, APCI, can increase the sensitivity of the laser desorption technique by several orders of magnitude due to its high ionization efficiency and the increased interaction cross-section. The APCI process is efficient for both polar and nonpolar molecules but it is commonly limited to small molecules (< 2,000 Da), thus preventing the analysis of proteins.

Electrospray ionization can also be used for the post-ionization of laser desorbed material as it is an atmospheric pressure technique, has a high ionization efficiency and

has a large interaction cross section. The advantage to ESI, compared to APCI, is that large biomolecules (> 2,000 Da), such as proteins, are easily ionized and mass analyzed. In electrospray post-ionization experiments, such as electrospray-assisted laser desorption ionization (*27*), matrix assisted laser desorption electrospray ionization (*28*) and laser ablation electrospray ionization (*29*), the charged droplets that are formed via electrospray processes (*1, 3*), capture and solvate the neutral molecules, nanoparticles and clusters ejected from the sample after ns laser irradiation. The droplets containing the analyte molecules will undergo several evaporation and Coulomb fission cycles until the final ion formation process, where charge is transferred to or from the analyte molecule depending on the charge of the droplet (*e.g.,* for a positively charged droplet, a positively charged adduct is transferred onto the analyte), thus softly ionizing the laser-desorbed sample.

Here, we present a new method for mass analysis of low vapor pressure molecules adhered to a substrate or in the aqueous state by using a fs laser pulse to induce vaporization of the condensed phase analyte. It will be demonstrated through the electrospray post-ionization of the vaporized material, which include: explosives, a lipid, biomolecules and protein, that neutral, unfragmented molecules, independent of molecular size or polarity, are transferred into the gas phase using fs laser pulses. This new method for atmospheric pressure mass analysis, fs laser vaporization with electrospray post-ionization, is known as laser electrospray mass spectrometry (LEMS).

3.3 Experimental

3.3.1 Materials

Two explosives, RDX (1 mg/mL, 1,3,5-trinitroperhydro-1,3,5-triazine) and HMTD (3, 4, 8, 9, 12, 13-hexaoxa-1, 6-diazabicyclo [4.4.4] tetradecane), were obtained in dilute acetonitrile:methanol (1:1) solution from Accustandard (New Haven, CT, USA). A solid sample of DHPC (1,2-dihexanoyl-*sn*-glycero-3-phosphocholine) was obtained from Avanti Polar Lipids (Alabaster, AL, USA). Undiluted human blood was obtained from a healthy volunteer in accordance with University policy and procedure. The reduced fat and whole milk were purchased from a local market. All samples were used without purification.

3.3.2 Sample preparation

The explosive samples was prepared by drying either a 50 μL aliquot of 1 x 10^{-3} M RDX or a 50 μL aliquot of 1 x 10^{-4} M HMTD on a stainless steel slide. The DHPC sample was diluted to 1 x 10^{-4} M in methanol. A 30 μL aliquot of the solution was deposited on a stainless steel slide (6 mm x 6 mm) and allowed to air dry prior to analysis.

Undiluted whole blood (20 μL) was deposited directly onto a stainless steel slide. A 2 μL aliquot of 1 x 10^{-3} M DHPC was added to the undiluted whole blood and mixed prior to analysis while in the aqueous state. A 300 μL aliquot of milk was deposited into a welled (45 mm x 6 mm x 1 mm) aluminum sample plate to deter evaporation. No further sample preparation was performed on the milk samples or the undiluted whole blood/DHPC mixture other than transfer to the sample plate. The sample slides were

placed on a three-dimensional translation stage which permitted the analysis of fresh sample by each laser shot.

3.3.3 Laser vaporization and ionization apparatus

A Ti:Sapphire oscillator seeded a regenerative amplifier to create 70 fs laser pulses centered at 800 nm with a pulse energy of 2.5 mJ. The laser pulse energy was reduced to 800 μJ/pulse (1.6 mJ/pulse for liquid samples) using a neutral density filter. The 500 Hz repetition rate of the laser was reduced to 10 Hz to couple to the electrospray system. The fs laser pulse was focused to a spot size of 250 μm in diameter using a 17.5 cm focal length lens, with an incident angle of 45° with respect to the sample (Figure 3.1), to induce vaporization of the analyte material. The metal sample plate holder was biased to -2 kV to correct for the distortion in the electric field between the needle and capillary inlet caused by the sample plate. This bias optimizes the entrance current of the ions into the dielectric capillary. The vaporized sample was captured and ionized by an electrospray solvent plume traveling perpendicular to the laser-ejected material. The electrospray solvent flow rate was 3 μL/min as set by a syringe pump.

3.3.4 Mass spectrometry

The ions enter the mass spectrometer system through a dielectric capillary before passing through the skimmer. The ions then enter a linear hexapole where they are trapped for 250 μs before being pulsed out of the source and transferred to the extraction region of the linear TOF mass analyzer by a second hexapole and ion optics. Once in the extraction region, the positive ions are pulsed orthogonally with respect to the electrospray ion optics into the TOF analyzer using two high voltage pulsers. The extraction region and field free flight tube were maintained at a pressure of ~10^{-6} Torr.

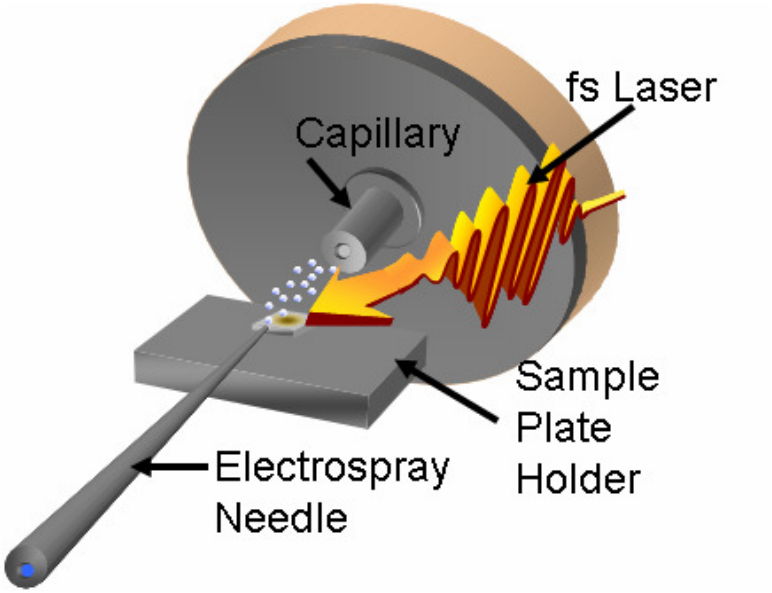

Figure 3.1. A schematic representation of the vaporization and ionization apparatus.

After mass analysis, the positive ions were detected and the resulting positive ion mass spectrum, with a resolution of m/Δm ~100 at mass-to-charge (*m/z*) 2122, was averaged for 50 laser shots using a digital oscilloscope.

An ESI solvent background mass spectrum (no laser present) was acquired before each experiment and subtracted from the laser vaporization measurement to produce the spectra shown. Significant differences in the intensity of the solvent mass spectrum were caused by the presence of the laser-vaporized molecules. The molecules compete for the charge in the electrosprayed solvent cluster, causing a change in the observed solvent signal. This leads to the formation of negative and positive solvent features seen in the subtracted mass spectra. Only analyte-related features are the labeled in the figures.

3.3.5 Remote detection

The remote detection of explosives was performed by depositing sample onto the sample plate holder which is positioned at a distance (2 m) from the electrospray source (Figure 3.2). The focused fs laser beam is used to vaporize the deposited molecules which are then transferred via tubing to the ionization region via a Venturi pump (VacMotion, Inc., Plymouth, MA, USA). The vaporized molecules exit the outlet feed of the tubing, above a biased metal plate, in the vicinity of the electrospray needle. The transferred, vaporized molecules interact with the electrosprayed solvent forming ions, which are directed into the capillary and analyzed by a mass spectrometer, as described above.

3.3.6 UV/VIS spectroscopy

A whole blood sample (~ 20 μL) was diluted in pure water (~ 6 mL) and characterized using a Jasco V-530 UV-VIS spectrometer in the wavelength range of 300 to 900 nm, with a resolution of 1 nm.

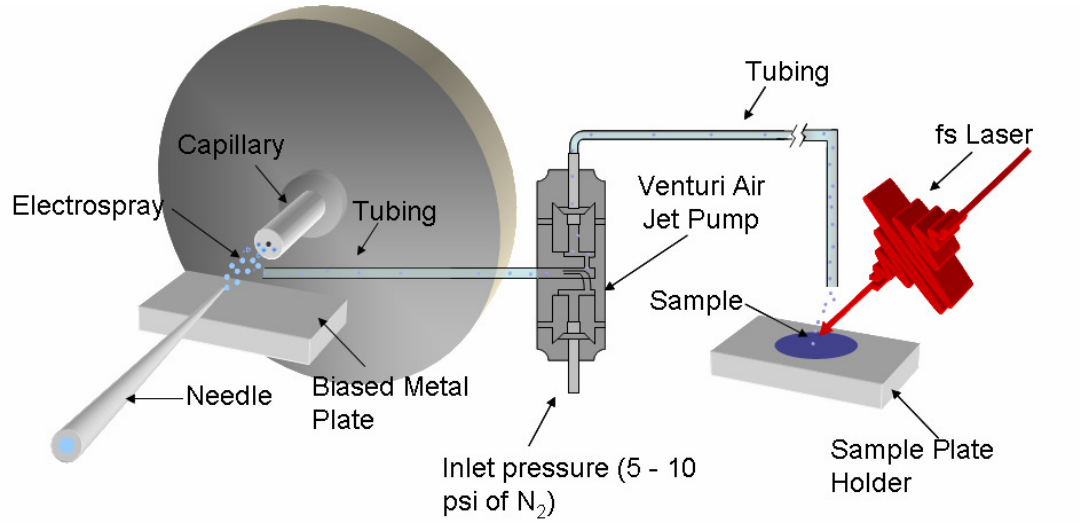

Figure 3.2. A schematic representation of the remote LEMS vaporization and ionization apparatus.

3.3.7 Safety considerations

Due to the nature of the explosive sample, small volumes were deposited onto the substrate and otherwise stored in dilute solutions. Appropriate laser eye protection was worn by all personnel and the high voltage area was enclosed in plexiglass to prevent accidental contact with the biased electrodes. An exposure control plan was approved by the University for the blood analysis under protocol number 13314 in accordance with the policy of the Department of Health and Human Services.

3.4 Results and discussion

3.4.1 Femtosecond laser vaporization of RDX

Explosives are highly unstable, fragile molecules. When a laser with a long pulse duration (*e.g.,* nanosecond) and high intensity (>10^8 W/cm^2) interacts with an explosive sample (solid or gas), fragmentation is observed (*30, 31*) yielding the elemental constituents (C, N, O and H). The high degree of dissociation typically yields no intact molecular ions that could be used for laser-based mass spectrometric identification due to the ladder switching mechanism that occurs during the time frame of the laser pulse. Therefore, soft techniques such as ESI (*4, 5*), MALDI (*32*) or desorption electrospray ionization (*33, 34*) have to be implemented to enable the detection of unfragmented explosive ions using mass spectrometry.

When a fs laser pulse at low pulse energy (<2 mJ/pulse) interacts with a film of explosive material, atomic emission lines from the elemental constituents are unable to be detected (*30, 35-37*). This suggests that a low energy fs laser does not induce fragmentation of the explosive material. Therefore, if the vaporized molecules were post-

ionized prior to mass analysis, intact, unfragmented ions should be observed. This was the case when RDX was vaporized from a metal substrate and post-ionized using an electrospray solvent composed of 7:3 (v:v) methanol:water solution with 0.5% sodium chloride and potassium chloride. The collected mass spectrum reveals the stable sodiated, $[M+Na]^+$, and potassiated, $[M+K]^+$, adducts of RDX at *m/z* 245 and 261, respectively (Figure 3.3). The peak at *m/z* 379 (marked with an asterix) is not observed in the solvent background spectrum and is consistent with a fragment of a dimer of RDX; however, the linear TOF employed in these measurements can not perform the MS^n technique needed to confirm the identity of the ion.

It is interesting to note that the addition of sodium and potassium to the electrospray solvent was required for detection of RDX. This is attributed to the formation of stable sodiated and potassiated adducts with the explosive molecule and has been observed with other mass analysis techniques (*33, 34, 38*). An acidified electrospray solvent resulted in no detectable protonated RDX ions. In addition, no detectable signal was observed in the mass spectrum without the electrospray solvent present. This suggests that the ionization mechanism occurs in the gas phase after interaction with the electrospray plume and is not a result of the vaporization process. The data alludes to the fact that neutral molecules are transferred into the gas phase allowing for their ionization using ESI. However, since sodium and potassium cations are common adduct ions observed in mass spectra resulting from the laser desorption of adsorbed molecules on metal substrates (*39*) additional experiments have to be performed to confirm whether the ionization is a result of ESI.

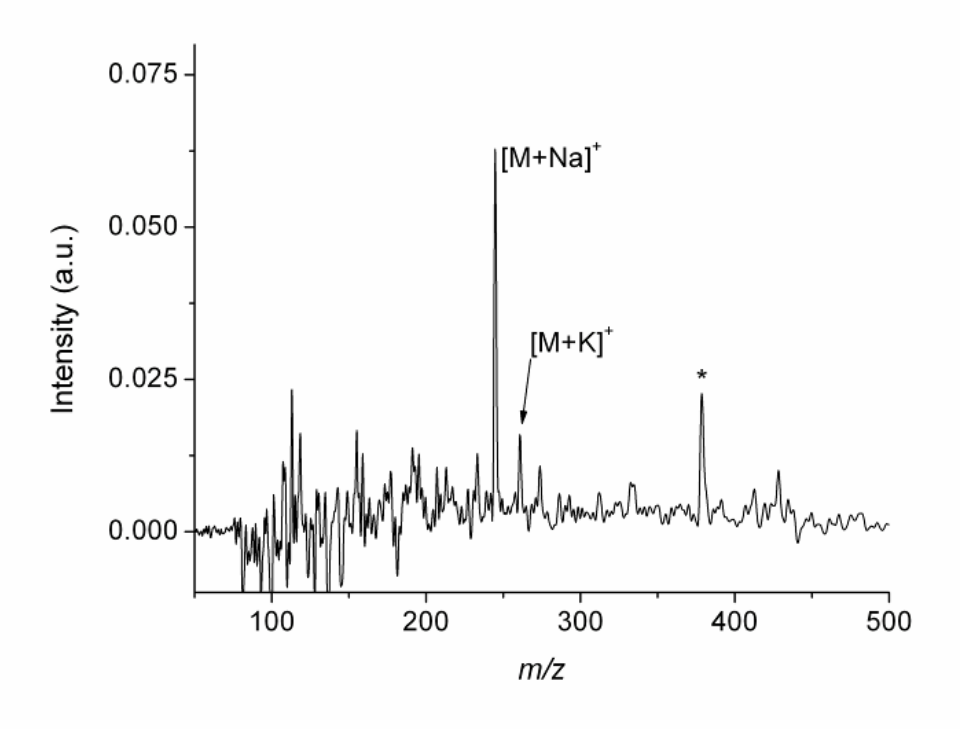

Figure 3.3. The LEMS mass spectrum resulting from the vaporization of RDX reveals the sodiated and potassiated adducts of RDX at *m/z* 245 and 261, respectively. The peak at *m/z* 379 (marked *) is not observed in the solvent background and is attributed to a fragment of a dimer of RDX.

Currently, most mass analysis instruments used to detect explosives can not investigate a surface directly at atmospheric pressure. Swabs are used in most solid probing methods to transfer materials from the surface to the analysis instrument (*40, 41*). Here, we demonstrated that LEMS allows for the direct investigation of an explosive contaminated solid surface without the need for wiping or an elution step. Detection of the sodiated and potassiated adduct ions of RDX reveals that intense, fs duration lasers can be used to transfer explosives from the condensed phase into the gas phase without *fragmentation* at atmospheric pressure. In addition, this demonstrates that a fs laser can increase the "vapor pressure" of the material by at least 8 orders of magnitude, possibly allowing for the detection via spectroscopic methods (*i.e.,* Raman spectroscopy) depending on the sensitivity of the spectroscopic technique and the quantity vaporized.

3.4.2 Femtosecond laser vaporization of an explosive propellant

The energetic ingredient in a formulation (containing plasticizers, stabilizers and/or binders) often has a lower vapor pressure than the energetic ingredient in its pure form. This makes gas phase sampling and detection methods more challenging and suggests that a direct probing of the solid phase is desirable as a detection strategy. To explore the direct analysis of an explosive in a formulation we investigate an RDX-based propellant using LEMS. Figure 3.4 shows the mass spectrum measured for a propellant composed of RDX, ethyl centralite ($C_{17}H_{20}N_2O$, a stabilizer) and nitrocellulose directly subjected to vaporization by the fs laser pulse. The sodiated and potassiated adduct ions of RDX, $[M+Na]^+$ and $[M+K]^+$, are detected at *m/z* 245 and 261, respectively. An RDX

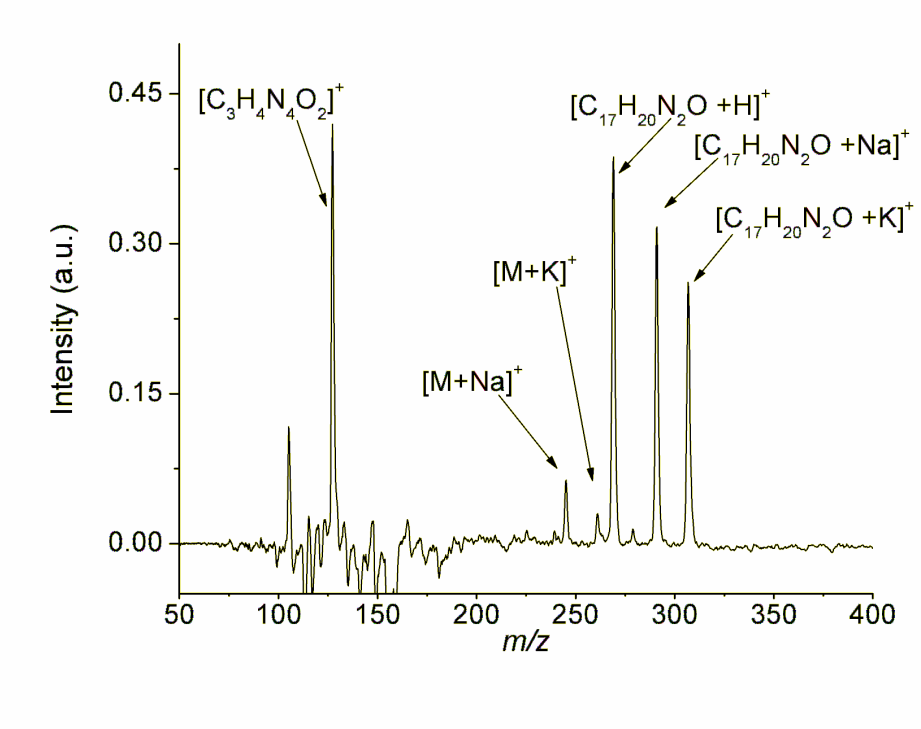

Figure 3.4. The background subtracted LEMS mass spectrum resulting from analysis of an RDX formulation containing RDX, plastizers and binders. The complexes of sodiated and potassiated adducts of RDX are both seen in the spectrum at *m/z* 245 and 261, respectively. The most intense peaks are the protonated, sodiated and potassiated adducts of ethyl centralite at *m/z* 269, 291 and 307, respectively. An RDX fragment is detected at *m/z* 128.

fragment, [$C_3H_4N_4O_2^+$], is also observed, at *m/z* 128 (*42*). There are a series of ion peaks that are detected at *m/z* 269, 291 and 307 that correspond to the protonated, sodiated and potassiated adducts of ethyl centralite, respectively. The difference in the signal intensity between the RDX adducts and the ethyl centralite adducts suggests that the explosive material does not have a high probability to form positive ions during the electrospray ionization process. The nitrocellulose contained in the propellant was not observed when the 7:3 (v:v) methanol:water solution containing 0.5% sodium chloride and potassium chloride was used as the electrospray solvent. Using the acidified solvent (7:3 (v:v) methanol:water with 1% acetic acid), no ions attributed to RDX were detected. The observation of the protonated, sodiated and potassiated adducts of ethyl centralite (in a similar ratio to that of Figure 3.4) was independent of the solvent system used.

3.4.3 Femtosecond laser vaporization of HMTD

Detection of fragile peroxide explosives is becoming increasingly important due to the relative ease with which these can be synthesized from common chemicals. When mass spectral methods are used for such peroxides, extensive fragmentation typically occurs (*43*). The ability to detect the $[M+H]^+$, $[M+Na]^+$ or $[M+K]^+$ ions is important for reducing false positive and false negative alarm rates. Thus, we investigated the analysis of a peroxide-based explosive, HMTD, using the LEMS method. The mass spectrum measured from a 50 μL aliquot of 10^{-4} M HMTD deposited onto a steel substrate is shown in Figure 3.5 using 7:3 (v:v) methanol:water solution containing 0.5% sodium chloride and potassium chloride as the electrospray solvent. The sodiated and potassiated ions of HMTD, $[M+Na]^+$ and $[M+K]^+$, are observed along with several fragment peaks. The peaks at *m/z* 229 ($[M-2H+Na]^+$) and *m/z* 245 ($[M-2H+K]^+$) suggest the loss of two

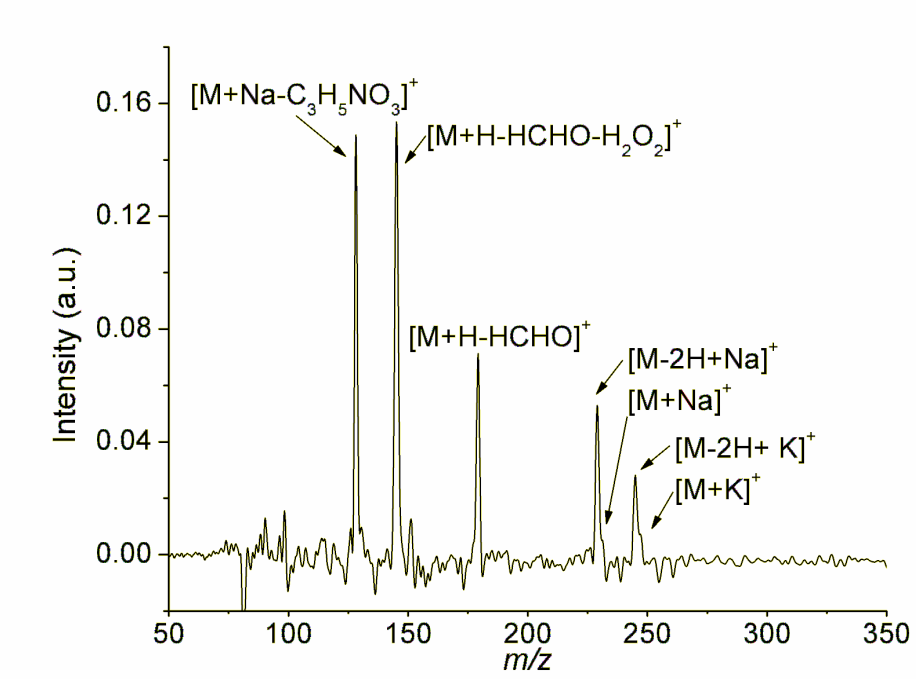

Figure 3.5. The background subtracted LEMS mass spectrum resulting from analysis of a 50 µL aliquot of 10^{-4} M HMTD dried on a metal surface.

hydrogen atoms during the vaporization/ionization process. The fragment peak at *m/z* 128 is consistent with the HMTD fragment $[M+Na-C_3H_7NO_3]^+$ while the peaks at *m/z* 145 and 179 are consistent with literature values for the HMTD fragments $[M+H-HCHO-H_2O_2]^+$ and $[M+H-HCHO]^+$, respectively (*33*). While there is more fragmentation observed in the mass spectrum of HMTD in comparison to RDX, the detection of the sodiated and potassiated adducts of HMTD using LEMS suggests that a fs laser is capable of transferring this rather fragile molecule into the gas phase without fragmentation for subsequent mass spectral analysis.

3.4.4 Remote detection of explosives

Remote sampling of explosives would decrease the risk to the operator performing the analysis and would facilitate detection, particularly in the field. To determine if LEMS was capable of remote sampling, 5.55 μg/cm^2 of RDX was applied to a metal slide. The sample was vaporized and transferred via 1.5 m of tubing to a Venturi air jet pump. Venturi air jet pumps include a constriction in a section of tubing and according to the Bernoulli's principle, a change in fluid pressure due to the constriction creates a vacuum which allows for the transfer of sample from the vaporization region to the ionization region. A vacuum of about 14 mm Hg is formed by the air jet pump when an inlet pressure of 5 – 10 mm Hg of N_2 is used (*44, 45*).

The sample was then transferred to the ionization region from the Venturi air jet pump via a 0.5 m length of tubing, for a total of 2 m. The resulting mass spectrum from the remote fs laser vaporization, transfer and ionization of RDX is shown in Figure 3.6. The sodiated and potassiated adducts of RDX are detected in the mass spectrum at *m/z* 245 and 261, respectively. Detection of the sodiated and potassiated adduct ions of

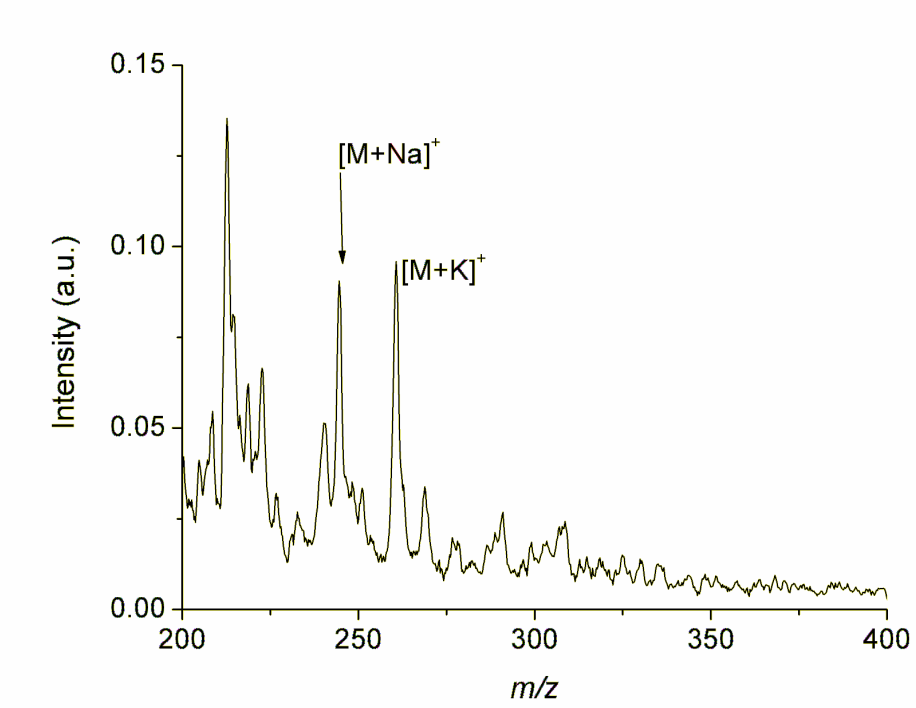

Figure 3.6. The LEMS mass spectrum resulting from the remote analysis of RDX dried on a metal surface at a coverage of 5.55 μg/cm^2. The complexes of sodiated and potassiated adducts of RDX are detected in the spectrum at *m/z* 245 and 261, respectively.

RDX reveals that intense, fs duration lasers can be used to transfer explosives remotely from one region to another. When only the fs laser was present no ions were observed in the acquired spectrum suggesting that the electrospray plume is responsible for the ionization of the explosive and is not due to the vaporization process. The spatial decoupling of the two processes, vaporization and ionization, provides further evidence that the fs laser results in vaporization of neutrals which are post-ionized in the electrospray plume.

3.4.5 Femtosecond laser vaporization of amphiphilic molecules

Amphiphilic molecules, such as lipids, are the main components in biological membranes. Lipids, when placed into aqueous solution, are capable of forming bilayers and can be used to create model membrane systems. The saturated phosphocholine lipid, DHPC, was analyzed to investigate the fs laser vaporization of precursor molecules to such model membrane systems and to offer more insight into the effect of molecular size on the vaporization mechanism. A 30 μL aliquot of the 1 x 10^{-4} M solution was spotted and dried on a metal slide. The molecular structure of DHPC is shown in the inset of Figure 3.7 and contains a C6:0 saturated diglyceride on the hydrophobic end and a phosphate and a choline group on the hydrophilic end. The mass spectrum for DHPC vaporized from stainless steel, shown in Figure 3.7, reveals the $[M+H]^+$ and $[M+Na]^+$ adduct ions at *m/z* 454 and 476, respectively, when using an electrospray solution composed of 1:1 (v:v) methanol:water with 1.0% acetic acid. A low abundance peak observed at *m/z* 907 is consistent with the formation of the dimer ion, $[2M+H]^+$ and is most likely due to dipolar interactions from the polar head groups on the lipid molecules

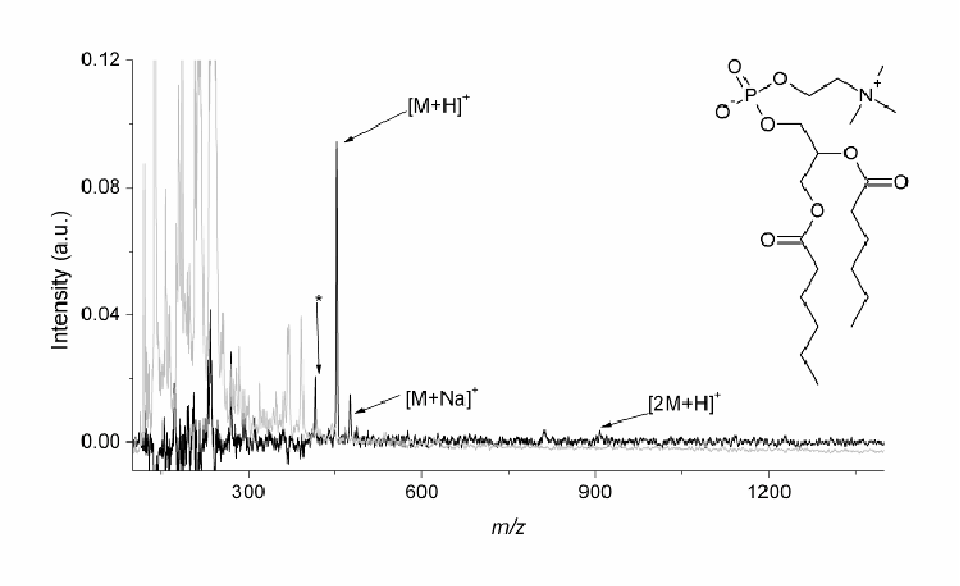

Figure 3.7. The background subtracted LEMS mass spectrum of DHPC vaporized and post-ionized in the electrospray plume. The gray line represents the solvent background measured just prior to laser vaporization and the black line represents the background subtracted LEMS mass spectrum of DHPC. The asterisk indicates the ion $[M\text{-}N(CH_3)_3\text{+}Na]^+$ for DHPC. All unlabeled peaks are solvent related.

and van der Waals interactions between the nonpolar hydrocarbon tails.

A lower abundance fragment of DHPC, consistent with the formation of the ion $[M\text{-}N(CH_3)_3+Na]^+$, was also observed at *m/z* 417 (indicated with a asterisk (*) in Figure 3.7). This fragment ions were not observed in control ESI-mass spectra of the lipids and are presumed to be the result of the vaporization/ionization process. Both the laser vaporization and dissociation processes are nonlinear and depend on the laser intensity. Thus, the vaporization of dimer molecules does not preclude minor dissociation pathways and vice versa. We conclude that fs laser vaporization of lipids containing phosphate and choline functional groups is possible while preserving non-covalent interactions. Therefore, fs laser vaporization and electrospray post-ionization allows for the mass analysis of a wide range of molecules with varying polarities and sizes.

3.4.6 Femtosecond laser vaporization of complex biological mixtures

3.4.6.1 Analysis of a complex biological fluid: Human blood

Matrix free laser desorption mass analysis of large biological molecules has been limited (*39*) due to the high degree of fragmentation that is associated with the lasers having a long pulse duration (*19*). This typically restricts desorption and analysis of molecules with mass < 1,500 Da (*39*). Analysis of larger compounds has been enabled but requires the addition of a matrix and therefore increases the required sample preparation. The use of ultrashort laser pulses may enable vaporization of intact large biomolecules since the coupling mechanisms are different. To explore this idea, lipids and proteins in complex mixtures were investigated to further determine the ability to vaporize larger macromolecules in LEMS without fragmentation. The complex mixture of lipids and proteins was prepared by placing a 20 μL aliquot of undiluted whole blood,

spiked with 2 μL of 10^{-3} M DHPC, onto a stainless steel sample slide. Lipids are typically solubilized in blood by lipoproteins, however in this experiment no proteins were added to the mixture. The vaporization of the lipid in the presence of hemoglobin allows for the simultaneous detection of both small and large biomolecules. The LEMS mass spectrum of whole blood spiked with DHPC in an approximate 1:1 molar ratio of DHPC to hemoglobin, shown in Figure 3.8, reveals the $[M+H]^+$ and $[M+Na]^+$ ions of DHPC. The signal intensities of the $[M+H]^+$ and $[M+Na]^+$ ions of DHPC are lower than expected based on similar amounts of sample deposited in control experiments. This is most likely due to ion suppression from the proteins (*e.g.,* human serum albumen), carbohydrates, minerals, hormones, platelets, etc. dissolved in blood. Such ion suppression effects are common when performing electrospray post-ionization and have been observed in literature (*46-48*).

Matrix-free ns laser-based desorption techniques are commonly limited to the analysis of molecules with low molecular weights (~1,500 Da) (*39*) due to the high degree of fragmentation from thermal mechanisms. However, no fragments were observed in the mass spectrum when fs lasers are used induce transfer of large molecules, such as hemoglobin, into the gas phase. Instead, ions corresponding to the multiply charged α and β subunits along with the heme B group of hemoglobin were detected and are consistent with previous conventional ESI-MS investigations (*49*). A previous investigation using laser-based desorption has also observed the α and β hemoglobin subunits from dried human blood (*50*) and the charge states measured are lower than those reported here. The difference in the observed charge states is most likely due to two

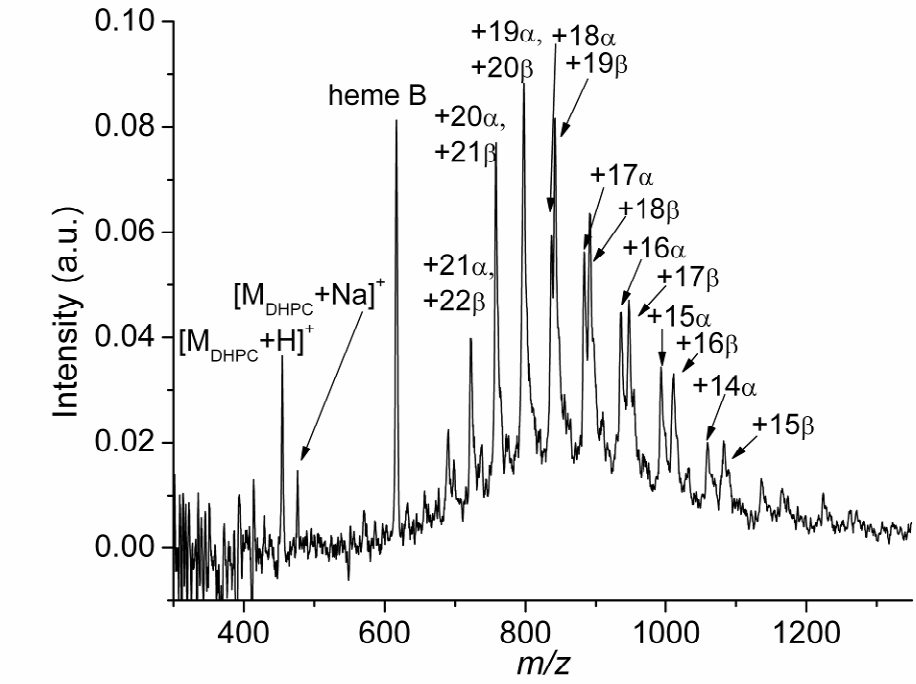

Figure 3.8. The background subtracted LEMS mass spectrum of laser vaporized human blood spiked with DHPC. The $[M+H]^+$ and $[M+Na]^+$ ions of DHPC can be observed along with the multiply charged α and β hemoglobin subunits and the heme B group of blood.

factors. The first is due to a higher concentration of acetic acid in the ESI solvent. This leads to lower pH and thus induces denaturation of the captured protein more readily than a solvent system containing 0.1% acetic acid. The second is the presence of methanol in the sample, due to the addition of DHPC, which can also cause denaturation and shifting of the charge states (*51*) to lower *m/z*. Nevertheless, the fs laser vaporization of blood demonstrates that the molecular size limit of ~1,500 Da does not apply when using fs laser pulses to transfer matrix-free molecules into the gas phase since intact α and β subunits are observed in the mass spectrum. It should be noted that whole blood does not act as a self matrix as there is no first order resonant absorption by whole blood at 800 nm (Figure 3.9). Another interesting observation is that the analysis of the blood/lipid mixture was performed while the sample was still in the aqueous state. Samples in the hydrated (aqueous) state form intrinsically homogeneous samples and therefore, dry drop methods or electrospray deposition are no longer necessary to produce samples with high reproducibility.

The investigation of whole human blood also allows for a clearer understanding of the ionization mechanism for which there are two main possibilities: photo-ionization or ESI. Laser ionization could lead to high charge states being formed in the protein after multiple ionization events. The highly charged protein would be left in an excited state due to the ladder climbing of excited electronic states. If this excited state is repulsive or is coupled to a repulsive state, the protein ion would likely fragment prior to mass analysis. This is shown when the polypeptide gramicidin D in the gas phase, under vacuum conditions, undergoes fragmentation after irradiation by a 10^{11} W/cm^2 fs laser pulse (*18*). However, if neutral, unfragmented molecules are vaporized by the fs laser

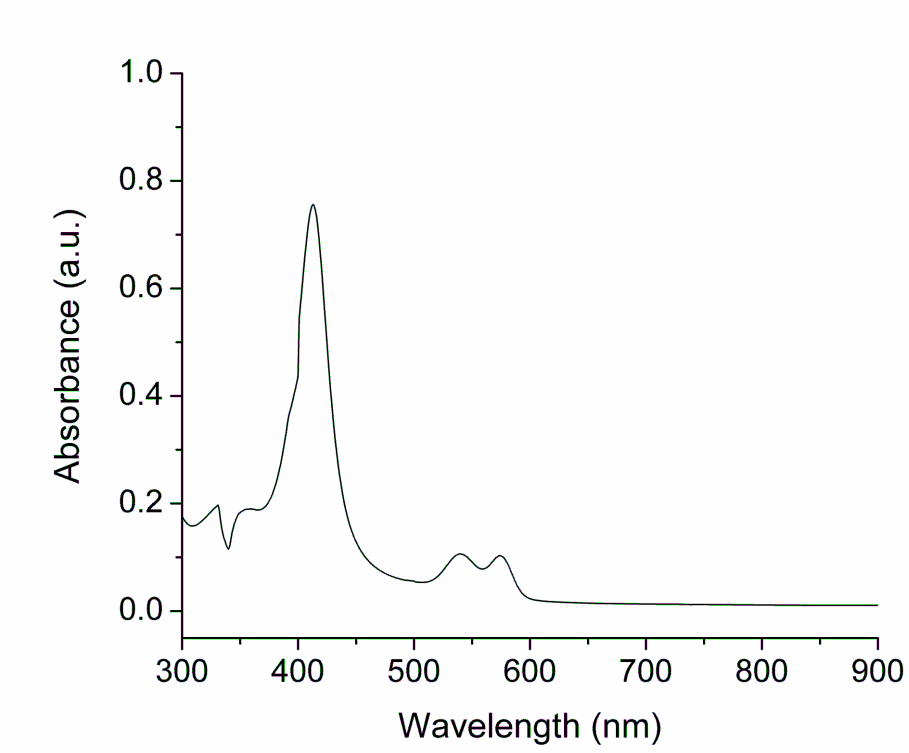

Figure 3.9. UV/VIS of absorption spectrum of whole blood.

pulse and captured by the electrospray plume, ionization can proceed via ESI. Electrospray ionization is known to produce highly charged, unfragmented ions which can be observed using mass spectrometry (*2*). To determine the predominant ionization mechanism, laser vaporization of aqueous protein was performed in the absence of the electrospray solvent. Upon irradiation of the blood sample, no signal in the mass spectrometer was observed demonstrating that the laser pulse does not result in any significant ionization. In addition, no ESI type processes (*52*) (*i.e.*, charging of the vaporized blood in the presence of the electric field) were occurring on the laser-vaporized blood sample, as seen in liquid samples subjected to atmospheric ns MALDI. This proves that the fs laser results in the formation of neutral molecules/clusters which are ejected perpendicular to the electrospray plume. The electrospray plume captures the vaporized protein and the lipid in the gas phase; solvating and ionizing the molecules via adduct formation. The successful detection of DHPC and the α and β hemoglobin subunits from undiluted whole blood suggests that other complex mixtures can be analyzed.

3.4.6.2 Analysis of a complex biological fluid: Milk

A complex biological fluid will contain a variety of polar, nonpolar and amphiphilic compounds. Milk, an example of a complex biological fluid, is mostly composed of water but contains approximately 5% carbohydrates, 3% fat/lipid, 3% protein and 1% vitamins and minerals by weight. The LEMS measurement for reduced fat milk vaporized from a welled sample plate is shown in Figure 3.10. While there are a large number of distinguishing peaks detected in the milk spectrum, only 16 peaks will be discussed here. Lactose is one of the major substituents of milk composing of ~5% (w/v).

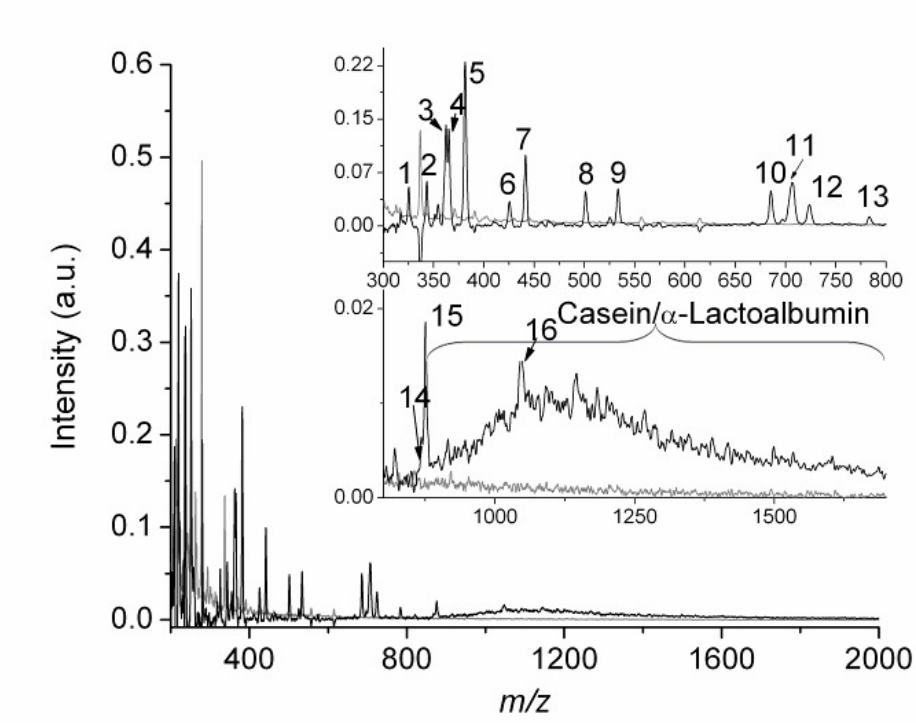

Figure 3.10. Peaks from lactose (1, 2, 4, 5, 10, 11 and 12), lipids (9, 13, 14, 15 and 16) and proteins γ-casein and α-lactoalbumin can be observed in the obtained background subtracted LEMS mass spectrum (black line) from reduced fat milk at low resolution in the high *m/z* region. The gray line represents the solvent background mass spectrum measured just prior to laser vaporization of the milk sample.

The peaks labeled 1, 2, 4, 5, 10, 11 and 12 correspond to the lactose (mass = 342 Da) ions $[M-H_2O+H]^+$, $[M+H]^+$, $[M+Na]^+$, $[M+K]^+$, $[2M+H]^+$, $[2M+Na]^+$ and $[2M+K]^+$, respectively, and are in agreement with previously reported mass spectral measurements (*53, 54*). There is a broad bell-shaped distribution ranging in *m/z* from 850 to 1750 in the milk mass spectrum. This distribution is consistent with the multiple charge states of the proteins γ-casein (mass = 24,010 Da) and α-lactoalbumin (mass = 14,175 Da) and were also observed by other groups that analyzed milk samples using laser-based methods (*46, 55, 56*). In the acquired mass spectrum (Figure 3.10), the instrument parameters were adjusted to provide a mass spectrum with the highest resolution in the lower *m/z* region. When the instrument parameters were tuned for high resolution in the higher *m/z* region, the peaks for γ-casein and α-lactoalbumin were better resolved (Figure 3.11). Previous investigations performing ns laser-based mass spectrometry on dried whole milk (*46, 57*) revealed only singly charged ion peaks at *m/z* 534, 705, 724, 868, 875, 1046 and 1065. The peaks at *m/z* 705 and 724 are consistent with the $[2M+Na]^+$ and $[2M+K]^+$ ions of lactose. However, due to the lack of MS^n analysis in the previous references and in our instrument, the identities of the other peaks could not be determined. The lack of protein peaks in the mass spectrum resulting from the ns laser-based desorption of whole milk was attributed to ion suppression since the lipid content of whole milk is 100 times higher than in reduced fat milk. When reduced fat milk was analyzed using ns laser-based techniques (*46*), the singly charged ions along with the charge state distributions for γ-casein and α-lactoalbumin were observed since the ion suppression effects were lower. Therefore, the singly charged peaks (at *m/z* 534, 868, 875, 1046 and 1065) were attributed by the authors to singly charged lipid ions found in milk. The peaks at *m/z* 534,

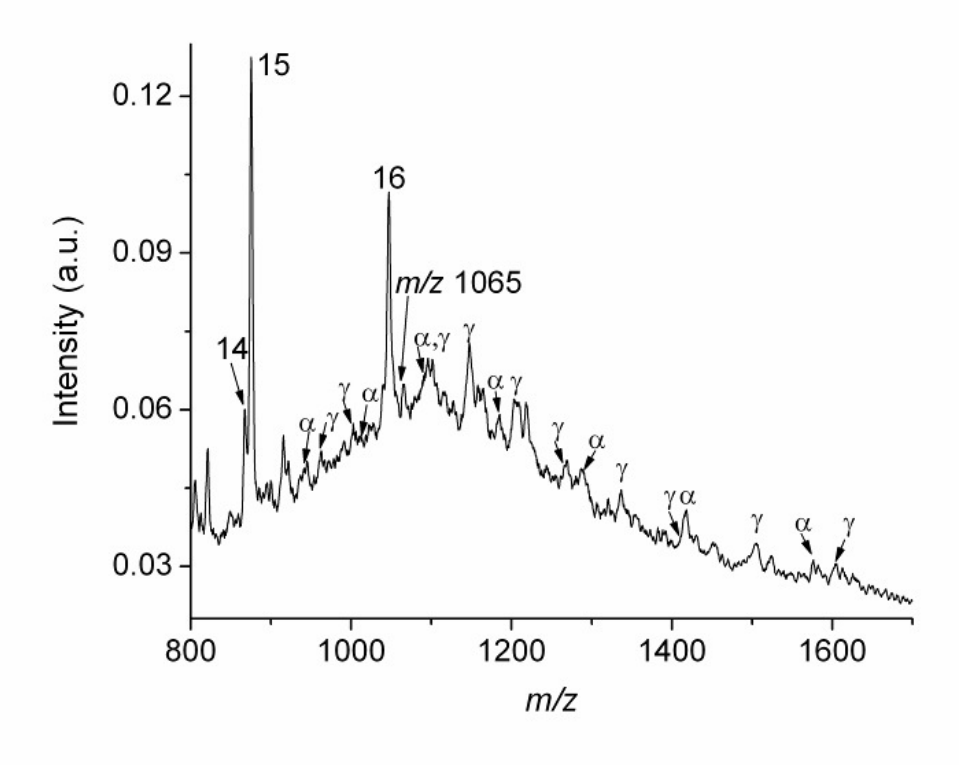

Figure 3.11. Peaks from lipids (14, 15 and 16) and proteins γ-casein and α-lactoalbumin can be observed in the obtained background subtracted LEMS mass spectrum (black line) from reduced fat milk at high resolution in the high *m/z* region.

868, 875 and 1046, labeled 9, 14, 15 and 16, were also observed in the LEMS mass spectrum of reduced fat milk. The peak at *m/z* 1065 can be observed in the high resolution LEMS spectrum, Figure 3.11, but is difficult to resolve in low resolution mass spectrum (Figure 3.10).

Upon analysis of three different brands of reduced fat milk and whole milk (Figure 3.10 and 3.12, respectively), each of the peaks labeled 1-16 and the charge state distributions for γ-casein and α-lactoalbumin can be observed in the LEMS measurements. However, the peaks labeled 6, 7, 8 and 13 observed at *m/z* 426, 442, 501 and 783, respectively, in Figure 3.12 are only observed when fs laser pulses were used to induce vaporization and were not detected in the ns laser-based measurements (*46, 54-57*). Therefore, the peaks detected are not unique to the brand or fat content of milk analyzed but appear to be unique to the fs vaporization of milk. The observation of carbohydrates, proteins and lipids in milk, regardless of fat content, demonstrates that LEMS is capable of analyzing complex biological fluids. In addition, the appearance of new peaks using fs vaporization with electrospray post-ionization suggests that ion suppression effects are less likely to occur despite the high concentration of interferents dissolved in the milk sample. The reduction in the ion suppression may be due to the fs laser vaporizing more neutral molecules at atmospheric pressure than ns laser-based techniques.

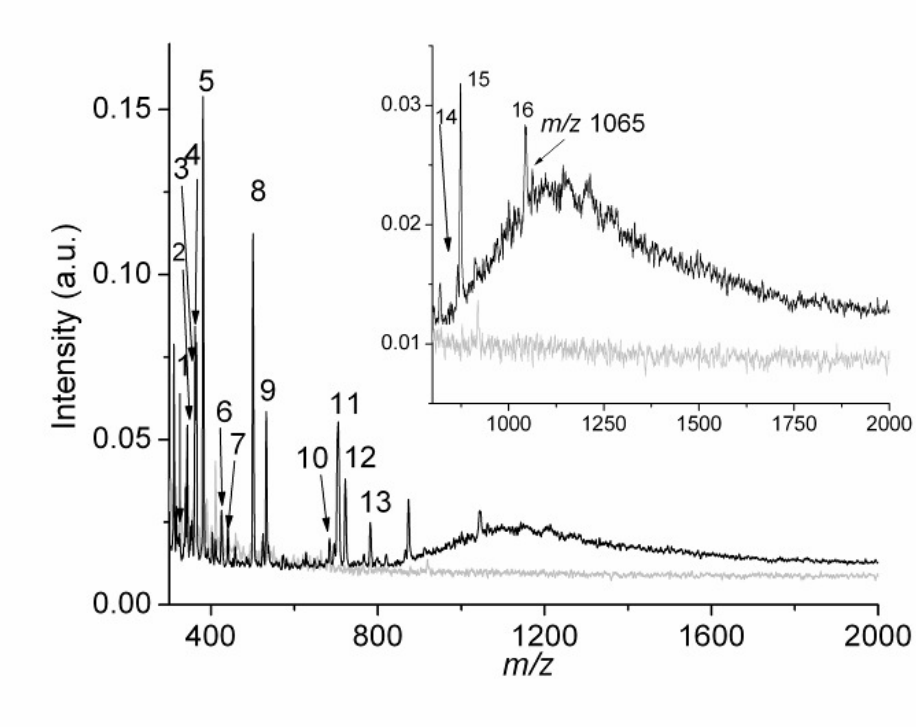

Figure 3.12. The LEMS mass spectrum acquired at low resolution in the high mass range for whole milk. The spectrum was acquired in this manner to demonstrate that each of the peaks labeled 1-16 and the charge state distributions for γ-casein and α-lactoalbumin can be observed in the LEMS measurements for milk, regardless of fat content.

3.5 Conclusions

The universal detection of materials is difficult due to the wide variety of chemical structures and the often exceedingly low vapor pressures. We demonstrate here that the combination of fs laser vaporization with electrospray post-ionization TOF mass spectrometry provides a new method to increase the vapor pressure of explosives, a lipid, biomolecules and proteins allowing for their detection. This method circumvents the challenge of detecting low vapor pressure molecules by inducing vaporization into the gas phase with ultrafast fs laser excitation. The fs laser has the capability to transfer small or large molecules, in the solid or liquid states independent of the molecules polarity, into the gas phase, suggesting that the laser must nonresonantly couple into the sample. The nonresonant coupling of the laser into the sample would allow for the mass analysis of any molecular system and would reduce the sample preparation requirements necessary with other resonant ns-laser based techniques. In addition, the fs laser pulse does not result in ionization of the molecules; instead, the molecules are ionized using electrospray ionization prior to TOF mass analysis. The use of an electrospray to post-ionize the vaporized molecules increases the ion abundance of the fs laser vaporization technique.

References

1. J. B. Fenn, M. Mann, C. K. Meng, S. F. Wong, C. M. Whitehouse, Electrospray ionization - principles and practice. *Mass Spectrom. Rev.* **9**, 37 (1990).
2. J. B. Fenn, M. Mann, C. K. Meng, S. F. Wong, C. M. Whitehouse, Electrospray ionization for mass-spectrometry of large biomolecules. *Science* **246**, 64 (1989).

3. J. V. Iribarne, B. A. Thomson, On the evaporation of small ions from charged droplets. *J. Chem. Phys.* **64**, 2287 (1976).

4. Y. Jehuda, E. M. Joseph, A. Y. Richard, Electrospray ionization tandem mass spectrometry collision-induced dissociation study of explosives in an ion trap mass spectrometer. *Rapid Commun. Mass Spectrom.* **11**, 1961 (1997).

5. Z. Wu, C. L. Hendrickson, R. P. Rodgers, A. G. Marshall, Composition of explosives by electrospray ionization Fourier transform ion cyclotron resonance mass spectrometry. *Anal. Chem.* **74**, 1879 (2002).

6. D. S. Moore, Instrumentation for trace detection of high explosives. *Rev. Sci. Instrum.* **75**, 2499 (2004).

7. T. P. Roddy, D. M. Cannon, C. A. Meserole, N. Winograd, A. G. Ewing, Imaging of freeze-fractured cells with *in situ* fluorescence and time-of-flight secondary ion mass spectrometry. *Anal. Chem.* **74**, 4011 (2002).

8. P. J. Todd, T. G. Schaaff, P. Chaurand, R. M. Caprioli, Organic ion imaging of biological tissue with secondary ion mass spectrometry and matrix-assisted laser desorption/ionization. *J. Mass Spectrom.* **36**, 355 (2001).

9. J. Cheng, N. Winograd, Depth profiling of peptide films with TOF-SIMS and a C-60 probe. *Anal. Chem.* **77**, 3651 (2005).

10. T. P. Roddy, D. M. Cannon, S. G. Ostrowski, A. G. Ewing, N. Winograd, Proton transfer in time-of-flight secondary ion mass spectrometry studies of frozen-hydrated dipalmitoylphosphatidylcholine. *Anal. Chem.* **75**, 4087 (2003).

11. S. G. Ostrowski, C. T. Van Bell, N. Winograd, A. G. Ewing, Mass spectrometric imaging of highly curved membranes during *Tetrahymena* mating. *Science* **305**, 71 (2004).

12. F. Hillenkamp, M. Karas, R. C. Beavis, B. T. Chait, Matrix-assisted laser desorption ionization mass-spectrometry of biopolymers. *Anal. Chem.* **63**, A1193 (1991).

13. E. Nordhoff *et al.*, Matrix-assisted laser desorption ionization mass-spectrometry of nucleic-acids with wavelengths in the ultraviolet and infrared. *Rapid Commun. Mass Spectrom.* **6**, 771 (1992).

14. L. Li, A. P. L. Wang, L. D. Coulson, Continuous-flow matrix-assisted laser desorption ionization mass-spectrometry. *Anal. Chem.* **65**, 493 (1993).

15. P. V. Tan, V. V. Laiko, V. M. Doroshenko, Atmospheric pressure MALDI with pulsed dynamic focusing for high-efficiency transmission of ions into a mass spectrometer. *Anal. Chem.* **76**, 2462 (2004).

16. S. G. Moyer, R. J. Cotter, Atmospheric pressure MALDI. *Anal. Chem.* **74**, 468A (2002).

17. R. Knochenmuss, Ion formation mechanisms in UV-MALDI. *Analyst* **131**, 966 (2006).

18. R. Weinkauf, P. Aicher, G. Wesley, J. Grotemeyer, E. W. Schlag, Femtosecond versus nanosecond multiphoton ionization and dissociation of large molecules. *J.Phys. Chem.* **98**, 8381 (1994).

19. K. W. D. Ledingham *et al.*, Multiply charged ions from aromatic molecules following irradiation in intense laser fields. *J. Phys. Chem. A* **103**, 2952 (1999).

20. J. J. Yang, D. A. Gobeli, M. A. El-Sayed, Change in the mechanism of laser multiphoton ionization-dissociation in benzaldehyde by changing the laser pulse width. *J. Phys. Chem.* **89**, 3426 (1985).

21. P. Demirev *et al.*, Matrix-assisted laser desorption with ultra-short laser pulses. *Rapid Commun. Mass Spectrom.* **6**, 187 (1992).

22. J. M. Wichmann, C. Lupulescu, L. Wöste, A. Lindinger, Matrix-assisted laser desorption/ionization by using femtosecond laser pulses in the near-infrared wavelength regime. *Rapid Commun. Mass Spectrom.* **23**, 1105 (2009).

23. R. B. Van Breemen, M. Snow, R. J. Cotter, Time resolved laser desorption mass spectrometry, I. Desorption of preformed ions. *Int. J. Mass Spectrom. Ion Processes* **49**, 35 (1983).

24. J. J. Coon, K. J. McHale, W. W. Harrison, Atmospheric pressure laser desorption/chemical ionization mass spectrometry: A new ionization method based on existing themes. *Rapid Commun. Mass Spectrom.* **16**, 681 (2002).

25. J. J. Coon, W. W. Harrison, Laser desorption-atmospheric pressure chemical ionization mass spectrometry for the analysis of peptides from aqueous solutions. *Anal. Chem.* **74**, 5600 (2002).

26. A. Leisner, A. Rohlfing, S. Berkenkamp, F. Hillenkamp, K. Dreisewerd, Infrared laser post-ionization of large biomolecules from an IR-MALD(I) plume. *J. Am. Soc. Mass Spectrom.* **15**, 934 (2004).

27. J. Shiea *et al.*, Electrospray-assisted laser desorption/ionization mass spectrometry for direct ambient analysis of solids. *Rapid Commun. Mass Spectrom.* **19**, 3701 (2005).

28. J. S. Sampson, A. M. Hawkridge, D. C. Muddiman, Generation and detection of multiply-charged peptides and proteins by matrix-assisted laser desorption electrospray ionization (MALDESI) Fourier transform ion cyclotron resonance mass spectrometry. *J. Am. Soc. Mass Spectrom.* **17**, 1712 (2006).

29. P. Nemes, A. Vertes, Laser ablation electrospray ionization for atmospheric pressure, *in vivo*, and imaging mass spectrometry. *Anal. Chem.* **79**, 8098 (2007).

30. Y. Dikmelik, C. McEnnis, J. B. Spicer, Femtosecond and nanosecond laser-induced breakdown spectroscopy of trinitrotoluene. *Opt. Express* **16**, 5332 (2008).

31. C. Mullen, D. Huestis, M. Coggiola, H. Oser, Laser photoionization of triacetone triperoxide (TATP) by femtosecond and nanosecond laser pulses. *Int. J. Mass Spectrom.* **252**, 69 (2006).

32. M. Zhang *et al.*, Using molecular recognition of β cyclodextrin to determine molecular weights of low-molecular-weight explosives by MALDI-TOF mass spectrometry. *J. Am. Soc. Mass Spectrom.* **17**, 189 (2006).

33. I. Cotte-Rodriguez, H. Hernandez-Soto, H. Chen, R. G. Cooks, *In situ* trace detection of peroxide explosives by desorption electrospray ionization and desorption atmospheric pressure chemical ionization. *Anal. Chem.* **80**, 1512 (2008).

34. I. Cotte-Rodriguez, Z. Takats, N. Talaty, H. Chen, R. G. Cooks, Desorption electrospray ionization of explosives on surfaces: Sensitivity and selectivity enhancement by reactive desorption electrospray ionization. *Anal. Chem.* **77**, 6755 (2005).

35. B. S. James, M. Caroline, in *Laser Applications to Chemical, Security and Environmental Analysis*. (Optical Society of America, 2008), pp. LThC2.

36. E. J. Judge, Ph.D Thesis, Temple University (2011).

37. J. L. Gottfried, F. C. De Lucia, C. A. Munson, A. W. Miziolek, Laser-induced breakdown spectroscopy for detection of explosives residues: A review of recent advances, challenges, and future prospects. *Anal. Bioanal. Chem.* **395**, 283 (2009).

38. G. Alexei, S. Michael, Y. Jehuda, Liquid chromatography/mass spectrometric analysis of explosives: RDX adduct ions. *Rapid Commun. Mass Spectrom.* **17**, 943 (2003).

39. M. A. Posthumus, P. G. Kistemaker, H. L. C. Meuzelaar, M. C. Ten Noever de Brauw, Laser desorption-mass spectrometry of polar nonvolatile bio-organic molecules. *Anal. Chem.* **50**, 985 (1978).

40. M. E. Sigman, C.-Y. Ma, In-injection port thermal desorption for explosives trace evidence analysis. *Anal. Chem.* **71**, 4119 (1999).

41. R. Waddell, D. E. Dale, M. Monagle, S. A. Smith, Determination of nitroaromatic and nitramine explosives from a PTFE wipe using thermal desorption-gas chromatography with electron-capture detection. *J. Chromatogr. A* **1062**, 125 (2005).

42. J. Yinon, D. J. Harvan, J. R. Hass, Mass spectral fragmentation pathways in RDX and HMX. A mass analyzed ion kinetic energy spectrometric/collisional induced dissociation study. *Org. Mass Spectrom.* **17**, 321 (1982).

43. E. S. Michael, C. D. Clark, F. Rebecca, L. G. Cherie, A. C. Christian, Analysis of triacetone triperoxide by gas chromatography/mass spectrometry and gas chromatography/tandem mass spectrometry by electron and chemical ionization. *Rapid Commun. Mass Spectrom.* **20**, 2851 (2006).

44. R. B. Dixon, J. S. Sampson, A. M. Hawkridge, D. C. Muddiman, Ambient aerodynamic ionization source for remote analyte sampling and mass spectrometric analysis. *Anal. Chem.* **80**, 5266 (2008).

45. R. B. Dixon, M. S. Bereman, D. C. Muddiman, A. M. Hawkridge, Remote mass spectrometric sampling of electrospray- and desorption electrospray-generated ions using an air ejector. *J. Am. Soc. Mass Spectrom.* **18**, 1844 (2007).

46. M. Z. Huang *et al.*, Characterization of the chemical components on the surface of different solids with electrospray-assisted laser desorption ionization mass spectrometry. *Rapid Commun. Mass Spectrom.* **21**, 1767 (2007).

47. S. Y. Lin, M. Z. Huang, H. C. Chang, J. Shiea, Using electrospray-assisted laser desorption/ionization mass spectrometry to characterize organic compounds separated on thin-layer chromatography plates. *Anal. Chem.* **79**, 8789 (2007).

48. Y. S. Shin, B. Drolet, R. Mayer, K. Dolence, F. Basile, Desorption electrospray ionization-mass spectrometry of proteins. *Anal. Chem.* **79**, 3514 (2007).

49. C. H. L. Shackleton, A. M. Falick, B. N. Green, H. E. Witkowska, Electrospray mass spectrometry in the clinical diagnosis of variant hemoglobins. *J. Chromatogr. B* **562**, 175 (1991).

50. M. Z. Huang, H. J. Hsu, L. Y. Lee, J. Y. Jeng, L. T. Shiea, Direct protein detection from biological media through electrospray-assisted laser desorption ionization/mass spectrometry. *J. Proteome Res.* **5**, 1107 (2006).

51. L. Konermann, D. J. Douglas, Acid-induced unfolding of cytochrome C at different methanol concentrations: Electrospray ionization mass spectrometry specifically monitors changes in the tertiary structure. *Biochemistry* **36**, 12296 (1997).

52. J. S. Sampson, A. M. Hawkridge, D. C. Muddiman, Development and characterization of an ionization technique for analysis of biological macromolecules: Liquid matrix-assisted laser desorption electrospray ionization. *Anal. Chem.* **80**, 6773 (2008).

53. L. Zhu, G. Gamez, H. Chen, K. Chingin, R. Zenobi, Rapid detection of melamine in untreated milk and wheat gluten by ultrasound-assisted extractive electrospray ionization mass spectrometry (EESI-MS) *Chem. Commun.*, 559 (2009).

54. J. S. Sampson, K. K. Murray, D. C. Muddiman, Intact and top-down characterization of biomolecules and direct analysis using infrared matrix-assisted laser desorption electrospray ionization coupled to FT-ICR mass spectrometry. *J. Am. Soc. Mass Spectrom.* **20**, 667 (2009).

55. J. Shiea *et al.*, Detection of native protein ions in aqueous solution under ambient conditions by electrospray laser desorption/ionization mass spectrometry. *Anal. Chem.* **80**, 4845 (2008).

56. S.-C. Cheng, T.-L. Cheng, H.-C. Chang, J. Shiea, Using laser-induced acoustic desorption/electrospray ionization mass spectrometry to characterize small

organic and large biological compounds in the solid state and in solution under ambient conditions. *Anal. Chem.* **81**, 868 (2009).

57. L. Jia, Q. Bo, L. Hai, Fingerprinting of yogurt products by laser desorption spray post-ionization mass spectrometry. *Rapid Commun. Mass Spectrom.* **24**, 1365 (2010).

CHAPTER 4

INSIGHT INTO THE VAPORIZATION MECHANISM IN LASER ELECTROSPRAY MASS SPECTROMETRY

4.1 Overview

It was previously shown that femtosecond laser pulses can be used to transfer neutral molecules into the gas phase as indicated by the obtained electrospray post-ionization mass spectra. Due to the wide range of polarities and size of molecules vaporized, it was suggested that the fs laser pulse must nonresonantly couple into the adsorbed molecule. In this chapter, nanosecond and femtosecond laser pulses are used to transfer rhodamine 6G, in the presence of matrix, into the gas phase. The measurements made using these two different pulse durations demonstrates that more neutral molecules are vaporized using fs laser pulses. Using this knowledge, the fs laser pulses were then used to induce vaporization of an amphiphilic lipid and hydrophobic proteins. The collected data indicates that the molecules are transferred into the gas phase via a nonthermal mechanism. Finally, the successful vaporization of dried lysozyme without matrix from various substrates suggests that the vaporization process proceeds via a molecule-molecule repulsion.

4.2 Introduction

The detection of large, non-volatile molecules with minimal sample preparation is important for biochemistry assays and forensic investigations. Two common soft vaporization/ionization techniques for analyzing large non-volatile molecules are

electrospray ionization (ESI) (*1, 2*) and matrix-assisted laser desorption ionization (MALDI) (*3, 4*). In ESI, a solution containing the analyte of interest is passed through a needle in the presence of an electric field inducing the formation of charged droplets. The analyte is transferred into the gas phase from the charged droplet via evaporation and desorption mechanisms allowing for mass analysis. Electrospray ionization has allowed for the mass analysis of a variety of analytes, such as lipid hydroperoxides (*5*) and proteins (*2*), but is limited in that only solution phase samples can be analyzed. Matrix-assisted laser desorption ionization mass spectrometry typically uses a nanosecond (ns) laser to excite a matrix, co-crystallized with the analyte, to a low lying state via a first order resonant absorption (*6*). A resonant absorption occurs when the spacing between energy levels is equal to the energy of one photon, $h\nu$, where h is Planck's constant and ν is the frequency of the photon (*7, 8*). For resonant absorption processes, the absorption cross section of the matrix increases approximately six orders of magnitude allowing for more energy to be absorbed in the resonant case when laser intensities are of the order of 10^6 - 10^7 W/cm^2 (*7*). The absorbed energy is thermalized by the matrix and is transferred into the condensed phase enabling desorption of both the matrix and the analyte. Most analyte molecules do not have a resonant excitation for a given laser frequency and thus requires the addition of a matrix, increasing sample preparation. Nevertheless, MALDI has been successful in analyzing a wide assortment of molecules, such as explosives (*9*) and proteins (*10*), despite the requirement of a matrix.

A series of ambient ionization techniques have been developed to reduce the complexity of sample preparation protocols prior to mass spectral analysis. Desorption electrospray ionization (DESI), (*11*) for instance, uses an electrospray plume to impinge

on a sample to desorb analytes via a droplet pickup mechanism. Samples analyzed by DESI include explosives (*12, 13*), carbohydrates (*14*) and biological tissues (*15*). Another set of ambient ionization techniques meant to reduce sample preparation are electrospray-assisted laser desorption ionization (ELDI) (*16*), matrix-assisted laser desorption electrospray ionization (MALDESI) (*17*) and laser ablation electrospray ionization (LAESI) (*18*). These techniques combine ns laser desorption with electrospray post-ionization for the transfer of analyte into the mass spectrometer at atmospheric pressure, avoiding the need for transferring samples into vacuum for subsequent laser desorption. Such laser-based techniques have allowed for the analysis of a variety of condensed phase samples such as proteins (*19*), peptides (*20*), caffeine and dyes (*21*).

The ELDI, MALDESI and LAESI techniques employ lasers wherein a first order resonant absorption excites molecules to a low lying state in the analyte or matrix to enable vaporization. The absorbed energy desorbs molecules via a thermal mechanism (*22, 23*) or a phase explosion mechanism (*24, 25*). For instance, LAESI uses a 100 ns, 2.94 μm laser pulse to resonantly excite the OH asymmetric stretch in water (*18*). Water-rich samples, analyzed at this wavelength and pulse duration, desorb via a phase explosion mechanism (*18*). However, the vast majority of molecules will not have a resonant excitation for a given laser frequency in the optical region. Hence, a specific matrix is used to absorb a particular excitation frequency.

While ns lasers are typically used for resonant excitation and vaporization of molecules in atmospheric laser-based desorption experiments, the coupling mechanisms of femtosecond (fs) duration lasers into molecules suggest that ultrafast excitation may be useful for such desorption experiments, as well. For the case of laser ionization under

vacuum conditions, more fragmentation is observed in the mass spectra of a biomolecule after interaction with a resonant ns laser in comparison with a resonant fs laser (for conditions providing similar ion intensities) (*26*). The additional fragmentation is due to a ladder switching mechanism during ns excitation/ionization. This mechanism allows the molecule to absorb energy and fragment during the excitation process in which the fragments subsequently absorb additional energy along the way to ionization, leading to extensive fragmentation. Ladder switching occurs because the molecular dissociation time is shorter than the laser pulse duration. During fs excitation, the molecule can not fragment during the pulse due to the ladder climbing mechanism (*i.e.,* the pulse duration is shorter than the molecular rearrangement time). For instance, gas phase gramicidin D in vacuum undergoes more fragmentation after irradiation by a resonant 5 ns pulse (260 nm) at an intensity of 10^7 W/cm^2 (50 mJ/cm^2) than a 500 fs pulse (245 – 265 nm) which is four orders of magnitude higher intensity (10^{11} W/cm^2, 50 mJ/cm^2) (*26*).

Nonresonant fs laser pulses have been used previously to transfer material into the gas phase, typically under vacuum conditions, for mass analysis (*27-29*). Irradiation of condensed cryogenic benzene, adsorbed onto a Pt (111) surface under vacuum conditions, using nonresonant fs laser pulses resulted in the intact transfer of material into the gas phase (*27-29*). These measurements suggest that a fs duration laser pulse would enable vaporization of intact molecules from a surface even in the case of nonresonant excitation. The use of nonresonant fs laser pulses to vaporize material is possible due to the nonlinear absorption of light, where two or more photons are absorbed through virtual states. The multiphoton absorption is required because the energy difference between the ground and pertinent excited energy levels is not equal to $nh\nu$ (*7, 8*). Such nonresonant

absorption processes typically require high laser intensity and therefore, short laser pulses. Nonresonant fs excitation should, in principle, couple into and vaporize all molecules, implying that sample preparation (elution, mixing with matrix and choosing samples with a particular electronic or vibrational transition) is not necessary. In addition, unlike the thermal mechanisms present in ns laser desorption experiments (*30*), the energy from a fs laser pulse is deposited into the system (substrate and analyte) on a timescale much faster than a thermal response. This suggests that if the fs laser pulse transfers analyte into the gas phase prior to thermalization to molecular modes, the anticipated decomposition can be avoided.

The previous laser electrospray mass spectrometry (LEMS) investigation demonstrated the ability to transfer a wide variety of molecules into the gas phase intact, using laser intensities on the order of 10^{13} W/cm^2, but provided little insight into a possible vaporization mechanism. Here, we probe the viable mechanism of nonresonant, nonthermal vaporization in experiments using fs laser pulses while investigating a range of molecules adsorbed on dielectric and metallic substrates. We investigate the molecules rhodamine 6G in the presence of matrix, a pseudoproline dipeptide, vitamin B12, an amphiphilic lipid and the proteins gramicidin and lysozyme.

4.3 Experimental

4.3.1 Materials

The solid samples of rhodamine 6G, pseudoproline dipeptide (Fmoc-Tyr(tBu)-Ser($\Psi^{Me,Me}$pro)-OH), vitamin B12, 1-monooleoyl-rac-glycerol and lysozyme were purchased from Sigma Aldrich (St. Louis, MO, USA), Novabiochem (Gibbstown, NJ,

USA), MP Biomedicals (Solon, OH, USA), MP Biomedicals and Sigma Aldrich, respectively. The solid hydrophobic protein mixture of gramicidin A, B and C isolated from *Bacillus aneurinolyticus* (*Bacillus brevis*) was purchased from Sigma Aldrich. The gramicidin mixture contained 80%, 6% and 14% of gramicidin A, B and C, respectively (*31*). The specific type of gramicidin is determined by the 11th amino acid in the 15 amino acid sequence. For example, gramicidin A has the sequence (*32, 33*) HCO-L-Val-Gly-L-Ala-D-Leu-L-Ala-D-Val-L-Val-D-Val-L**-**Trp-D-Leu-**L-Trp**-D-Leu-L-Trp**-**D-Leu-L-Trp-NH$(CH_2)_2$OH (mass = 1881 Da) while gramicidin B has the sequence HCO-L-Val-Gly-L-Ala-D-Leu-L-Ala-D-Val-L-Val-D-Val-L**-**Trp-D-Leu-**L-Phe**-D-Leu-L-Trp**-**D-Leu-L-Trp-NH$(CH_2)_2$OH (mass = 1842 Da). Gramicidin C (mass = 1858 Da) has the sequence HCO-L-Val-Gly-L-Ala-D-Leu-L-Ala-D-Val-L-Val-D-Val-L**-**Trp-D-Leu-**L-Tyr**-D-Leu-L-Trp**-**D-Leu-L-Trp-NH$(CH_2)_2$OH.

4.3.2 Sample preparation

The matrix-assisted samples were prepared in two steps. First, stock solutions of rhodamine 6G, pseudoproline dipeptide and vitamin B12 were prepared to a concentration of 1 x 10^{-4} M in methanol (1 x 10^{-3} M for vitamin B12). In the MALDI experiments, the stock solutions were then mixed with the matrix, 2,5-dihydroxybenzoic acid (50 mg/mL in methanol, Sigma Aldrich), in a 1000:1 molar ratio of DHB:analyte prior to drying a 250 μL aliquot on a dielectric (glass) slide (2.54 cm x 2.54 cm). To analyze a neat (matrix-free) sample of vitamin B12, a 250 μl aliquot of 1 x 10^{-3} M solution in methanol was dried on a dielectric (glass) slide (2.54 cm x 2.54 cm).

The lipid and gramicidin samples were diluted to 1 x 10^{-4} M in methanol. Matrix-free samples of the lipid and gramicidin were prepared by depositing a 30 μL aliquot of

each stock solution on separate stainless steel or transparent dielectric (glass) slides (7 mm x 7 mm) and allowed to air dry prior to analysis.

Hen egg white lysozyme was diluted to 1 x 10^{-3} M in deionized water. A matrix-free sample of lysozyme was prepared by depositing a 15 μL aliquot of the stock solution on slides (of varying composition) and allowed to air dry prior to analysis. The sample plates were placed on a three dimensional stage which permits analysis of fresh sample by each laser shot.

4.3.3 UV/VIS spectroscopy

The 1-monooleoyl-rac-glycerol and gramicidin samples were diluted to 1 x 10^{-6} M in methanol. A rhodamine 6G sample was diluted to 1 x 10^{-5} M. The prepared samples were characterized using a Jasco V-530 UV-VIS spectrometer in the wavelength range of 200 to 800 nm, with a resolution of 1 nm.

4.3.4 Matrix-assisted laser desorption/ionization mass spectrometry

4.3.4.1 Nanosecond and femtosecond matrix-assisted laser desorption/ionization

Two types of matrix-assisted laser desorption/ionization (MALDI) techniques were performed. The first was MALDI using ns laser pulses. For ns laser desorption, a 10 Hz, tripled (355 nm) Nd:YAG laser (Continuum, Santa Clara, CA, USA) with a pulse energy of 500 μJ and duration of 4 ns was used to transfer the sample into the gas phase.

The second MALDI technique utilized fs laser pulses (provided by a second laser) for vaporization. A Ti:Sapphire oscillator (Kapteyn-Murnane Laboratories Inc., Boulder, Co, USA) seeded a regenerative amplifier (Coherent Inc., Santa Clara, CA, USA) which created a 2.5 mJ pulse centered at 800 nm with a 70 fs pulse duration at a repetition rate of 10 Hz. The energy of the fs laser pulse was reduced to 800 μJ/pulse using neutral

density filters. The laser beams (ns and fs) were then focused to a spot size of ~ 250 μm in diameter using a 17.5 cm focal length lens, with an incident angle of 45° with respect to the sample. The intensity of the ns and fs laser pulses at the substrate was approximately 2.5 x 10^8 W/cm^2 and 2 x 10^{13} W/cm^2, respectively. A schematic of the laser vaporization region is shown in Figure 4.1

4.3.4.2 Mass spectrometry

The ionized gas phase sample entered a time-of-flight (TOF) mass analysis system via a dielectric capillary (both ends coated with metal) biased to -5 kV. The positive ions passed through a skimmer and a hexapole which was operated in trapping mode, where the positive ions are collected at 10 Hz. After exiting the hexapole, the ions are transferred to the extraction region by a second hexapole where they are injected linearly into the TOF analyzer via two high voltage pulsers. The positive ions were then detected and the resulting mass spectra were averaged for 60 seconds (600 mass spectra) using a digital oscilloscope. It should be noted that the dielectric capillary, the skimmer, the hexapoles, the ion optics and the TOF analyzer were along the same axis for the MALDI experiments. As a result, low resolution mass spectra were obtained when in this configuration. A schematic of the mass spectrometer used in these experiments is shown in Figure 4.2.

4.3.5 Laser vaporization with electrospray post-ionization mass spectrometry

4.3.5.1 Nanosecond and femtosecond matrix-assisted laser desorption/vaporization with electrospray post-ionization

Two types of vaporization experiments were performed. The first experiment used a 355 nm, 4 ns laser at a repetition rate of 10 Hz with an energy of 500 μJ to induce

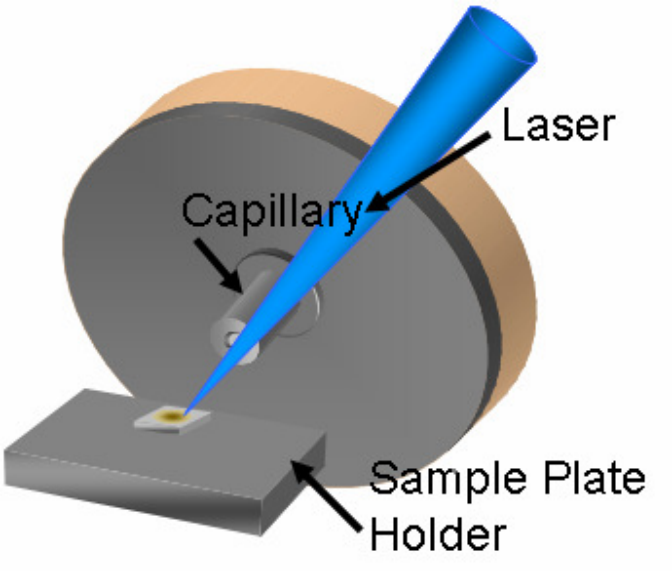

Figure 4.1. A schematic of the atmospheric MALDI apparatus. The analyte is desorbed from a sample plate holder that is mounted to a three-dimensional stage to allow translation. The laser used to vaporize the sample had an angle of incidence of 45° with respect to the sample plate.

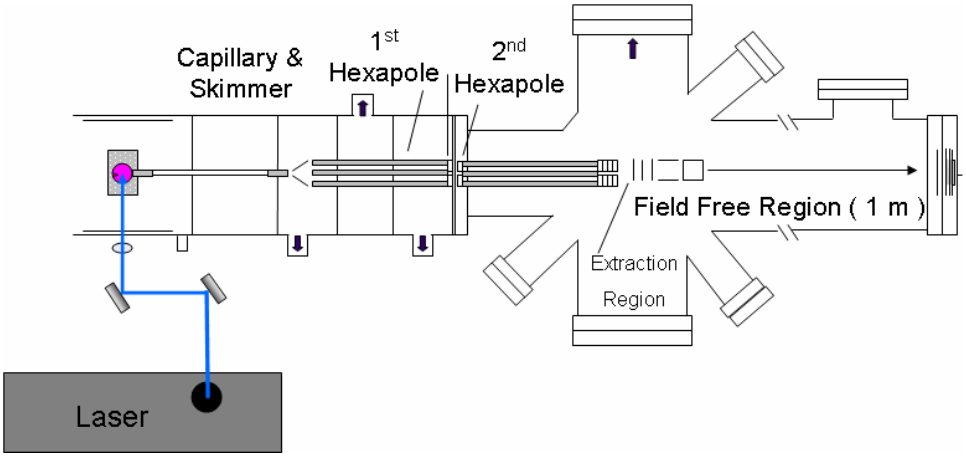

Figure 4.2. Schematic view of the atmospheric pressure MALDI mass spectrometer.

desorption. The second vaporization technique utilized fs laser pulses. A Ti:Sapphire oscillator seeded a regenerative amplifier which created a 2.5 mJ pulse centered at 800 nm with a 70 fs pulse duration at a repetition rate of 10 Hz. The energy of the fs laser pulse was reduced to 800 μJ/pulse using neutral density filters. The laser beam (ns or fs) was then focused to a spot size of ~ 250 μm in diameter using a 17.5 cm focal length lens, with an incident angle of 45° with respect to the sample. The intensity of the ns and fs laser pulse at the substrate was approximately 2.5 x 10^8 W/cm^2 and 2 x 10^{13} W/cm^2, respectively.

The vaporized sample interacted with an electrospray plume, ionizing any neutral molecules transferred into the gas phase. The electrospray plume was formed by pumping solvent through a grounded hypodermic needle at a rate of 3.0 μl/min, as set by a syringe pump (Harvard Apparatus, Holliston, MA, USA). The solvent exits the needle in the presence of an electric field producing a plume of charged droplets. A schematic of the laser vaporization region is shown in Figure 4.3

4.3.5.2 Mass spectrometry

The electrospray-ionized gas phase sample entered a TOF mass analysis system (in a linear configuration for the rhodamine 6G experiments as described above, or an orthogonal configuration for all other experiments, as described in Chapter 2) via a dielectric capillary (both ends coated with metal) biased to -5 kV. The positive ions passed through a skimmer and a hexapole operated in trapping mode. After exiting the hexapole, the ions are transferred to the extraction region by a second hexapole where they are injected into the linear TOF analyzer via two high voltage pulsers. The positive ions were then detected and the resulting mass spectra were averaged.

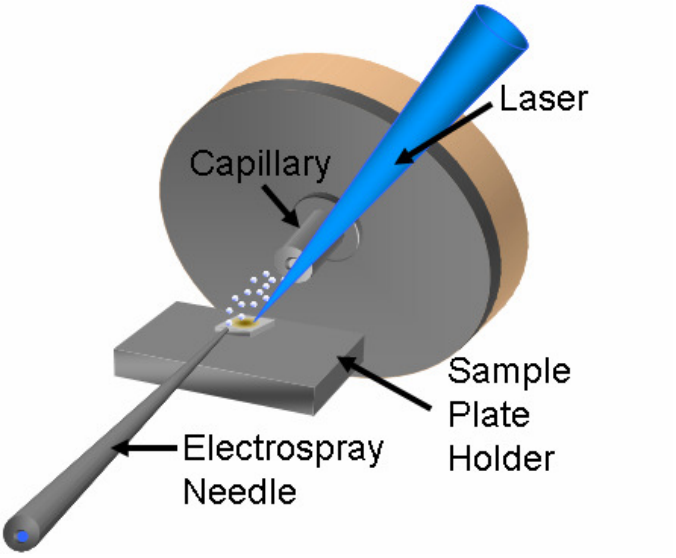

Figure 4.3. A schematic representation of the laser vaporization and electrospray ionization apparatus. The analyte is desorbed from a sample plate holder that is mounted to a three-dimensional stage to allow translation. The laser used to vaporize the sample had an angle of incidence of 45° with respect to the sample plate.

4.3.6 Safety consideration

Appropriate laser eye protection was worn by all personnel and the high voltage area was enclosed in plexiglass to prevent accidental contact with the biased electrodes.

4.4 Results and discussion

4.4.1 Neutral molecule production during femtosecond laser vaporization

Matrix-assisted laser desorption/ionization (MALDI) is commonly used to desorb molecules adsorbed onto a surface (*34*) by dispersing the sample to be analyzed in a great excess of an appropriate matrix (*e.g.,* 2,5-dihyrdoxybenzoic acid (DHB)). A ns laser pulse couples into the matrix through a one-photon resonant excitation process at a laser intensity of approximately $10^6 – 10^7$ W/cm^2 (*35*). The absorbed energy is transferred from the matrix to the condensed phase allowing for desorption of both the matrix and analyte. To demonstrate the resonant desorption process that occurs with MALDI, rhodamine 6G was dispersed in the matrix DHB and irradiated with a resonant ns laser pulse. Desorption of the sample from the condensed phase yielded a peak for the intact molecular ion, $[M\text{-}Cl]^+$, at mass-to-charge (*m/z*) 443 (Figure 4.4). The peak to the left of the $[M\text{-}Cl]^+$ ion signal, in Figure 4.4 and throughout this section, is an artifact of the ESI-TOF system in the linear configuration and is due to a portion of the ion packet being in the acceleration region when pulsed. Nonetheless, observation of the $[M\text{-}Cl]^+$ supports the fact that intact molecular ions are formed during atmospheric resonant ns-MALDI analysis.

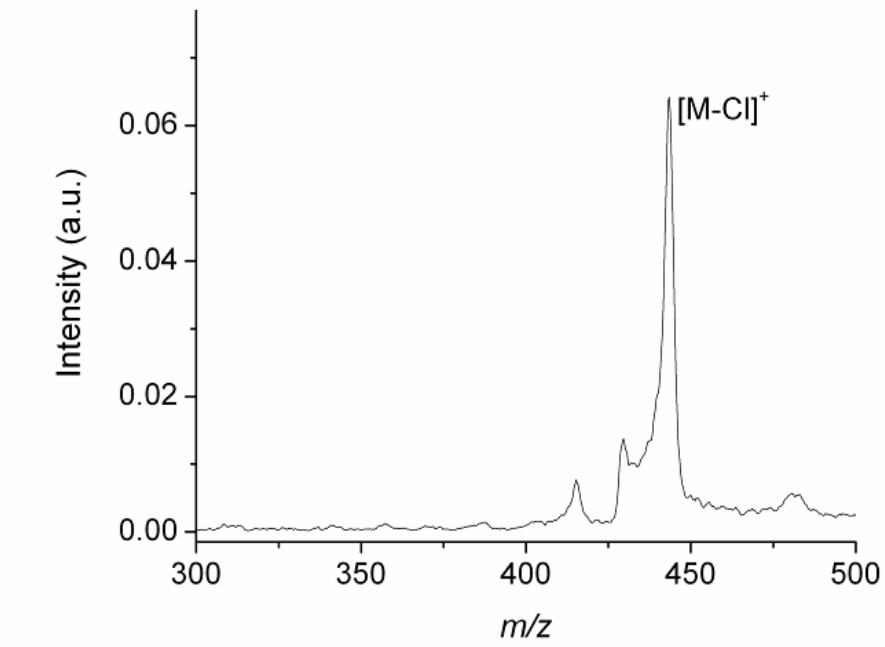

Figure 4.4. The mass spectrum corresponding to the resonant ns-MALDI analysis of a 1000:1 molar solution of DHB and rhodamine 6G spotted on a dielectric substrate.

The ultrashort duration of the fs laser pulse enables nonresonant absorption due to the high intensity at the focus (~ 10^{13} W/cm^2). To determine if such nonlinear absorption processes can enable vaporization as suggested in the previous chapter, rhodamine 6G was dispersed in the DHB matrix and irradiated using a nonresonant (800 nm) fs laser pulse. Neither the DHB matrix (*36-38*) nor the rhodamine 6G analyte (Figure 4.5) has an absorption band at the wavelength used in this experiment (800 nm), yet the intact molecular ion for rhodamine 6G, $[M\text{-}Cl]^+$, is observed at *m/z* 443 when using nonresonant fs-MALDI (Figure 4.6). Vaporization of the matrix and the rhodamine 6G is enabled via a nonresonant mulitphoton processes in the sample. Although this demonstrates that the molecule rhodamine 6G can be vaporized using nonresonant fs-MALDI, a reduction in the ion abundance (~125x lower) is observed when compared to that obtained from resonant ns-MALDI analysis. The reduction in ion abundance using nonresonant fs-MALDI is not due to an increase in fragmentation since no peaks are observed in the low *m/z* region of the mass spectrum. In addition, the decrease in ion abundance is not due to the analysis being performed at atmospheric pressure as other groups also observed a similar trend when comparing fs-MALDI to ns-MALDI under vacuum conditions (*39, 40*). However, one possible explanation for the decrease in ion abundance is that fs-MALDI produces more neutral molecules (less ions) than ns-MALDI.

To determine the relative number of neutrals produced upon laser irradiation, rhodamine 6G was dispersed in DHB and irradiated using a resonant ns laser pulse. However, in these experiments the desorbed sample interacts with an electrospray solvent (methanol with 1.0 % acetic acid). The electrospray plume will post-ionize a portion of

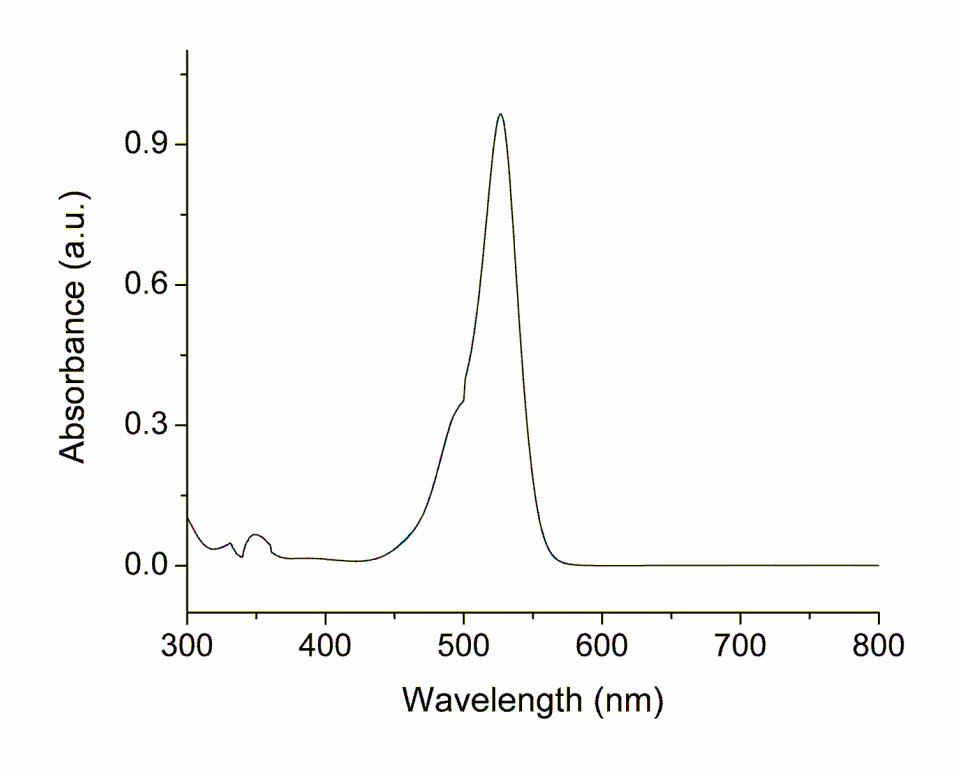

Figure 4.5. UV/VIS absorption spectrum of rhodamine 6G.

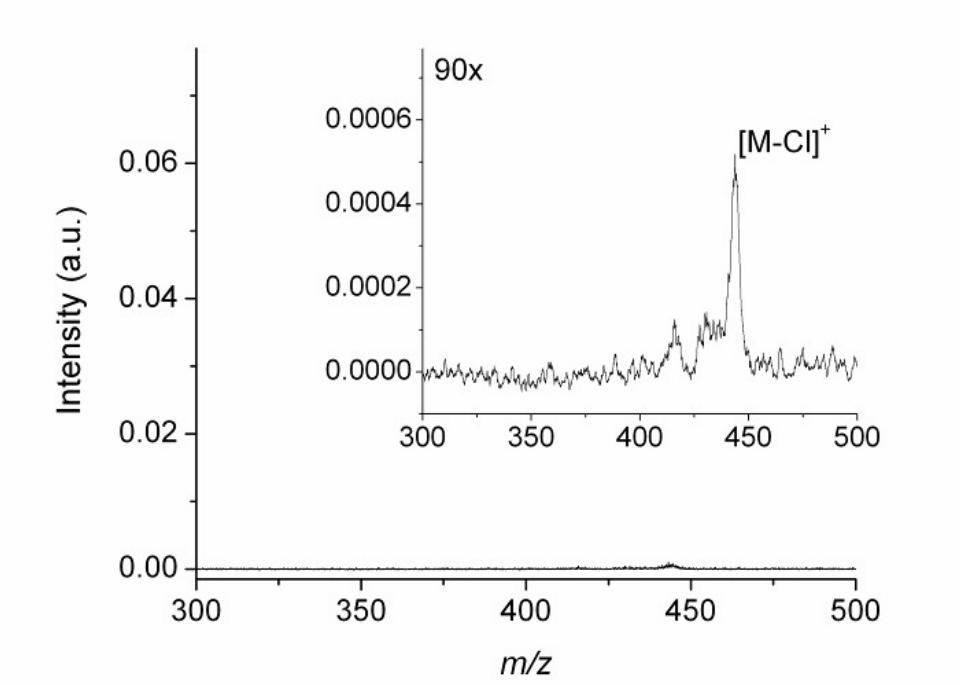

Figure 4.6. The mass spectrum corresponding to the nonresonant fs-MALDI analysis of a 1000:1 molar solution of DHB and rhodamine 6G spotted on a dielectric substrate. The inset display is a 90 x zoom of the peak at *m/z* 443.

the desorbed neutral molecules enabling their detection. Upon analysis of the collected mass spectrum using this scheme (Figure 4.7), a reduction in the ion abundance is observed when compared to ns-MALDI alone (no electrospray plume). The decrease in the ion abundance is in contrast to previous electron impact post-ionization experiments (*41*). However, the suggested gain in ion abundance is observed when fs laser pulses are used for vaporization (Figure 4.8). The interaction of the fs laser vaporized material with the electrospray plume (methanol with 1.0 % acetic acid) results in an increase in the ion abundance when compared to nonresonant fs-MALDI alone (~125x greater). The increase in the ion abundance for rhodamine 6G suggests that fs laser pulses transfer more neutral molecules (a molecule-to-ion ratio of >100:1) into the gas phase than the ns laser pulses used in these experiments. Therefore, this demonstrates and further confirms that the nonresonantly vaporized neutral molecules are captured by the electrospray plume enabling ionization as suggested in the previous chapter.

Traditional MALDI ionization mechanisms (*42*), such as gas phase proton transfer, are not dominant when using fs laser pulses. In fact, ion signal was only observed for the *salt* rhodamine 6G when using nonresonant fs-MALDI alone. When nonresonant fs-MALDI was performed on a dipeptide mixed with DHB no ion signal was observed. However, upon post-ionization of the vaporized material using an electrospray solvent (1:1 (v:v) methanol:water with 1.0 % acetic acid), intact protonated molecular ion $[M+H]^+$ at *m/z* 588 was observed for the dipeptide (Figure 4.9). This demonstrates the capability to transfer neutral molecules in the presence of matrix into the gas phase using a nonresonant fs laser pulse. The ionization of the dipeptide sample occurs when the vaporized neutral molecules are captured by the electrospray droplets and not through the

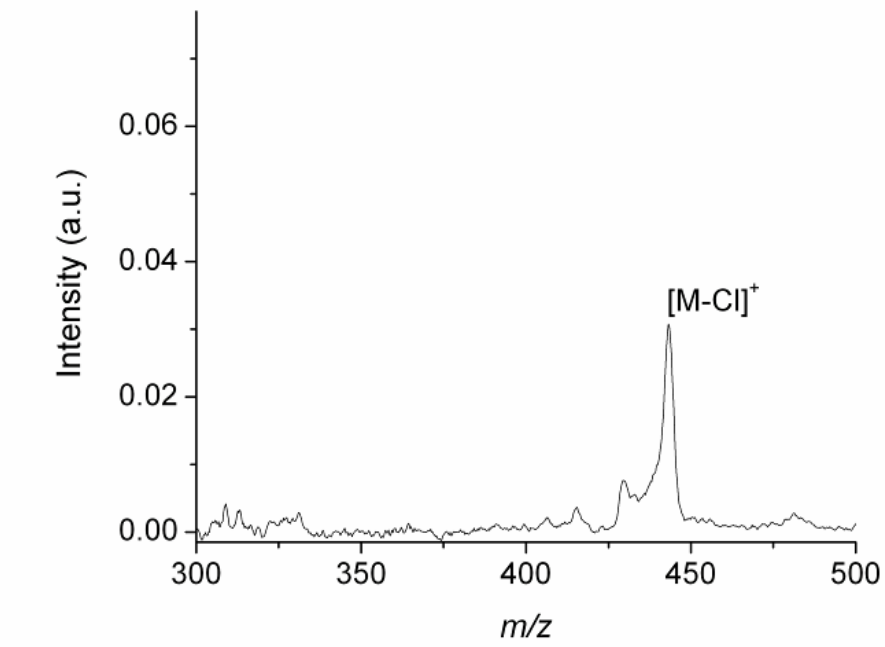

Figure 4.7. The mass spectrum corresponding to the resonant ns laser desorption with electrospray post-ionization analysis of a 1000:1 molar solution of DHB and rhodamine 6G spotted on a dielectric substrate.

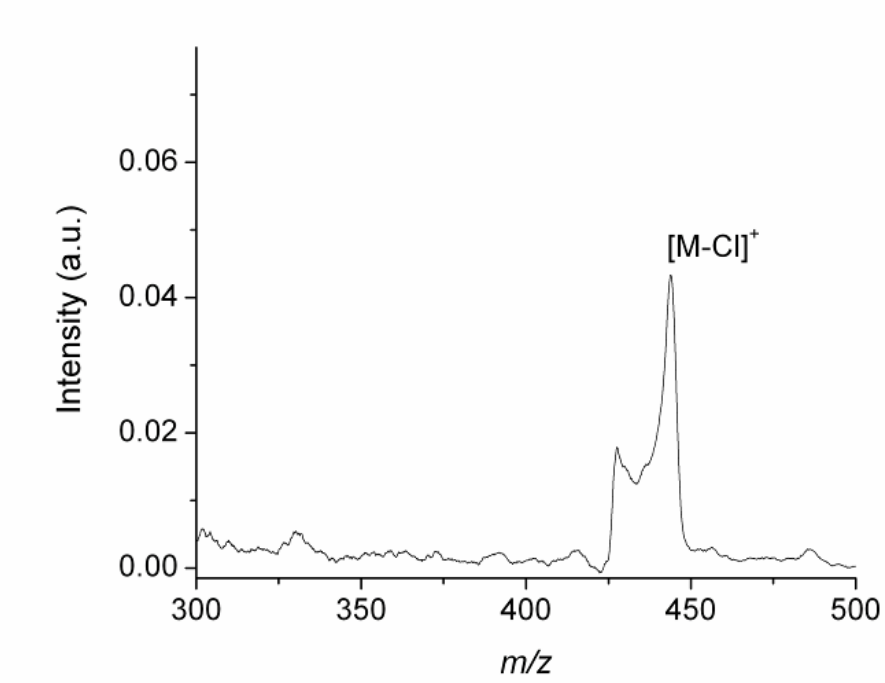

Figure 4.8. The mass spectrum corresponding to the nonresonant fs laser vaporization with electrospray post-ionization analysis of a 1000:1 molar solution of DHB and rhodamine 6G spotted on a dielectric substrate.

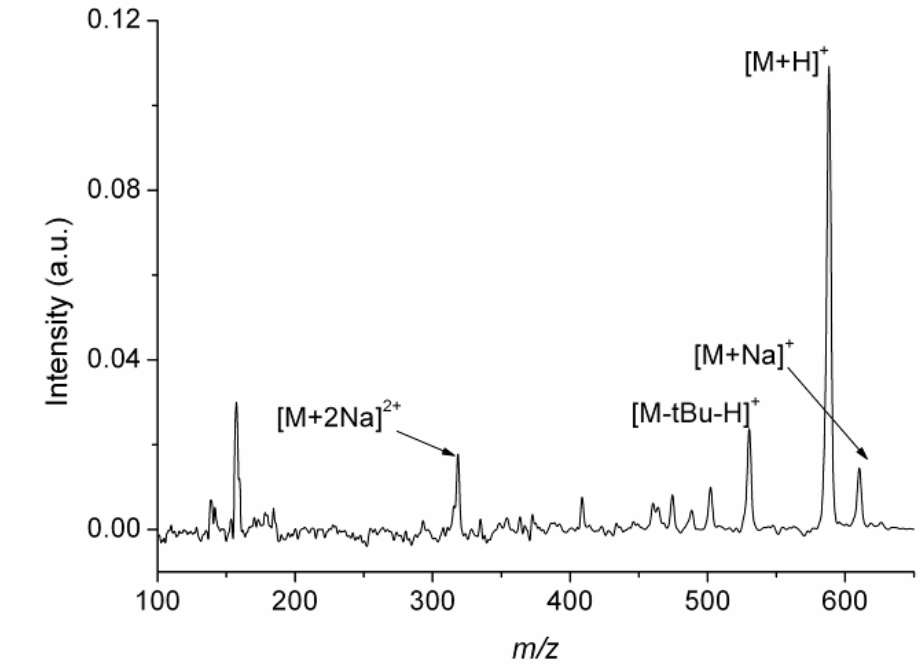

Figure 4.9. The mass spectrum corresponding to the nonresonant fs laser vaporization with electrospray post-ionization analysis of a 1000:1 molar solution of DHB and dipeptide spotted on a dielectric substrate. All unlabeled peaks are solvent-related.

traditional MALDI ionization mechanisms (*42*). Nevertheless, the ultrafast excitation of the DHB/dipeptide mixture allows for vaporization to proceed via a nonresonant absorption mechanism. This would not be possible using high intensity ns lasers at the same wavelength because increased fragmentation would be observed due to the intensities required to enable nonresonant excitation (*43*) of the solid sample into the gas phase. This suggests that the nonresonant fs laser pulses employed here do produce more intact neutral molecules than resonant ns lasers and allows for coupling into and vaporization of all molecules, implying that sample preparation (elution, mixing with matrix and choosing samples with a particular electronic or vibrational transition) is not necessary.

4.4.2 Energy deposition during femtosecond laser vaporization: Vitamin B12

Nanosecond MALDI results in the formation of intact molecular ions, while direct ns laser desorption can lead to extensive fragmentation (*22, 44*). However, some molecules, such as vitamin B12, have been shown to undergo fragmentation even when desorbed from matrices (*45*). This is attributed to the molecule being desorbed with a high degree of internal energy, which leads to dissociation. To further investigate the vaporization mechanism, vitamin B12 was mixed with DHB and deposited onto a dielectric surface. The mass spectrum (Figure 4.10) resulting from the vaporization of the vitamin B12/DHB sample using nonresonant fs laser pulses revealed the intact ion $[M+H]^+$ at *m/z* 1356, and the doubly charged ions $[M+2H]^{2+}$ and $[M+H+Na]^{2+}$ at *m/z* 679 and 690, respectively, for vitamin B12. Only one fragment ion was observed in the mass spectrum at *m/z* 666, which is consistent with $[M-CN+2H]^{2+}$, but its identity can not be confirmed without MS^n. No ions were observed in the mass spectrum without the

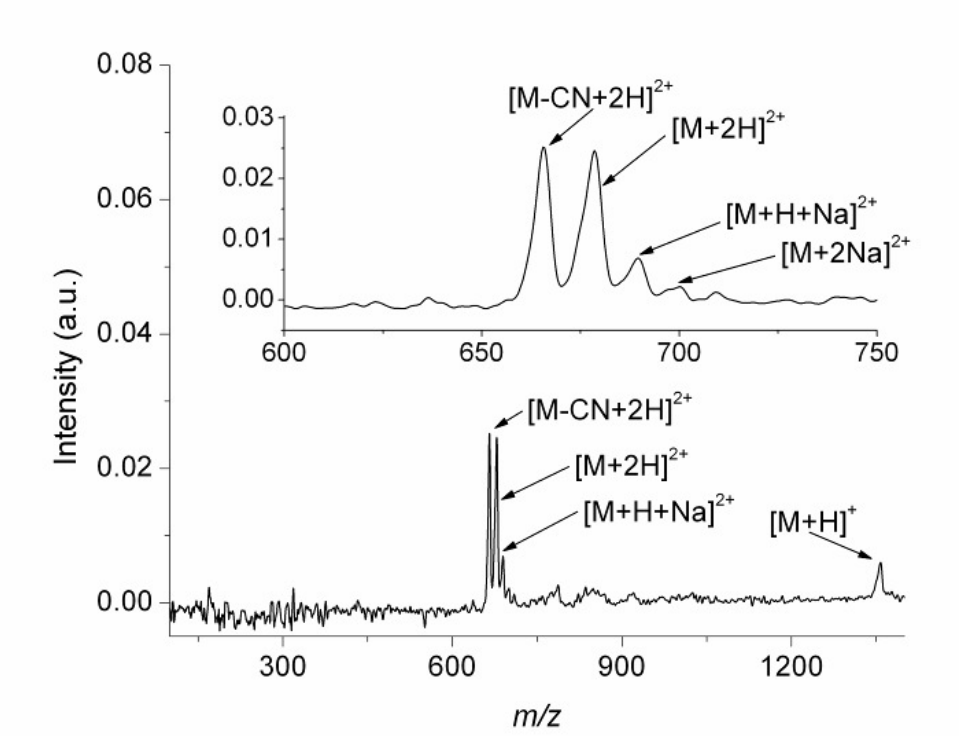

Figure 4.10. The mass spectrum corresponding to the nonresonant fs laser vaporization with electrospray post-ionization analysis of a 1000:1 molar solution of DHB and vitamin B12 spotted on a dielectric substrate shows the singly and doubly protonated molecules. The inset displays a 2x magnification of the doubly charged parent molecules. All unlabeled peaks are solvent related.

electrospray plume present during vaporization of vitamin B12. This once again suggests that secondary ionization mechanisms (*e.g.*, proton transfer in the plume) (*42*) seen in resonant ns-MALDI do not result in any observable ionization when using ultrashort nonresonant laser pulses.

When matrix-free vitamin B12 was vaporized with nonresonant fs laser pulses, the intact molecular ion was observed (Figure 4.11) at *m/z* 1356. Fragments were also observed at *m/z* 132, 147, 666, 914 and 1331 which are consistent with the pentose fragment, the dimethylbenzimidazole (base) fragment, $[M\text{-}CN+2H]^{2+}$ and [M-Co-CN-base-sugar-PO4]$^{+}$, respectively. These fragment peaks are not contained in the conventional ESI-MS of vitamin B12; therefore, the fragments are presumed to be the result of the vaporization/ionization process. However, previous studies using ns-MALDI have shown that direct photo-desorption could not explain the observed fragmentation in vitamin B12 (*45*). It was suggested that the observed fragmentation in the previous experiment is dependent on the enthalpy of the proton transfer reaction and the internal energy of the vaporized molecule (*45-47*). If the proton transfer is sufficiently exothermic, *i.e.,* the proton affinity of the analyte is greater than the proton affinity of the Brønsted acid (*e.g.,* H_3O^+), the excess energy becomes available to the newly formed ion. The excess of internal energy leads to fragmentation (*46-48*) in the molecule. In the matrix-assisted sample, the DHB absorbs a significant portion of the laser pulse energy allowing for vitamin B12 to vaporize with relatively low internal energy. The addition of a matrix lowers the internal energy of vitamin B12 via collisional cooling (*49, 50*) in the gas phase after vaporization. Once captured by the electrospray plume, ionization occurs via proton transfer in the charged droplet. However, the excess energy that is deposited

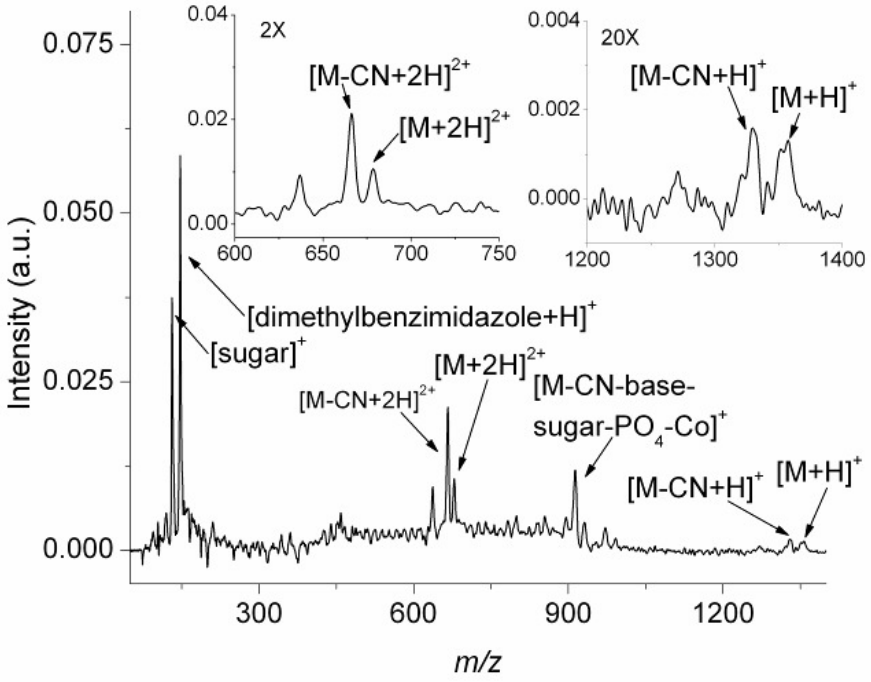

Figure 4.11. The mass spectrum corresponding to the nonresonant fs laser vaporization with electrospray post-ionization analysis of a matrix-free sample of vitamin B12 spotted on a dielectric substrate, shows the singly and doubly protonated molecules. The insets are a 2x magnification of the doubly charged molecules (left) and a 20x magnification the protonated molecule (right). All unlabeled peaks are solvent related.

into the molecule upon proton transfer is not sufficient to cause fragmentation, leading to the detection of intact ions (Figure 4.11). However, when the neat vitamin B12 was vaporized, the laser pulse energy is nonresonantly absorbed by vitamin B12, transferring the molecule into the gas phase with high internal energy. Since there is no matrix to undergo collisions with the sample in the gas phase, the internal energy of the molecule remains high. Upon proton transfer via electrospray ionization processes, excessive energy is deposited into the ion leading to the observed fragmentation in the mass spectrum of vitamin B12. This suggests that the fragments observed in LEMS are not photo-dissociation products but a result of two processes: fs laser vaporization and ESI. Proper selection of the Brønsted acid may eliminate the observed fragmentation in the collected mass spectrum completely.

4.4.3 Femtosecond laser vaporization mechanism: Analysis of 1-monooleoyl-rac-glycerol

The vaporization of lipids at atmospheric pressure using intense ultrafast laser pulses was investigated next. Monoglyceride lipids are fatty acids that play a role in biological structure and processes in both plants and animals. The fatty acid, 1-monooleoyl-rac-glycerol or monoolein, was analyzed as a model system using LEMS. The structure of monoolein, shown as the inset in Figure 4.12, contains a C18:1 unsaturated monoglyceride (where C18:1 signifies an 18 carbon chain with one unsaturated bond) on the hydrophobic end and two hydroxyl groups on the hydrophilic end. The fs laser vaporization of matrix-free monoolein from a steel substrate reveals the $[M+H]^+$, $[M+NH_4]^+$ and the $[M+Na]^+$ ions of monoolein at *m/z* 357, 374 and 379, respectively in the LEMS mass spectrum shown in Figure 4.12. The ions at *m/z* 374 and

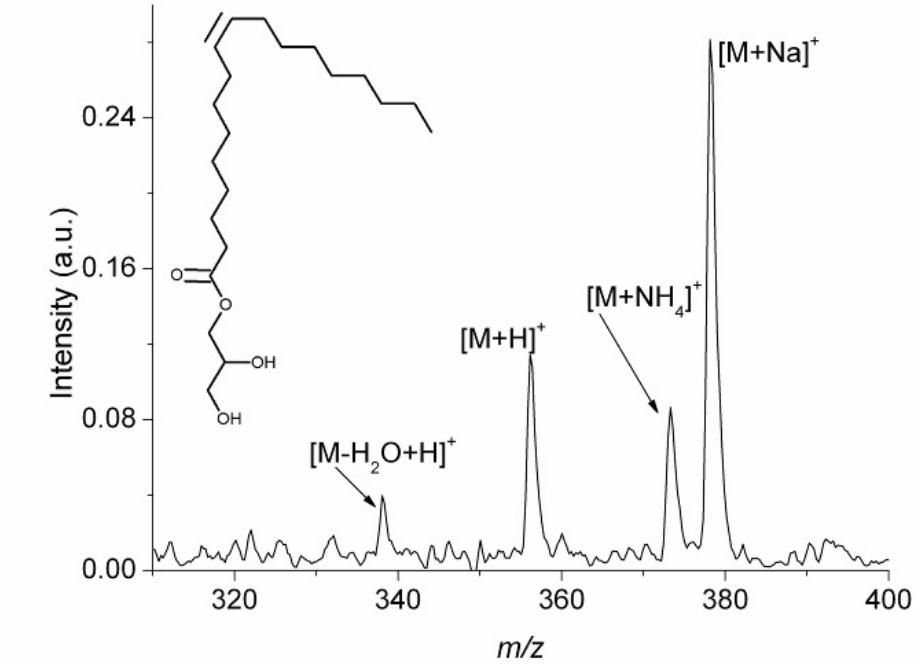

Figure 4.12. The background subtracted mass spectrum of 1-monooleoyl-rac-glycerol (monoolein) vaporized from metal using nonresonant fs laser vaporization with electrospray post-ionization analysis. The inset shows the molecular structure of monoolein.

379 have been observed in literature from solutions containing ammonium acetate when performing conventional ESI-MS analysis (*51*). A fragment observed at *m/z* 339, consistent with the ion $[M\text{-}H_2O+H]^+$, is due to hydrolysis in the electrospray droplet (*52*).

The mechanism of intense nonresonant fs laser-induced vaporization remains an unanswered question. In the case of ns laser-based desorption techniques, rapid heating of the substrate likely occurs and therefore the substrate plays an important role as shown when basic blue 7 dye was desorbed from a variety of substrates without a matrix (*23*). The highest ion abundance was observed when the dye was desorbed from a stainless steel surface, which is consistent with the efficient absorption of the ns laser pulse energy by the steel substrate leading to rapid heating and thermal desorption of the analyte.

Therefore, to address the nature of the vaporization mechanism for lipids using intense fs laser pulses, monoolein was deposited and dried on a dielectric substrate. The dielectric, glass, is transparent at 800 nm and therefore, no first order resonant transitions occur in that region of the electromagnetic spectrum. In addition, monoolein does not have an electronic transition in the 800 nm region, as shown in the UV/VIS absorption spectrum (Figure 4.13). The optical penetration depth of glass at 800 nm is much greater than that for metal, allowing the light to be transmitted through the dielectric substrate. Since there is no coupling (absorption) of the laser into the dielectric, there is no heating and no possibility for thermal desorption. Thus, the vaporization of monoolein deposited on a dielectric substrate would demonstrate the nonthermal nature of the fs vaporization process. The mass spectrum of matrix-free monoolein vaporized using intense fs laser pulses from a dielectric substrate is shown in Figure 4.14. The $[M\text{-}H_2O+H]^+$, $[M+H]^+$, $[M+NH_4]^+$ and $[M+Na]^+$ ions are observed for the LEMS analysis of monoolein

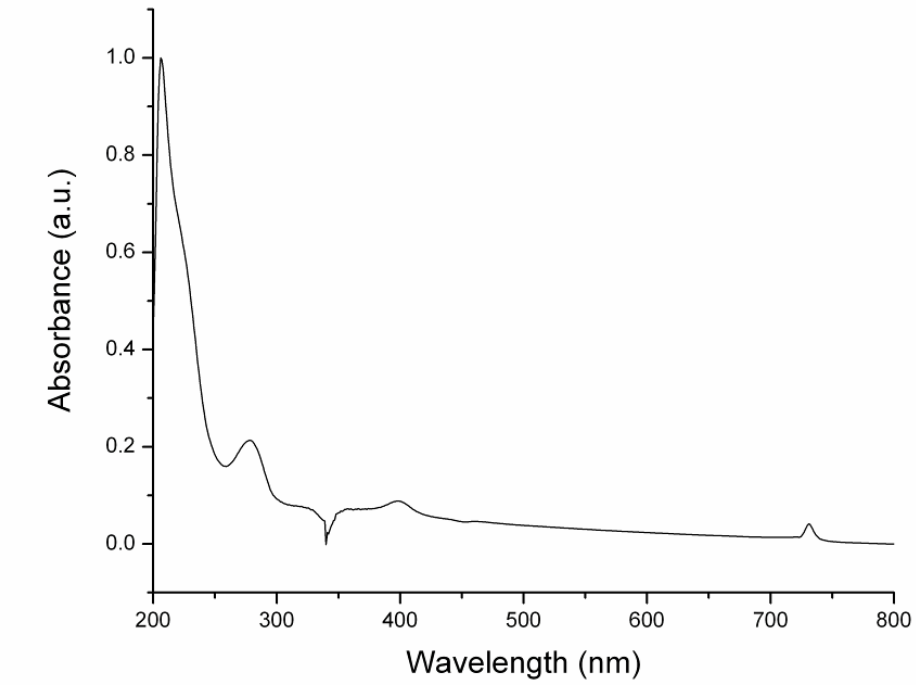

Figure 4.13. UV/VIS absorption spectrum of monoolein

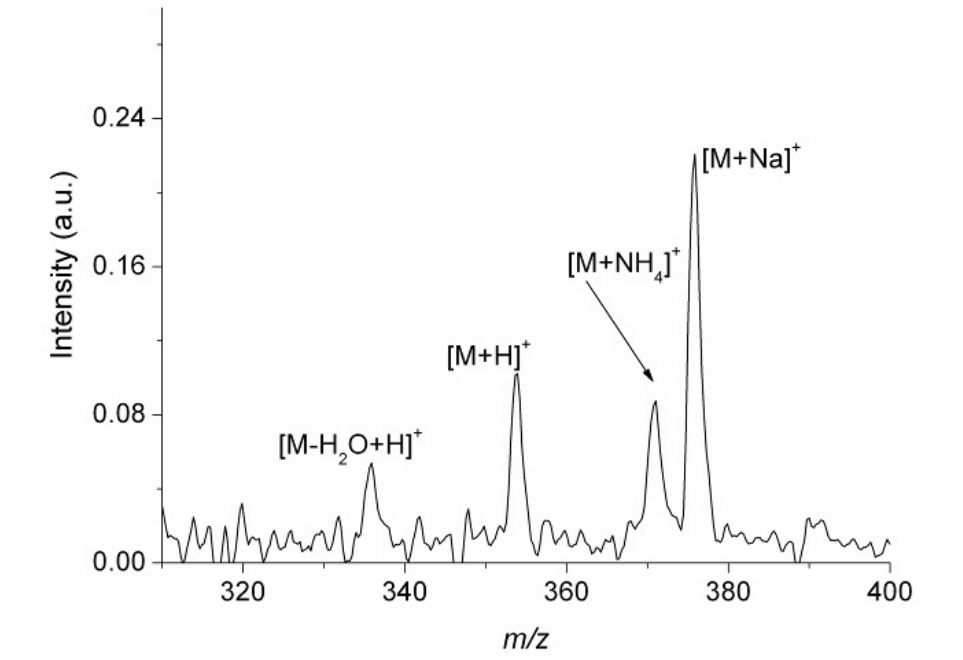

Figure 4.14. The background subtracted mass spectrum of monoolein vaporized from a dielectric substrate using nonresonant fs laser vaporization with electrospray post-ionization analysis.

vaporized from a dielectric substrate; however, the ion abundance decreases presumably due to the dielectric's surface undergoing patch charging. This causes a distortion of the electrospray plume resulting in a decrease in the observed ion abundance for the laser vaporized material (*53*). The vaporization of monoolein is due to the fs laser pulses depositing its energy into the molecule nonresonantly and on a timescale much faster than a thermal response leading to nonthermal vaporization. Thus, the vaporization mechanism of the lipid from an insulating dielectric surface after fs laser excitation demonstrates that thermal desorption is not required for transferring molecules into the gas phase.

4.4.4 Femtosecond laser vaporization of membrane-derived proteins

Lipids are commonly found in the membrane of cells from living organisms. Within these membranes reside membrane-bound proteins, the detection of which remains a major challenge for analytical science. Membrane-bound proteins are typically nonpolar, hydrophobic molecules making detection challenging using conventional mass spectrometric methods (*10, 54, 55*). Several processing steps are required to extract hydrophobic, membrane-bound proteins for conventional ESI-MS analysis. We have demonstrated previously that nonresonant fs laser pulses coupled with electrospray post-ionization is capable of vaporizing, ionizing and analyzing a hydrophobic porphyrin without any preprocessing steps other than deposition onto a substrate (*56*). This suggests that LEMS may be capable of vaporization, ionization and analysis of hydrophobic proteins. Here, we investigate the fs laser vaporization of the hydrophobic membrane-derived proteins gramicidin A, B and C, a class of proteins that possess antibiotic

properties. Like the lipid monoolein, gramicidin A, B and C are not soluble in water and constitute an important test for hydrophobic macromolecule analysis using LEMS.

The mass spectrum resulting from the fs laser vaporization and electrospray post-ionization of the matrix-free proteins gramicidin A, B and C deposited and dried on a steel slide is shown in Figure 4.15. A broad feature corresponding to the singly charged gramicidin ions was observed at *m/z* 1882 and is consistent with the $[M_A+H]^+$ ion of gramicidin A. The resolution (m/Δm) of the linear TOF at *m/z* 2122 is ~ 100 and the singly charged features for gramicidin are not resolved in this *m/z* range. In the lower *m/z* region, the resolution is higher (m/Δm at *m/z* 922 ~ 120) and the mass spectral features are better resolved. The peaks observed at *m/z* 922, 930, 941.5, 952, 963 and 972 correspond to the doubly charged gramicidin $[M_B+2H]^{2+}$, $[M_C+2H]^{2+}$, $[M_A+2H]^{2+}$, $[M_C+2Na]^{2+}$, $[M_A+2Na]^{2+}$ and $[M_A+H_2O+2Na]^{2+}$ ions, respectively. It should be noted that no ions were observed in the acquired mass spectrum without the presence of the electrospray plume during the vaporization of gramicidin A, B and C.

The peak observed at *m/z* 1183, indicated by an asterisk, was not observed in the conventional ESI-MS of gramicidin and is consistent with a fragment formed via the vaporization/ionization process. The fragment at *m/z* 1183 was also observed when gramicidin was trapped in an ion cyclotron resonance cell and irradiated with a CO_2 laser pulse (*57*). These LEMS measurements demonstrate the capability to detect hydrophobic membrane-derived proteins from a metal substrate.

To confirm that a nonthermal vaporization is the underlying mechanism for the transfer of hydrophobic proteins into the gas phase, matrix-free gramicidin was deposited and dried on a dielectric substrate prior to fs laser vaporization. The LEMS mass

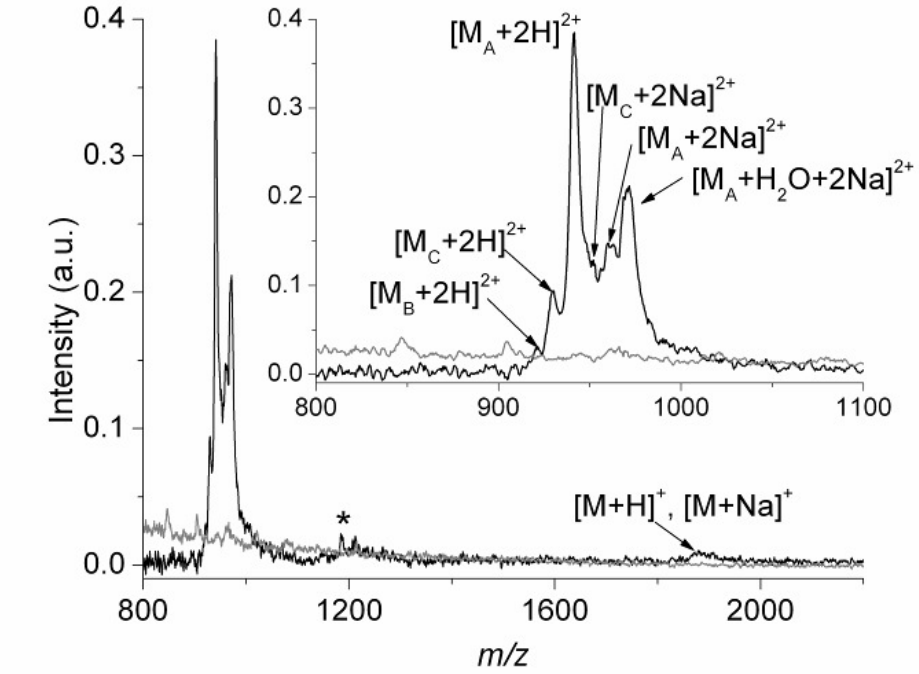

Figure 4.15. The background subtracted mass spectrum of gramicidin A, B and C from a steel surface resulting from nonresonant fs laser vaporization with electrospray post-ionization analysis. The gray line represents the solvent background measured just prior to laser vaporization of the analyte. The marked peak (∗) denotes fragment of gramicidin.

spectrum of gramicidin deposited on the dielectric, shown in Figure 4.16, reveals the gramicidin A, B and C singly and doubly charged ions along with the fragment ion at *m/z* 1183. This is similar to the spectrum of gramicidin vaporized from steel with the only difference in the spectra being that vaporization from a dielectric substrate results in lower ion abundance, which is most likely a result of patch charging. While neither the dielectric substrate nor gramicidin have a resonant transition in the 800 nm region and are thus transparent at this wavelength (Figure 4.17) at low intensity, there is a higher probability for multiphoton excitation to occur in gramicidin since the lowest electronic transition in gramicidin is less than the band gap energy of the dielectric substrate. We note that there is no plasma generation, etching or pitting of the dielectric's surface after fs laser vaporization of the gramicidin. These results demonstrate that the fs pulse must couple nonresonantly into the gramicidin molecule to enable vaporization via a nonthermal mechanism. This suggests that the fs laser pulse will transfer a wide range of molecules into the gas phase regardless of electronic structure, overcoming the need for resonant transitions in molecules or substrates.

4.4.5 Femtosecond laser vaporization mechanism of a large protein

The nonresonant ultrafast laser vaporization of small hydrophobic proteins from a transparent dielectric substrate has been demonstrated suggesting that the nonresonant coupling of the laser can occur at atmospheric pressure. We presume that at such high intensities, a sufficient number of amino acids are excited in a protein subunit upon *n*-photon absorption allowing the molecule to access a molecule-molecule repulsive surface that results in vaporization. Therefore, the vaporization process should not be affected by the composition of the substrate or the molecule since the laser nonresonantly couples

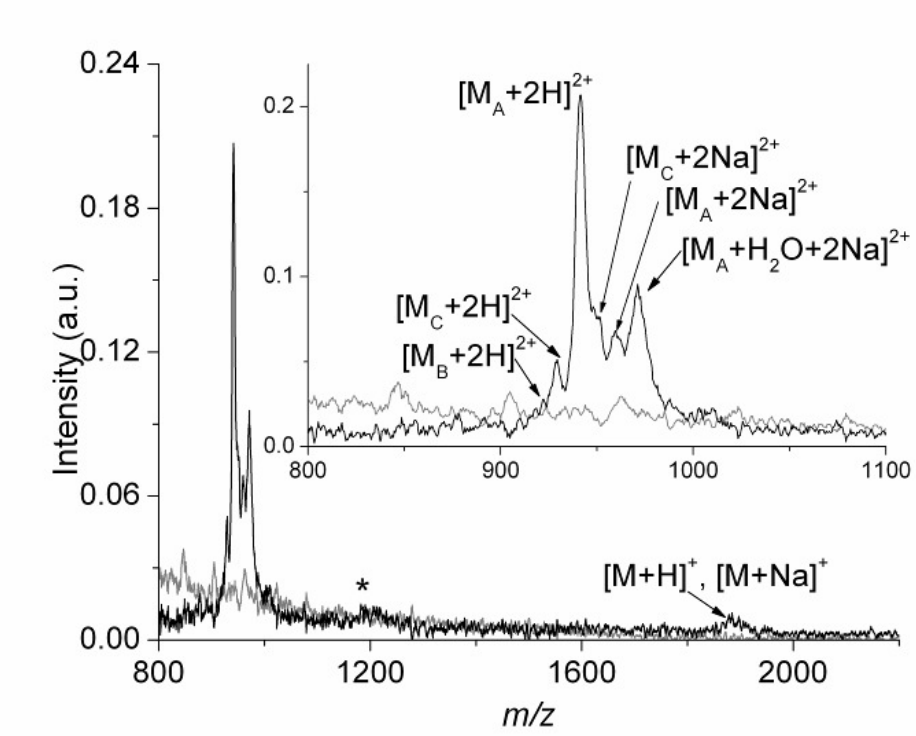

Figure 4.16. The background subtracted mass spectrum of gramicidin A, B and C from a dielectric substrate resulting from nonresonant fs laser vaporization with electrospray post-ionization analysis. The gray line represents the solvent background measured just prior to laser vaporization of the analyte. The marked peak (∗) denotes a fragment of gramicidin.

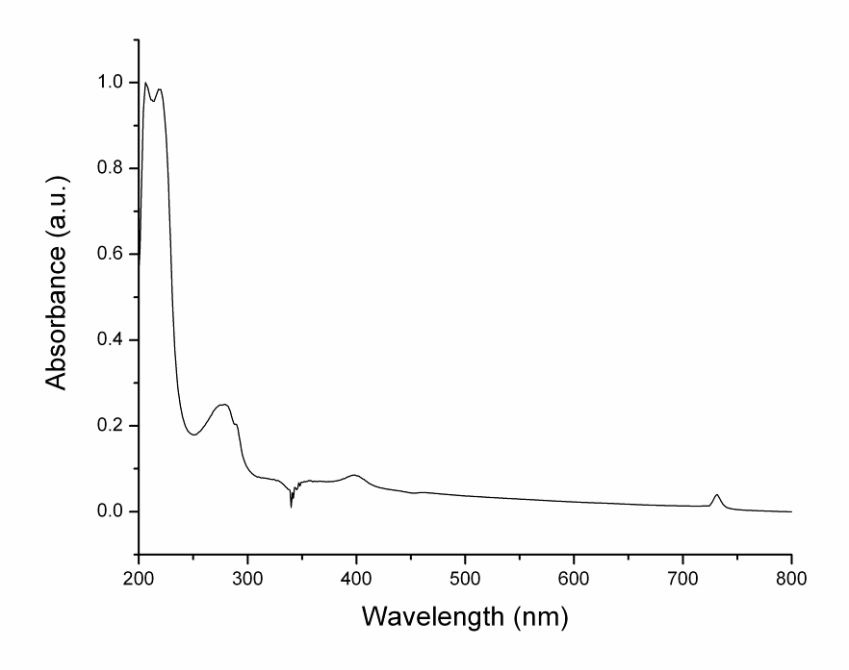

Figure 4.17. UV/VIS absorption spectrum of gramicidin.

into the analyte. To demonstrate the nonresonant, nonthermal vaporization mechanism for large biomolecules, lysozyme, a 14.3 kDa protein, was vaporized from several substrates of varying composition including, a transparent dielectric, a silicon wafer and a stainless steel surface. It was found that vaporization from a transparent dielectric substrate yields intact lysozyme ions ranging in *m/z* from 1,000 to 2,250 (Figure 4.18), with each ion corresponding to a different charge state. The observed distribution was centered at the 9+ charge state (the n+ charge state represents the $[M+nH]^{n+}$ ion, where M is the mass of the molecule and n is the number of additional protons bound to the molecule). In the mass spectrum (Figure 4.18), higher charges states (indicative of unfolded protein (*58*)) are observed and are a result of lysozyme partially unfolding as the protein solution dries on the surface (*59*). Nevertheless, it was found that the surface does not significantly affect the shape of the distribution or the vaporization yield of the protein (Figure 4.19). Vaporization from stainless steel results in approximately the same integrated ion abundance as vaporization from a dielectric substrate, demonstrating that the ultrafast laser pulse nonresonantly couples into analyte directly, transferring sample into the gas phase via a nonthermal mechanism regardless of size. The variance in the ion abundance resulting from the vaporization of lysozyme from different substrates suggests that the wide range of substrate electronic properties do not affect the transfer of protein into the gas phase, excluding a molecule-substrate repulsive vaporization mechanism. Rather, it is presumed that at such intensities a sufficient number of amino acids are excited in a protein subunit via a *n*-photon absorption process by the fs laser pulse. This allows the adsorbed protein to access a molecule-molecule repulsive surface that results in vaporization of the protein into the gas phase.

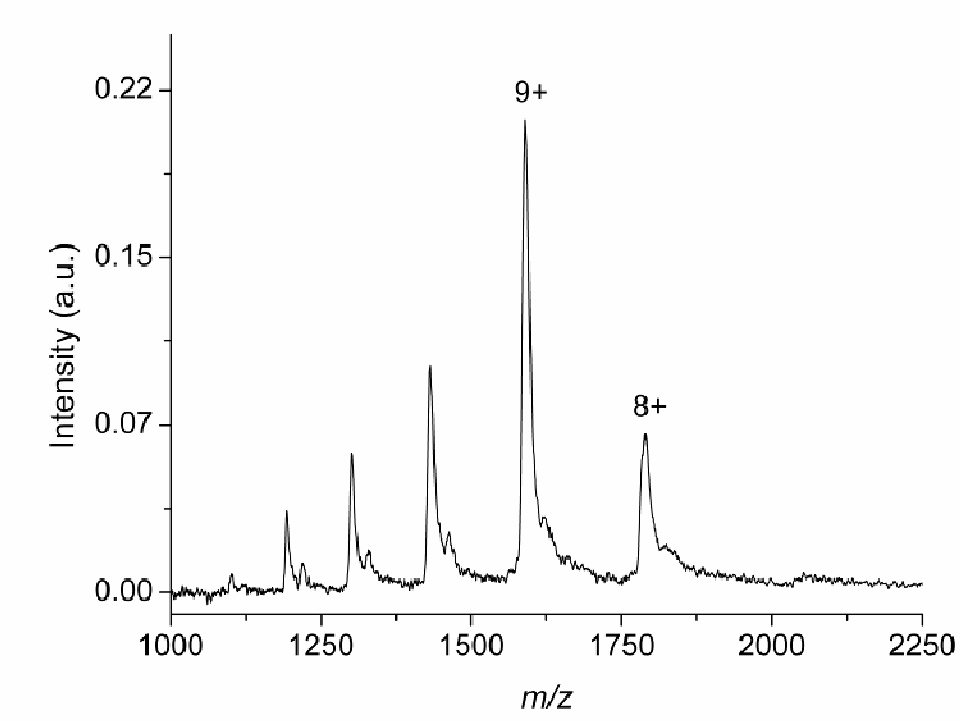

Figure 4.18. The nonresonant fs laser vaporization with electrospray post-ionization analysis of aqueous lysozyme from a transparent dielectric substrate.

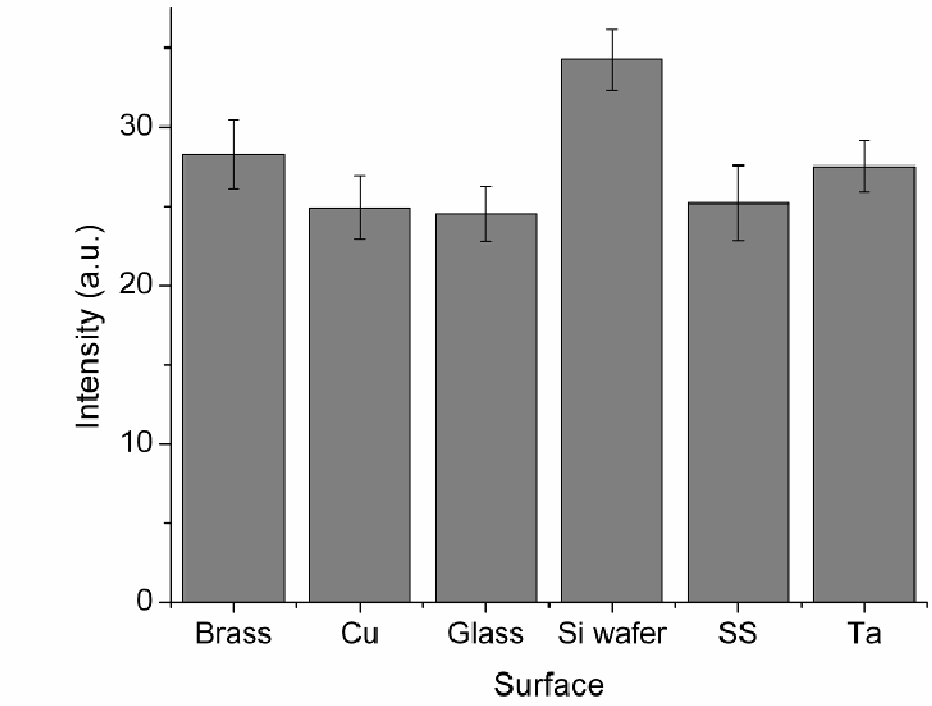

Figure 4.19. The integrated ion abundance of lysozyme vaporized from brass, copper (Cu), glass, a silicon (Si) wafer, stainless steel (SS) and a tantalum (Ta) substrate.

4.5 Conclusions

The universal detection of biological molecules is difficult due to the wide variety of chemical structures, polarities and low vapor pressures for samples of interest. We have shown that LEMS is capable of detecting an amphiphilic lipid, a dipeptide, vitamin B12 and the proteins, gramicidin and lysozyme, from dielectric substrates. The detection of macromolecules from a dielectric substrate indicates that the molecules undergo vaporization via a nonresonant, nonthermal mechanism. Once vaporized, the molecules are captured and ionized in an electrospray plume. These measurements further demonstrate that the intense nonresonant fs laser may be capable of delivering molecules into the gas phase without altering their structural conformation, allowing for the condensed phase conformational analysis of protein samples.

References

1. J. B. Fenn, M. Mann, C. K. Meng, S. F. Wong, C. M. Whitehouse, Electrospray ionization - principles and practice. *Mass Spectrom. Rev.* **9**, 37 (1990).
2. J. B. Fenn, M. Mann, C. K. Meng, S. F. Wong, C. M. Whitehouse, Electrospray ionization for mass-spectrometry of large biomolecules. *Science* **246**, 64 (1989).
3. F. Hillenkamp, M. Karas, R. C. Beavis, B. T. Chait, Matrix-assisted laser desorption ionization mass-spectrometry of biopolymers. *Anal. Chem.* **63**, A1193 (1991).
4. E. Nordhoff *et al.*, Matrix-assisted laser desorption ionization mass-spectrometry of nucleic-acids with wavelengths in the ultraviolet and infrared. *Rapid Commun. Mass Spectrom.* **6**, 771 (1992).

5. C. M. Spickett, A. R. Pitt, A. J. Brown, Direct observation of lipid hydroperoxides in phospholipid vesicles by electrospray mass spectrometry. *Free Radic. Bio. Med.* **25**, 613 (1998).

6. C. Y. Cheng *et al.*, Electrospray-assisted laser desorption/ionization mass spectrometry for continuously monitoring the states of ongoing chemical reactions in organic or aqueous solution under ambient conditions. *Anal. Chem.* **80**, 7699 (2008).

7. N. B. Delone, V. P. Krainov, *Mulitphoton processes in atoms*. (Springer-Verlag Berlin Heidelberg, ed. Second, 1999), pp. 314.

8. J. H. Posthumus, The dynamics of small molecules in intense laser fields. *Rep. Prog. Phys.* **67**, 623 (2004).

9. M. Zhang *et al.*, Using molecular recognition of β cyclodextrin to determine molecular weights of low-molecular-weight explosives by MALDI-TOF mass spectrometry. *J. Am. Soc. Mass Spectrom.* **17**, 189 (2006).

10. B. Rosinke *et al.*, Matrix-assisted laser desorption/ionization mass-spectrometry (MALDI-MS) of membrane-proteins and noncovalent complexes. *J. Mass Spectrom.* **30**, 1462 (1995).

11. Z. Takats, J. M. Wiseman, B. Gologan, R. G. Cooks, Mass spectrometry sampling under ambient conditions with desorption electrospray ionization. *Science* **306**, 471 (2004).

12. I. Cotte-Rodriguez, H. Hernandez-Soto, H. Chen, R. G. Cooks, *In situ* trace detection of peroxide explosives by desorption electrospray ionization and

desorption atmospheric pressure chemical ionization. *Anal. Chem.* **80**, 1512 (2008).

13. I. A. Popov, H. Chen, O. N. Kharybin, E. N. Nikolaev, R. G. Cooks, Detection of explosives on solid surfaces by thermal desorption and ambient ion/molecule reactions. *Chem. Commun.*, 1953 (2005).

14. M. S. Bereman, T. I. Williams, D. C. Muddiman, Carbohydrate analysis by desorption electrospray ionization Fourier transform ion cyclotron resonance mass spectrometry. *Anal. Chem.* **79**, 8812 (2007).

15. R. G. Cooks, Z. Ouyang, Z. Takats, J. M. Wiseman, Ambient mass spectrometry. *Science* **311**, 1566 (2006).

16. J. Shiea *et al.*, Electrospray-assisted laser desorption/ionization mass spectrometry for direct ambient analysis of solids. *Rapid Commun. Mass Spectrom.* **19**, 3701 (2005).

17. J. S. Sampson, A. M. Hawkridge, D. C. Muddiman, Generation and detection of multiply-charged peptides and proteins by matrix-assisted laser desorption electrospray ionization (MALDESI) Fourier transform ion cyclotron resonance mass spectrometry. *J. Am. Soc. Mass Spectrom.* **17**, 1712 (2006).

18. P. Nemes, A. Vertes, Laser ablation electrospray ionization for atmospheric pressure, *in vivo*, and imaging mass spectrometry. *Anal. Chem.* **79**, 8098 (2007).

19. M. Z. Huang, H. J. Hsu, L. Y. Lee, J. Y. Jeng, L. T. Shiea, Direct protein detection from biological media through electrospray-assisted laser desorption ionization/mass spectrometry. *J. Proteome Res.* **5**, 1107 (2006).

20. I. X. Peng, J. Shiea, R. R. O. Loo, J. A. Loo, Electrospray-assisted laser desorption/ionization and tandem mass spectrometry of peptides and proteins. *Rapid Commun. Mass Spectrom.* **21**, 2541 (2007).

21. S. Y. Lin, M. Z. Huang, H. C. Chang, J. Shiea, Using electrospray-assisted laser desorption/ionization mass spectrometry to characterize organic compounds separated on thin-layer chromatography plates. *Anal. Chem.* **79**, 8789 (2007).

22. C. D. Calvano, F. Palmisano, C. G. Zambonin, Laser desorption/ionization time-of-flight mass spectrometry of triacylglycerols in oils. *Rapid Commun. Mass Spectrom.* **19**, 1315 (2005).

23. M.-Z. Huang, S.-S. Jhang, C.-N. Cheng, S.-C. Cheng, J. Shiea, Effects of matrix, electrospray solution, and laser light on the desorption and ionization mechanisms in electrospray-assisted laser desorption ionization mass spectrometry. *Analyst* **135**, 759 (2010).

24. A. Peterlongo, A. Miotello, R. Kelly, Laser-pulse sputtering of aluminum - vaporization, boiling, superheating, and gas-dynamic effects. *Phys. Rev. E* **50**, 4716 (1994).

25. J. H. Yoo, S. H. Jeong, R. Greif, R. E. Russo, Explosive change in crater properties during high power nanosecond laser ablation of silicon. *J. App. Phys.* **88**, 1638 (2000).

26. R. Weinkauf, P. Aicher, G. Wesley, J. Grotemeyer, E. W. Schlag, Femtosecond versus nanosecond multiphoton ionization and dissociation of large molecules. *J. Phys. Chem.* **98**, 8381 (1994).

27. H. Arnolds, R. J. Levis, D. A. King, Vibrationally assisted DIET through transient temperature rise: The case of benzene on Pt{111}. *Chem. Phys. Lett.* **380**, 444 (2003).

28. H. Arnolds, C. Rehbein, G. Roberts, R. J. Levis, D. A. King, Femtosecond near-infrared laser desorption of multilayer benzene on Pt{111}: A molecular Newton's cradle? *J. Phys. Chem. B* **104**, 3375 (2000).

29. H. Arnolds, C. E. M. Rehbein, G. Roberts, R. J. Levis, D. A. King, Femtosecond near-infrared laser desorption of multilayer benzene on Pt{111}: Spatial origin of hyperthermal desorption. *Chem. Phys. Lett.* **314**, 389 (1999).

30. J. M. Hicks, L. E. Urbach, E. W. Plummer, H.-L. Dai, Can pulsed laser excitation of surfaces be described by a thermal model? *Phys. Rev. Lett.* **61**, 2588 (1988).

31. A. S. Bourinbaiar, C. F. Coleman, The effect of gramicidin, a topical contraceptive and antimicrobial agent with anti-HIV activity, against herpes simplex viruses type 1 and 2 *in vitro*. *Arch. Virol.* **142**, 2225 (1997).

32. R. Sarges, B. Witkop, Gramicidin a. V. The structure of valine- and isoleucine-gramicidin a. *J. Am. Chem. Soc.* **87**, 2011 (1965).

33. R. K. Chitta, M. L. Gross, Electrospray ionization-mass spectrometry and tandem mass spectrometry reveal self-association and metal-ion binding of hydrophobic peptides: A study of the gramicidin dimer. *Biophys. J.* **86**, 473 (2004).

34. E. H. Seeley, S. R. Oppenheimer, D. Mi, P. Chaurand, R. M. Caprioli, Enhancement of protein sensitivity for MALDI imaging mass spectrometry after chemical treatment of tissue sections. *J. Am. Soc. Mass Spectrom.* **19**, 1069 (2008).

35. K. Dreisewerd, M. Schürenberg, M. Karas, F. Hillenkamp, Influence of the laser intensity and spot size on the desorption of molecules and ions in matrix-assisted laser desorption/ionization with a uniform beam profile. *Int. J. Mass Spectrom.* **141**, 127 (1995).

36. D. A. Allwood, P. E. Dyer, Quantitative fluorescence measurements performed on typical matrix molecules in matrix-assisted laser desorption/ionization. *Chem. Phys.* **261**, 457 (2000).

37. D. A. Allwood, R. W. Dreyfus, I. K. Perera, P. E. Dyer, Optical absorption of matrix compounds for laser-induced desorption and ionization (MALDI). *App. Surf. Sci.* **110**, 154 (1997).

38. D. A. Allwood, R. W. Dreyfus, I. K. Perera, P. E. Dyer, UV optical absorption of matrices used for matrix-assisted laser desorption/ionization. *Rapid Commun. Mass Spectrom.* **10**, 1575 (1996).

39. P. Demirev *et al.*, Matrix-assisted laser desorption with ultra-short laser pulses. *Rapid Commun. Mass Spectrom.* **6**, 187 (1992).

40. J. M. Wichmann, C. Lupulescu, L. Wöste, A. Lindinger, Matrix-assisted laser desorption/ionization by using femtosecond laser pulses in the near-infrared wavelength regime. *Rapid Commun. Mass Spectrom.* **23**, 1105 (2009).

41. R. Van Breemen, M. Snow, C. R. M., Time resolved laser desorption mass spectrometry, I. Desorption of preformed ions. *Int. J. Mass Spectrom. Ion Processes* **49**, 35 (1983).

42. R. Zenobi, R. Knochenmuss, Ion formation in MALDI mass spectrometry. *Mass Spectrom. Rev.* **17**, 337 (1998).

43. M. J. Dewitt, R. J. Levis, Near-infrared femtosecond photoionization dissociation of cyclic aromatic-hydrocarbons. *J. Chem. Phys.* **102**, 8670 (1995).

44. M. A. Posthumus, P. G. Kistemaker, H. L. C. Meuzelaar, M. C. Ten Noever de Brauw, Laser desorption-mass spectrometry of polar nonvolatile bio-organic molecules. *Anal. Chem.* **50**, 985 (1978).

45. G. R. Kinsel, L. M. Preston, D. H. Russell, Fragmentation of vitamin B12 during 337 nm matrix-assisted laser-desorption ionization. *Biol. Mass Spectrom.* **23**, 205 (1994).

46. J. P. Speir, I. J. Amster, Substrate-assisted laser desorption of neutral peptide molecules. *Anal. Chem.* **64**, 1041 (1992).

47. J. P. Speir, G. S. Gorman, D. S. Cornett, I. J. Amster, Controlling the dissociation of peptide ions using laser desorption chemical ionization Fourier-transform mass-spectrometry. *Anal. Chem.* **63**, 65 (1991).

48. A. G. Harrision, *Chemical ionization mass spectrometry*. (CRC Press, Boca Raton, FL, 1983), pp. 156.

49. R. Tembreull, D. M. Lubman, Pulsed laser desorption of biological molecules in supersonic beam mass spectrometry with resonant two-photon ionization detection. *Anal. Chem.* **59**, 1082 (1987).

50. R. Tembreull, D. M. Lubman, Resonant two-photon ionization of small peptides using pulsed laser desorption in supersonic beam mass spectrometry. *Anal. Chem.* **59**, 1003 (1987).

51. I. Eide, K. r. Zahlsen, Chemical fingerprinting of biodiesel using electrospray mass spectrometry and chemometrics: Characterization, discrimination, identification, and quantification in petrodiesel. *Energ. Fuels* **21**, 3702 (2007).

52. N. Shibayama, S. Q. Lomax, K. Sutherland, E. R. d. l. Rie, Atmospheric pressure chemical ionization liquid chromatography mass spectrometry and its application to conservation: Analysis of triacylglycerols. *Stud. Conserv.* **44**, 253 (1999).

53. E. J. Judge, J. J. Brady, D. R. Dalton, R. J. Levis, Mass analysis of pharmaceutical compounds from glass, cloth, steel and wood surfaces at atmospheric pressure using non-resonant femtosecond laser vaporization and electrospray ionization *Anal. Chem.* **82**, 3231 (2010).

54. S. P. Mirza, B. D. Halligan, A. S. Greene, M. Olivier, Improved method for the analysis of membrane proteins by mass spectrometry. *Physiol. Genomics* **30**, 89 (2007).

55. C. C. Wu, J. R. Yates, The application of mass spectrometry to membrane proteomics. *Nat. Biotechnol.* **21**, 262 (2003).

56. J. J. Brady, E. J. Judge, R. J. Levis, Mass spectrometry of intact neutral macromolecules using intense non-resonant femtosecond laser vaporization with electrospray post-ionization. *Rapid Commun. Mass Spectrom.* **23**, 3151 (2009).

57. D. P. Little, J. P. Speir, M. W. Senko, P. B. O'Connor, F. W. McLafferty, Infrared multiphoton dissociation of large multiply charged ions for biomolecule sequencing. *Anal. Chem.* **66**, 2809 (1994).

58. R. Grandori, Origin of the conformation dependence of protein charge-state distributions in electrospray ionization mass spectrometry. *J. Mass Spectrom.* **38**, 11 (2003).

59. A. Sethuraman, G. Vedantham, T. Imoto, T. Przybycien, G. Belfort, Protein unfolding at interfaces: Slow dynamics of α-helix to β-sheet transition. *Proteins* **56**, 669 (2004).

CHAPTER 5

LEMS ANALYSIS OF AQUEOUS PROTEINS PRESERVES FOLDED CONFORMATION

5.1 Overview

In this chapter, the *in vitro* measurement of protein conformation using laser-based mass spectrometry at atmospheric pressure is presented. Cytochrome c and lysozyme are vaporized from the condensed phase into the gas phase intact when exposed to an intense (10^{13} W/cm^2), nonresonant (800 nm), ultrafast (75 femtosecond) laser pulse. Electrospray post-ionization mass spectrometry reveals that the vaporized protein maintains the solution-phase conformation through measurement of the charge state distribution and the collision-induced dissociation channels produced. This suggests that nonresonant fs laser vaporization with electrospray post-ionization of aqueous protein is a softer vaporization/ionization technique than conventional electrospray ionization mass spectrometry.

5.2 Introduction

The interaction of intense, ultra-short laser pulses with matter has resulted in a number of remarkable new phenomena including above threshold ionization (1, 2), high harmonic generation (3-5), Coulomb explosion (6), nonadiabatic excitation of polyatomic molecules (7, 8), neutron emission from clusters (9, 10) and the creation of attosecond laser pulses (5). Intense laser-matter interactions are currently used to determine polyatomic molecular electronic structure (11) and nuclear dynamics (12). Biomolecular

structure determination represents a new frontier for ultra-intense laser experiments. In this regard, methods to deliver non-volatile biological molecules intact into the gas phase, preferably maintaining condensed phase structure, are of interest. The previous chapter demonstrated that intense, nonresonant, ultrafast laser pulses could be used to deliver proteins with molecular weights of 14 kDa and larger (13) into the gas phase without fragmentation. One motivation for this investigation is that for femtosecond (fs) laser vaporization to be of value for protein structural determination, the vaporization must ideally preserve the condensed phase primary, secondary and tertiary conformation. Another motivation for these investigations is the fact that the analysis of biological structure *in situ* presents a significant challenge. As a first step toward this goal, we investigate the conformation of proteins vaporized from the solution phase, *in vitro,* using intense, nonresonant, fs laser pulses.

The biological function of a protein is determined by both primary sequence and structural conformation, with the latter governed by inter- and intra-molecular covalent and noncovalent interactions. Techniques such as x-ray crystallography (14), NMR spectroscopy (15) and hydroxyl-radical protein footprinting (16) are commonly used to determine protein conformation and to probe noncovalent interactions. However, another method, electrospray ionization mass spectrometry (ESI-MS) (17) can be used to assess protein conformation in the electrospray solvent solution since small folded proteins typically displays one or two intense peaks in the mass spectrum (18). Protein in an unfolded conformation results in a bell-shaped distribution of the peaks with the centroid of the distribution occurring at a lower mass-to-charge (*m/z*) value (than the folded features) due to the basic amino acids being revealed and protonated (18). Changes in

temperature, solvent, pH and salt concentration will alter the equilibrium concentration of folded and unfolded protein and thus alter the observed mass spectrum. Although remarkably successful, the aforementioned methods are not amenable for *ex vivo* studies of protein conformation and require extensive sample manipulation prior to measurement. For example, the extraction and preparation steps typically result in denaturing conditions, altering the equilibrium concentration of folded/unfolded protein. Therefore, a key question concerns whether protein can be transferred from the condensed phase into the gas phase without altering the structural conformation.

Nanosecond (ns) duration laser-based methods provide the opportunity to directly sample condensed phase material, but requires the addition of a matrix to transfer analyte into the gas phase. For example, matrix-assisted laser desorption/ionization (MALDI) has been used for *ex vivo* spatial distribution analysis of protein (19). In MALDI, the ns laser pulse couples into the externally applied matrix through a one-photon resonant excitation process at a laser intensity of approximately $10^6 - 10^7$ W/cm^2. The absorbed energy is transferred from the matrix to the condensed phase allowing for desorption and ionization of both the matrix and protein (20). Although MALDI-MS has successfully analyzed a variety of molecules, there is no provision for directly obtaining structural information for a protein. Such information requires extensive sample manipulation (21-23).

The coupling of laser-based desorption with electrospray post-ionization can allow not only for identification but also structural information for a given protein. Post-electrospray ionization of laser desorbed proteins has been achieved using techniques such as laser ablation electrospray ionization (24), electrospray-assisted laser desorption ionization (25) and matrix-assisted laser desorption electrospray ionization (26, 27). The

aqueous proteins are delivered into the gas phase at atmospheric pressure using a ns laser resonant with a vibrational transition in water. The deposition of energy into the water induces a phase explosion similar to MALDI, transferring material into the gas phase (24). The accompanying heating in the ns laser desorption event presumably causes the aqueous protein to unfold. For example, unfolded bovine cytochrome c is observed in the mass spectrum upon infrared ns laser desorption with electrospray post-ionization (25-28).

The use of nonresonant fs laser pulses for vaporization may prevent thermal processes since the energy of the laser pulse is deposited into the system on a timescale much faster than that required for any ensuing thermal response. Time-resolved measurements in metallic systems reveal that after the initial electronic excitation, the internal modes of the condensed phase system heat on the picosecond to nanosecond timescale (29). If the nonequilbrium channel of vaporization occurs prior to thermalization to protein modes, dissociation can be avoided. In fact, the interaction of intense, nonresonant, fs laser pulses (70 fs, 10^{13} W/cm^2) with a condensed phase sample at atmospheric pressure results in the intact vaporization of a wide variety of non-volatile polyatomic molecules in systems ranging from explosive formulations to plant tissue (30-33). The discovery that a strong field fs laser pulse can transfer neutral macromolecules into the gas phase *intact* (34) was unanticipated since isolated molecules in vacuum exposed to an intense laser pulse will ionize and possibly fragment (35, 36). The nonresonant fs laser pulse can, in principle, couple into and vaporize all molecules in a given sample. This implies that the sample preparation steps of elution and mixing with a matrix are not necessary. Direct analysis of molecules ranging in size from

pharmaceuticals (~ 300 Da) to proteins (> 40 kDa) has been performed using the laser electrospray mass spectrometry (LEMS) method (13, 30-34) where ionization, mass analysis and detection of the fs laser vaporized sample is achieved via atmospheric pressure electrospray ionization time-of-flight mass spectrometry.

In this work, we investigate the interaction of intense nonresonant fs laser pulses with aqueous proteins to determine whether nonequilibrium processes enable the transfer of protein into the gas phase without altering the initial condensed phase structural conformation. The conformation of the vaporized protein is probed by measuring the resulting electrospray post-ionization mass spectrometry charge state distribution as well as the collision-induced dissociation (CID) channels. The LEMS measurements, as a function of electrospray solvent pH and sample pH, are compared to conventional ESI-MS experiments.

5.3 Experimental

5.3.1 Sample preparation

A solid sample of cytochrome c was purchased from Sigma Aldrich (St. Louis, MO, USA) and used without purification. For the conventional ESI-MS samples, a stock solution of 2 x 10^{-4} M was prepared in 10 mM ammonium acetate buffer. A 1 x 10^{-5} M solution was then prepared by diluting an aliquot of the stock solution in a pH controlled 1:1 (v:v) methanol:water solution containing 5 mM ammonium acetate (pH range 7-4). A 8 x 10^{-4} M cyctochrome c solution was prepared in deionized water for LEMS analysis. A denatured cytochrome c sample was also prepared for LEMS analysis by diluting a portion of the 8 x 10^{-4} M cytochrome c solution in a 1:1 (v:v) ratio with 1:1 (v:v)

methanol:water containing 5 mM ammonium acetate (pH 4). This solution was further acidified with acetic acid to a pH ~3.

A solid sample of hen egg white lysozyme was purchased from Sigma Aldrich and used without purification. For the conventional ESI-MS samples, a 1 x 10^{-4} M solution of lysozyme was prepared in 1:1 (v:v) acetonitrile:water with 1.0% acetic acid. For the LEMS analysis, a 1 x 10^{-3} M of lysozyme was prepared in deionized water.

The LEMS analysis was performed in the aqueous state with a 10 μL aliquot of each solution being deposited on separate stainless steel substrates prior to analysis. The substrate was supported by a three dimensional translation stage which permitted the analysis of fresh sample.

5.3.2 Laser vaporization and ionization apparatus

A Ti:Sapphire oscillator seeded a regenerative amplifier to create a 2.5 mJ pulse centered at 800 nm with a duration of 70 fs. The 500 Hz repetition rate of the laser was reduced to 10 Hz to couple to the electrospray system. The energy of the laser pulse was reduced to 1.5 mJ/pulse using neutral density filters prior to being directed to the sample by a mirror. The laser was focused to a spot size of ~ 250 μm in diameter using a 17.5 cm focal length lens, with an incident angle of 45° with respect to the sample (Figure 5.1). The intensity of the laser at the substrate was approximately 4.3 x 10^{13} W/cm^2. The vaporized sample was captured and ionized by an electrospray plume composed of pH adjusted 5 mM ammonium acetate buffer in 1:1 (v:v) methanol:water (cytochrome c experiments) or 1:1 (v:v) acetonitrile:water acidified with 1.0% glacial acetic acid (lysozyme experiments) traveling perpendicular to the laser-vaporized material at a flow rate of 3 μL/min as set by a syringe pump. The charged droplets containing the captured

sample were dried by counter propagating nitrogen gas at 180°C prior to entering the inlet capillary.

5.3.3 Mass spectrometry

The ionized sample enters the electrospray source via a dielectric capillary (both ends coated with metal). The positive ions pass through the capillary where they are directed to a skimmer and a hexapole. The ions are transferred to the extraction region by electrospray source ion optics and a second hexapole. Once the positive ions enter the extraction region two high voltage pulsers are used to transfer the ions into the linear time-of-flight mass analyzer. The positive ions were then detected and the resulting mass spectra were averaged for 5 seconds (50 mass spectra) using a digital oscilloscope.

For the conventional ESI-MS measurements reported here, the solution to be analyzed was electrosprayed at a flow rate of 0.6 μL/min and 200 spectra were collected and averaged. The electrosprayed solutions were composed of the same solvent as that used for the LEMS analysis of the respective protein samples. No laser was present during the ESI-MS measurements and no background subtraction was performed on the collected ESI mass spectrum. The ESI experiments had the same voltage conditions as the LEMS to ensure uniform conditions for all experiments.

5.3.4 Collision induced dissociation (CID) experiments

In the region between the electrospray capillary exit and the skimmer in the ESI source there is ~1.2 Torr of N_2 gas which induces a large number of protein-N_2 collisions (Figure 5.1). Energy is imparted into the molecule upon collision with this background gas molecule. The maximum energy that can be transferred into the internal modes of a protein via a collision with the background N_2 gas scales with the magnitude of the

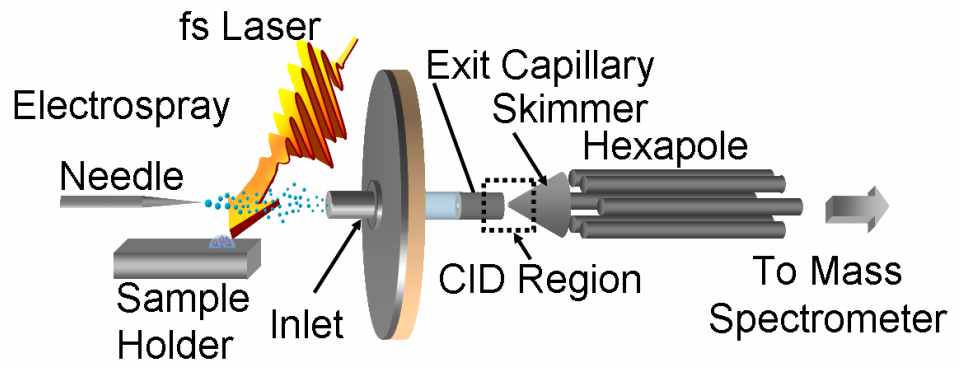

Figure 5.1. A schematic of the LEMS technique. A nonresonant fs laser irradiates an aqueous sample, vaporizing the analyte molecules. The molecules are captured and ionized by the electrospray plume prior to entering the mass spectrometer. The ions are then mass analyzed or undergo collision-induced dissociation with subsequent mass analysis.

acceleration potential as set by the voltage difference between the capillary exit and the skimmer in the electrospray source. The acceleration potential can be adjusted by varying the voltage difference between the capillary exit and the skimmer in the electrospray source (50 V- 390 V). Ten mass averaged spectra were acquired at each acceleration potential for both the conventional ESI-MS and LEMS experiments.

5.3.5 Safety consideration

Appropriate laser eye protection was worn by all personnel and the high voltage area was enclosed in plexiglass to prevent accidental contact with the biased electrodes.

5.4 Results and discussion

5.4.1 Conventional ESI-MS of cytochrome c as a function of pH

The mass spectral charge state distribution of an electrosprayed protein provides a direct indication of the structural conformation, folded versus unfolded (*18*). Thus, the conventional ESI mass spectrum of cytochrome c can be measured as a function of acid concentration to serve as a calibrant for the analysis of protein structure after fs laser vaporization and electrospray post-ionization. The ESI mass spectrum of cytochrome c electrosprayed from a solvent at pH 7.18 displays two distributions: one containing predominantly the 8+ and 7+ charge states and the second containing a bell-shaped distribution (ranging from 17+ to 9+) centered at the 12+ charge state (Figure 5.2). The n+ charge state represents the ion with *m/z* (M+n)/(n), where *M* is the mass of the molecule and *n* is the number of additional protons (H^+) bound to the molecule. The 8+ and 7+ charge states correspond to a folded conformation of cytochrome c as revealed by

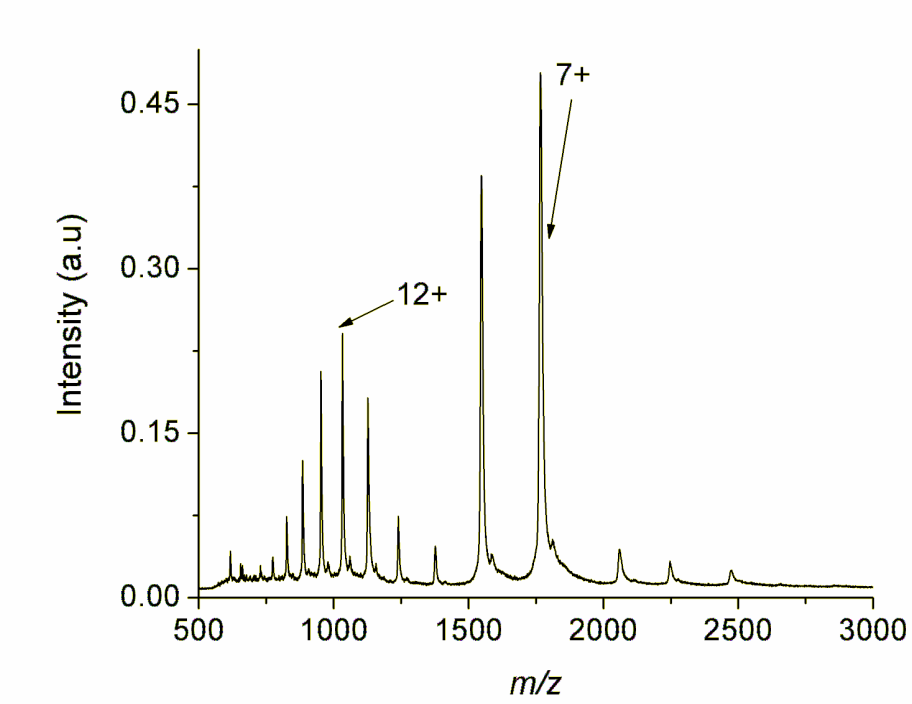

Figure 5.2. The conventional ESI mass spectrum of cytochrome c collected at pH 7.18.

nano-ESI-MS experiments (*37*). However, it should be noted that each charge state may contain several different conformations of the three dimensional structure (*38*).

The charge state distribution observed in the ESI mass spectrum centered at 12+ corresponds to an unfolded conformation of cytochrome c (*37, 39, 40*). Unfolded cytochrome c is detected in the conventional ESI mass spectrum at neutral pH where only folded protein is expected. This is due to denaturing in the electrospray solvent containing 50% methanol by volume (*41, 42*) and a decrease in pH in the electrospray droplet during the electrospray process (*43, 44*).

The structural conformation of cytochrome c is sensitive to pH and should shift to higher charge states (with more states populated) as the pH decreases (*42*). As anticipated, the unfolded state of cytochrome c dominates the distribution under increasingly acidic solvent conditions (pH 6 to 4, Figures 5.3 to 5.5). The conventional ESI-MS spectra obtained (Figures 5.2 to 5.5) are in agreement with previous ESI-MS measurements as a function of pH (*42*).

5.4.2 LEMS analysis of cytochrome c as a function of electrospray solvent pH

When a fs laser pulse interacts with a condensed phase system, electrons are excited resonantly via a single photon, or nonresonantly via multiphoton excitation. In either case, the energy of the nascent, "hot" electrons is transferred into the phonon modes of the system on the picosecond timescale (*29, 45*), a timescale which is many orders of magnitude shorter than that required for protein unfolding (*46*). If the protein is vaporized prior to achieving thermal equilibrium, the initial conformation may be

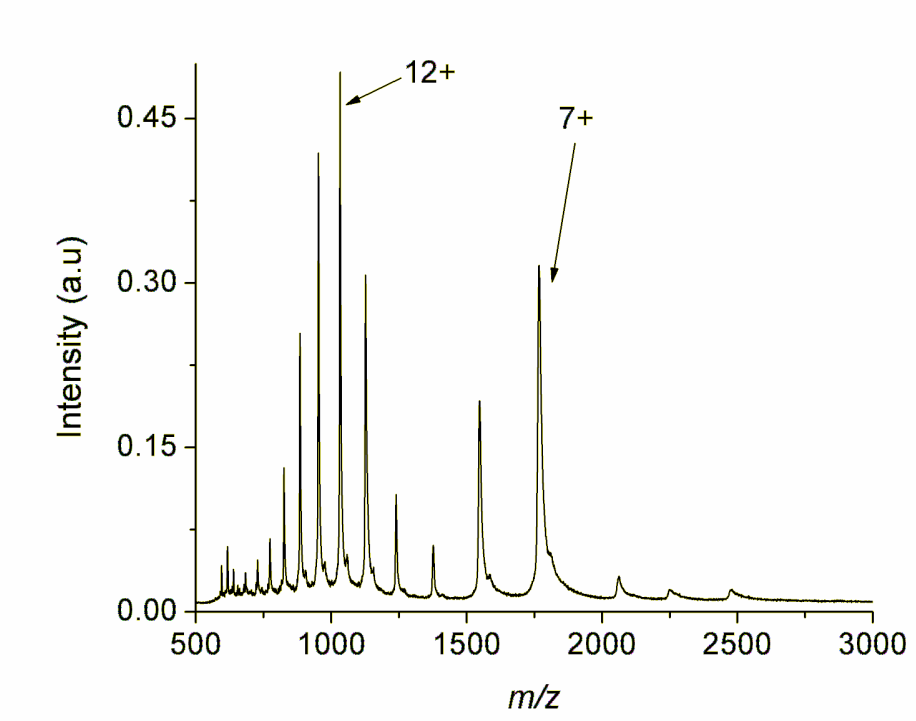

Figure 5.3. The conventional ESI mass spectrum of cytochrome c collected at pH 6.07.

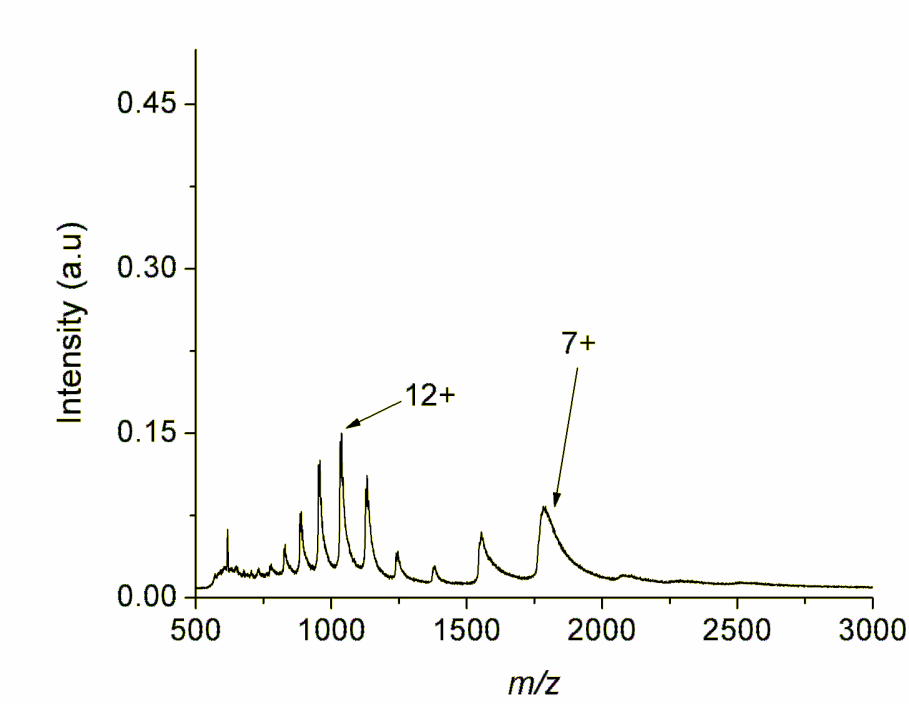

Figure 5.4. The conventional ESI mass spectrum of cytochrome c collected at pH 5.06.

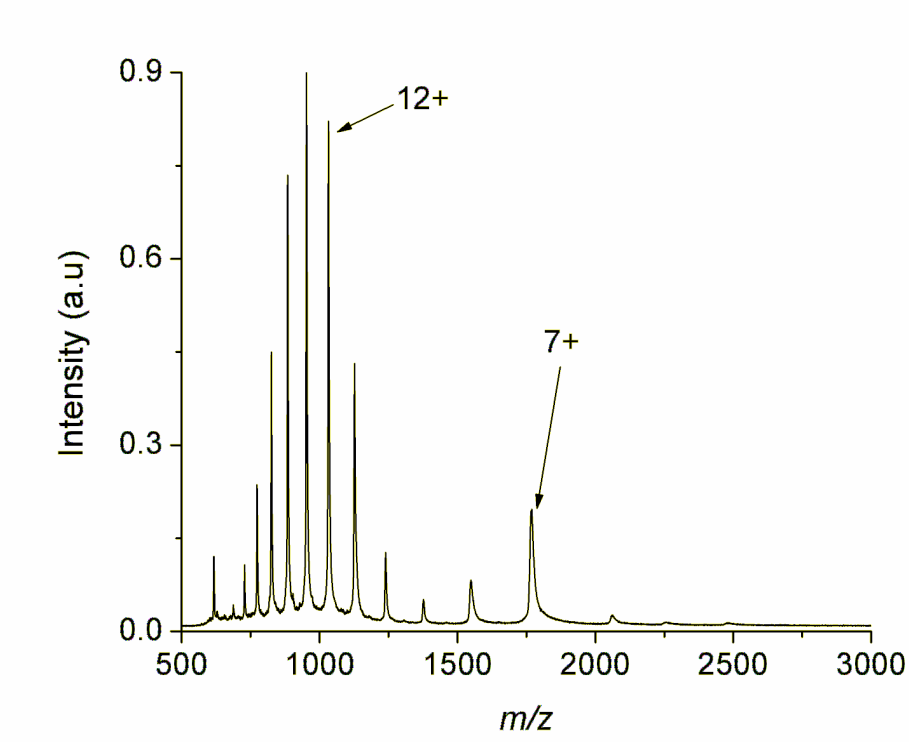

Figure 5.5. The conventional ESI mass spectrum of cytochrome c collected at pH 4.06.

maintained in the gas phase. The charge state distribution of aqueous cytochrome c was analyzed to determine whether nonresonant fs laser vaporization alters a protein's tertiary structure via thermal denaturation. The protein sample was dissolved to a concentration of 8 x 10^{-4} M in deionized (DI) water at pH 7 where native (folded) noncovalent interactions are preserved (*47*). A 10 μL aliquot was deposited onto a stainless steel slide for LEMS analysis. After interaction with the fs laser, the vaporized protein was captured in the same series of solvents (buffered 1:1 (v:v) water:methanol, pH adjusted) used for the conventional ESI-MS measurements. The measured charge state distributions (Figure 5.6 to 5.9) resulting from the intense, nonresonant fs laser vaporization with subsequent capture and ionization in an electrospray plume are quite different in comparison with conventional ESI-MS. Only the folded conformation (as revealed by the 8+ and 7+ charge states) is detected when the vaporized protein was captured and ionized by an electrospray plume at pH 7.18 (Figure 5.6) or 6.07 (Figure 5.7). The data suggests that intense, nonresonant fs laser vaporization prevents thermal denaturation and therefore allows for the condensed phase conformation of the protein to be preserved upon transfer into the gas phase. In addition, intense, nonresonant fs laser vaporization with electrospray post-ionization preserves the condensed phase conformation even when a denaturant (methanol) is present in the electrospray solvent. However, unfolded protein is observed in the mass spectrum when vaporized into an electrospray plume at pH 5.06 (Figure 5.8) and 4.06 (Figure 5.9), suggesting that the denaturation rate increases at higher acid concentrations in the electrospray plume

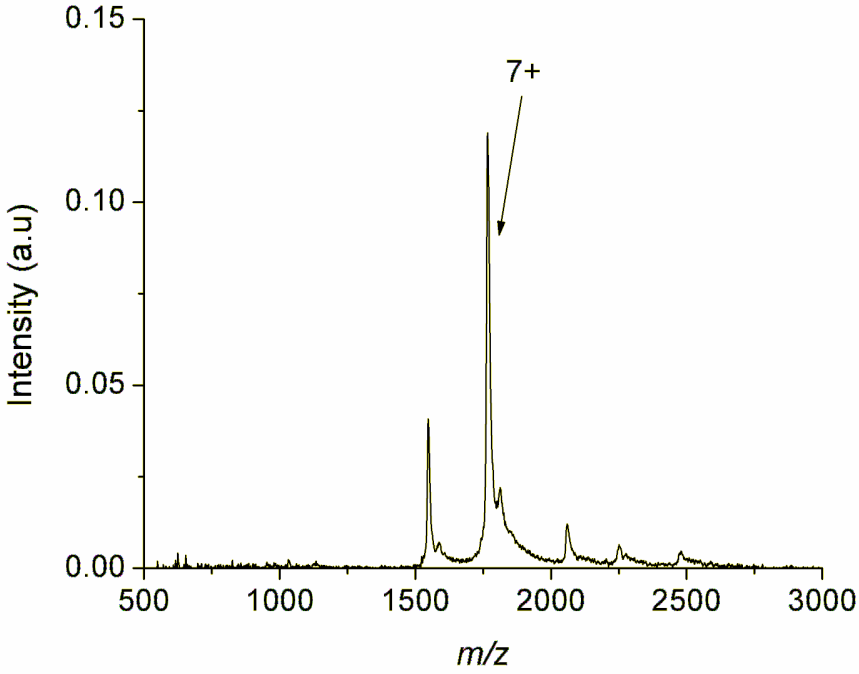

Figure 5.6. The LEMS mass spectrum resulting from the nonresonant fs laser-induced vaporization of aqueous cytochrome c followed by capture and ionization in an electrospray plume at pH 7.18.

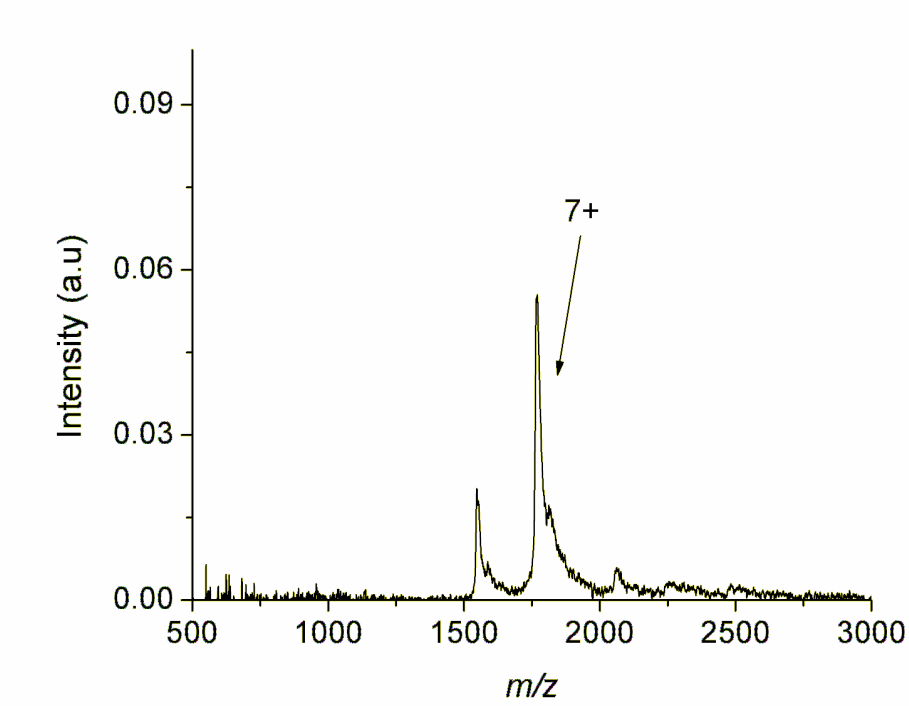

Figure 5.7. The LEMS mass spectrum resulting from the nonresonant fs laser-induced vaporization of aqueous cytochrome c followed by capture and ionization in an electrospray plume at pH 6.07.

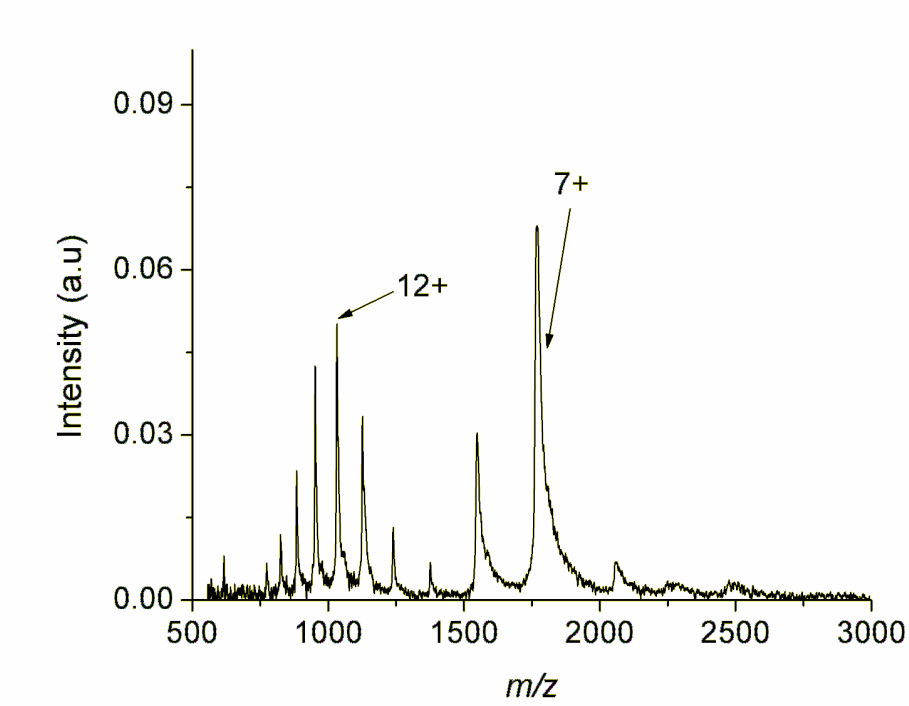

Figure 5.8. The LEMS mass spectrum resulting from the nonresonant fs laser-induced vaporization of aqueous cytochrome c followed by capture and ionization in an electrospray plume at pH 5.06.

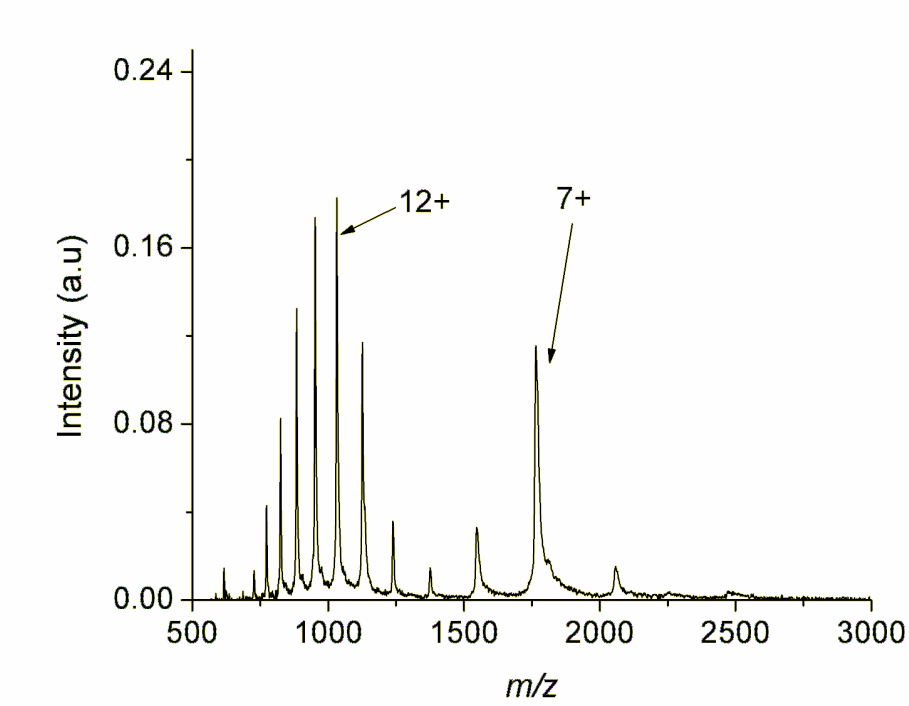

Figure 5.9. The LEMS mass spectrum resulting from the nonresonant fs laser-induced vaporization of aqueous cytochrome c followed by capture and ionization in the electrospray plume at pH 4.06.

5.4.3 LEMS analysis as a function of pH of the vaporized sample

To further explore the hypothesis that LEMS preserves the condensed phase conformation of protein, we measured the charge state distribution as a function of pH of the protein solution deposited onto the sample plate. When cytochrome c is vaporized from a non-denaturing solution (pH 7) and captured and ionized by an electrospray solvent at neutral pH, only folded protein is observed in the mass spectrum (Figure 5.6). This is expected since the pH of both solvent systems (sample solution and electrospray solvent) are non-denaturing. However, when cytochrome c is vaporized from a denaturing solution (pH 3) prior to capture and ionization by a non-denaturing electrospray solvent (pH 7), unfolded protein is observed in the mass spectrum (Figure 5.10). This reveals that the conformation of the condensed phase protein, whether folded or unfolded, is reflected in the ESI charge state distribution and may be due to the short interaction time with the electrospray plume. Nevertheless, these measurements further support the hypothesis that intense, nonresonant fs laser vaporization of protein maintains the condensed phase conformation.

5.4.4 Quantification of the charge state distributions of cytochrome c as a function of electrospray pH

The ratio of folded cytochrome c to the total protein signal was plotted as a function of electrospray solvent pH for both techniques in Figure 5.11. At every pH measured, the fraction of folded protein is higher for the LEMS experiment in comparison to conventional ESI-MS experiment. At pH 7.18 and 6.07, only folded protein is observed for the LEMS experiments while ~ 40% of the protein resides in the

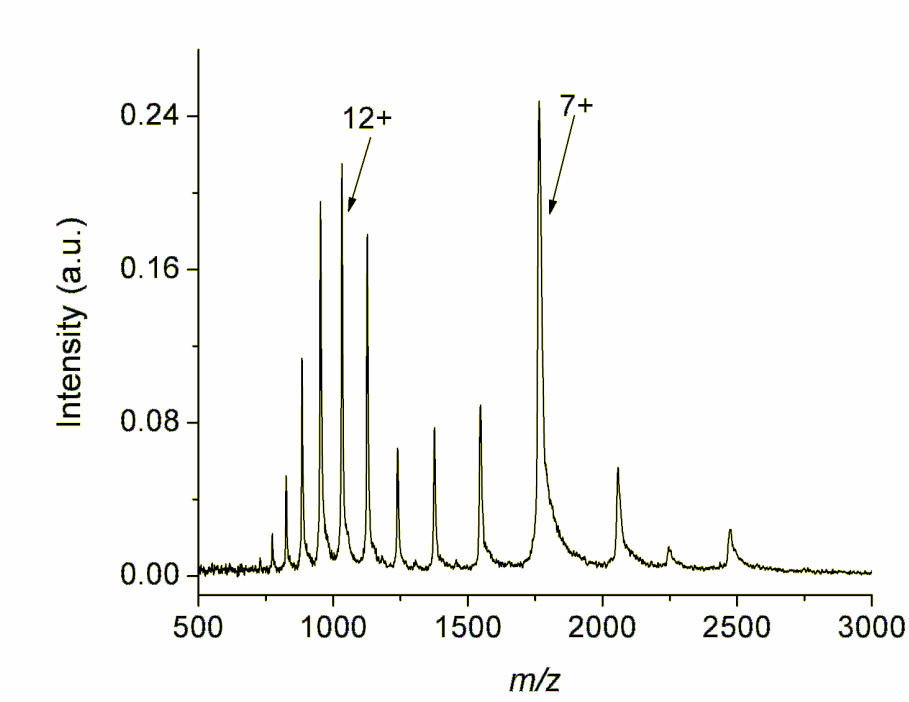

Figure 5.10. The LEMS mass spectrum resulting from the nonresonant fs laser-induced vaporization of aqueous cytochrome c dissolved in DI water acidified with acetic acid followed by capture and ionization in an electrospray plume at pH 7.06.

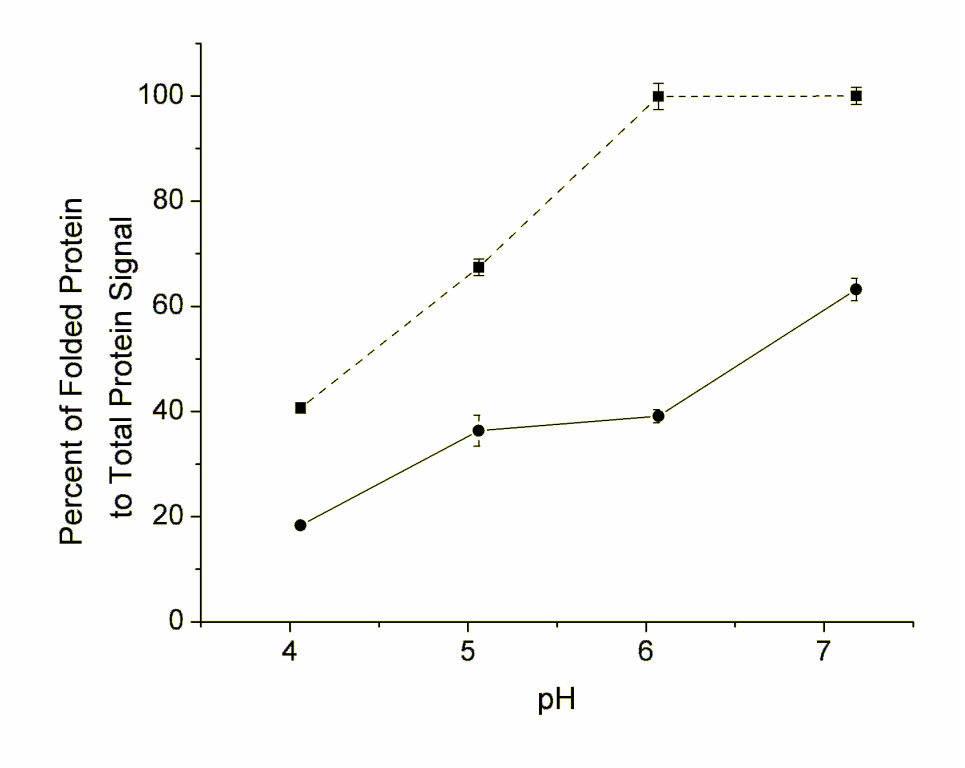

Figure 5.11. The percent of folded protein vs. the total protein signal resulting from the LEMS experiments (■, dashed line) and the conventional ESI-MS experiments (●, solid line).

unfolded state for conventional ESI-MS experiments. In the ESI-MS experiments, the protein spends minutes in solution allowing the folded/unfolded ratio to reach equilibrium at a given pH. In the LEMS experiment, the protein remains in the electrospray solvent for approximately 100 ms upon capture, which is short compared to the time scale of several seconds required for unfolding to a denatured state (*48*). Therefore, the condensed phase conformation is detected in the mass spectrum due to the mismatch in these time scales. In addition, the detection of folded protein in the LEMS experiments could be partially due to the capture, solvation and ionization of the vaporized sample by smaller droplets in the electrospray plume. Smaller droplets prevent a decrease in pH during the electrospray droplet formation process, reducing denaturation conditions in a manner similar to that seen in high gas flow ESI measurements (*49, 50*). However, as the pH of the electrospray solvent decreases, the denaturation rate increases to a point that unfolding can occur during the short transit time spent in the solvent droplet (*51*), prior to evaporation, allowing for a higher fraction of the protein to be observed in the unfolded conformation. Thus, we conclude that the limited interaction time of the vaporized protein with the denaturing electrospray plume enables LEMS to be a much softer mass spectrometric method than conventional ESI-MS. A softer vaporization/ionization method allows for direct determination of a protein's condensed phase conformation without further time consuming experiments or sample preparation.

5.4.5 Conventional ESI-MS of lysozyme as a function of CID energy

Collision-induced dissociation (CID) studies have been used to probe the structural conformation (*52, 53*) of a gas phase protein. Gas phase dissociation of analyte can be induced depending on the CID cross section, the number of collisions and the

energy transferred to the molecules. The CID cross section for lysozyme in a folded and unfolded conformation is approximately 750 $Å^2$ and 1,125 $Å^2$, respectively (*54*). Unfolded lysozyme will undergo more collisions as compared to folded lysozyme, and on average, more energy per collision will be transferred into the unfolded protein. In the CID experiment, the maximum energy (E_T) that can be transferred into the internal modes of the protein, via a collision between an ion of mass m_i and a background target gas molecule of mass m_n, is given by $E_T = qV_D\ [m_n/\ (\ m_n + m_i)]$ where q is the charge of the ion and V_D is the voltage differential between the skimmer and capillary (acceleration potential) in the ESI source (*55*). To provide some point of reference, the maximum energy that will be transferred into the internal modes of lysozyme for the folded (9+) and unfolded (12+) conformations at an acceleration potential of 390 V after a collision with N_2 is approximately 6.8 eV and 9.1 eV, respectively. However, a protein in an unfolded conformation has a lower probability of redistributing the collision energy into other available internal modes. Thus, the folded protein should survive an energetic collision with a background gas molecule without fragmentation (*56, 57*), while an unfolded protein will have a higher probability to fragment (*57*).

The CID experiment represents another means to probe the gas phase conformation of the protein (*52, 53*). To test the hypothesis that LEMS transfers protein into the gas phase without conformational change, a second protein, hen egg white lysozyme was investigated first using conventional ESI-MS. The conventional ESI mass spectra of lysozyme (pH 3.25) at different acceleration potentials reveal that the observed charge state distribution is highly sensitive to the collision energy (Figure 5.12). At an acceleration potential of 50 V, a bell-shaped distribution corresponding to the charge

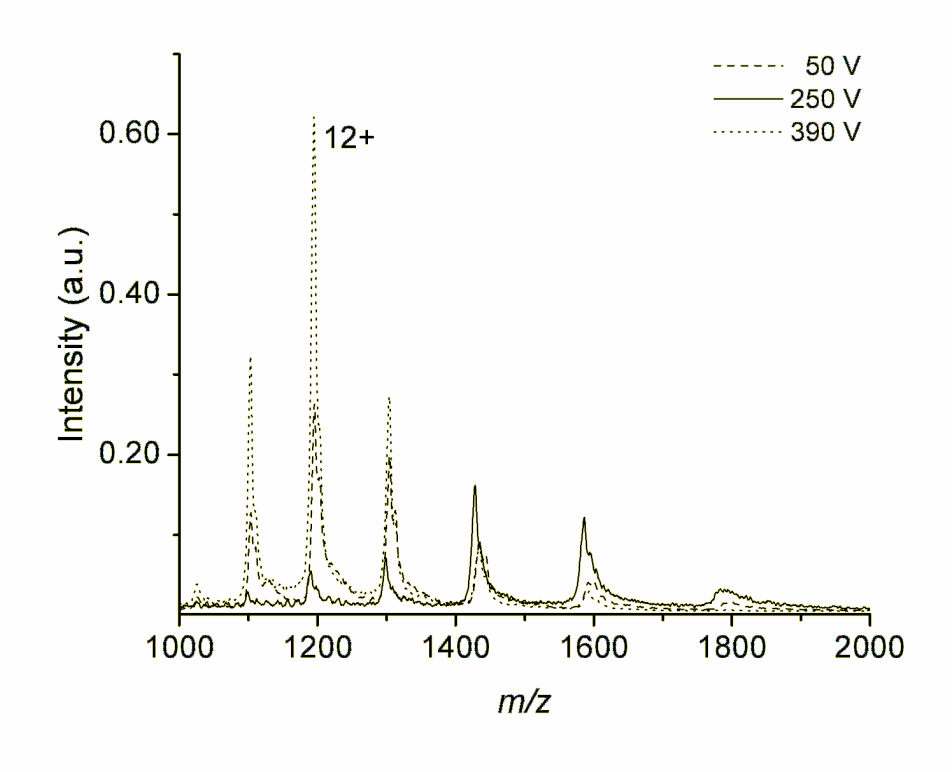

Figure 5.12. The conventional ESI mass spectra of hen egg white lysozyme for the acceleration potentials of 50 V (dash), 250 V (dot) and 390 V (solid).

states ranging from 13+ to 8+ is measured, suggesting that the protein is in an unfolded conformation (*37, 42, 58*). The bell-shaped distribution is maintained as the acceleration potential approaches 250 V, but increases in abundance. The increase in the ion abundance at higher acceleration potentials is attributed to the fact that the protein ions are moving at a higher velocity toward the skimmer, decreasing the expansion of ions to regions outside of the skimmer inlet radius due to space charge (Coulomb repulsion) effects. In addition, the increase in the ion abundance is due to the removal of adducts (water and acetonitrile molecules) that are loosely bound to the lysozyme ion. The removal of the adducts transfers ion abundance from the shoulder peak ($[M+3H_2O+CH_3CN+nH^+]^{n+}$) into the adduct free lysozyme peak (n+, i.e., $[M+nH^+]^{n+}$). As the acceleration potential is increased to 390 V, a decrease in ion abundance is observed and the charge states shift (*e.g.,* $[M+nH]^+$ to $[M+(n-1)H]^+$) due to the collision-induced loss of loosely bound cations (*59, 60*). It should be noted that the observed charge states correspond to an unfolded conformation of lysozyme with the disulfide bonds intact. If the disulfide bonds in lysozyme were reduced, higher charge states, ranging from 20+ to 12+, would be observed in the ESI mass spectrum (*61*).

5.4.6 LEMS analysis of lysozyme as a function of CID energy

In this set of experiments, a 10 μL aliquot of lysozyme solution (1×10^{-3} M, dissolved in DI water) was deposited onto a steel surface and vaporized using a fs laser pulse prior to capture and ionization in the electrospray plume (1:1 (v:v) acetonitrile:water with 1.0% acetic acid). The CID measurements of the LEMS analysis are quantitatively different than those for conventional ESI-MS. The LEMS mass spectrum collected at low collision energy (acceleration potential = 100 V) displays the

10+ and 9+ charge states which corresponds to a folded conformation (Figure 5.13) (*18, 62*). Upon increasing the acceleration potential to 390 V, an increase in the ion abundance was observed with no additional fragmentation or change in the charge state distribution. The increase in ion abundance at high acceleration potentials is attributed to the decrease in space charge effects and removal of loosely bound adducts, as seen with the conventional ESI-MS of lysozyme. The folded protein signal is dominant for the LEMS measurements in comparison to the conventional ESI-MS experiments at each collision energy, again suggesting that the folded structure (*18, 62*) is preserved under the intense laser pulse conditions.

5.4.7 Quantification of the charge state distributions of lysozyme as a function of acceleration potential (CID energy)

To further explore the hypothesis that LEMS analysis preserves the folded structure of proteins under conditions where conventional ESI-MS does not, we measured the integrated ion abundance from the various charge states as a function of collision energy for both techniques. The total ion abundance contained in the conventional ESI mass spectra was plotted as a function of acceleration potential as shown in Figure 5.14. As the acceleration potential increases to ~ 250 V, the lysozyme signal monotonically increases due to the reduction of space charge effects and loss of non-covalently bound adducts. However, above 250 V, a decrease in the intact ion abundance is measured due to charge reduction and fragmentation, which is consistent with the notion that a denatured protein has a larger CID cross section.

In the case of the fs laser-induced vaporization with electrospray post-ionization, the integrated ion abundance as a function of acceleration potential reveals no evidence

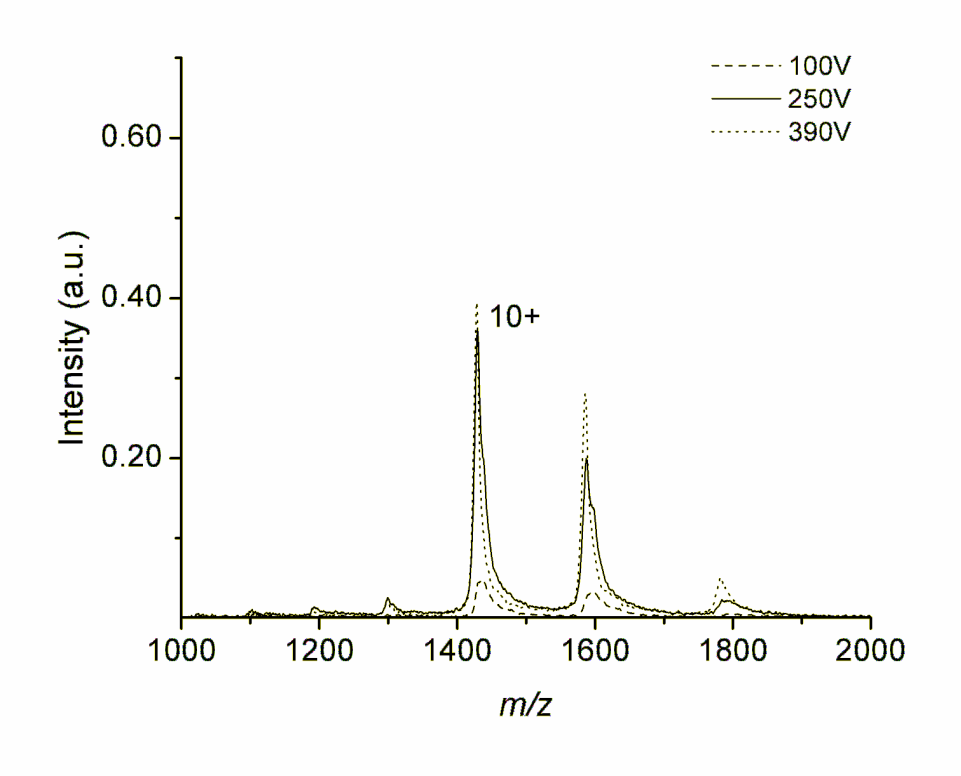

Figure 5.13. The LEMS mass spectra of hen egg white lysozyme for the acceleration potentials of 100 V (dash), 250 V (dot) and 390 V (solid).

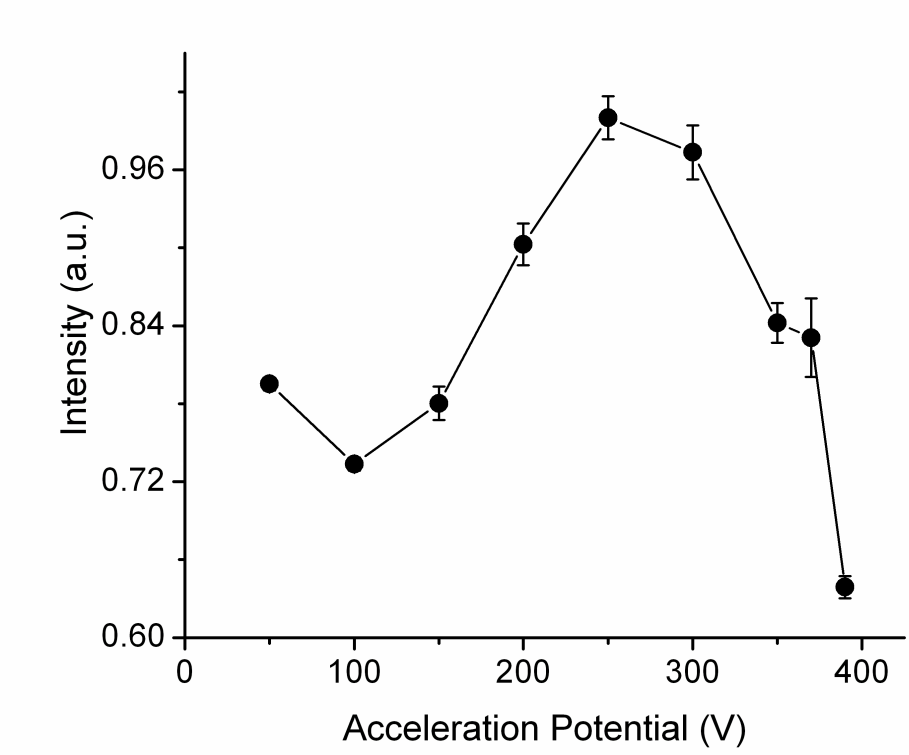

Figure 5.14. The integrated ion abundance of lysozyme as a function of acceleration potential using conventional ESI.

for fragmentation at higher collision energy (Figure 5.15). The lack of fragmentation and the absence of charge reduction is consistent with vaporization of folded protein. There is no decrease in signal above an acceleration potential of 250 V because the folded structure suffers fewer collisions. Any energy deposited during the collision is rapidly transferred away from the impact site due to the folded conformation providing multiple points of contact facilitating intramolecular energy redistribution. Therefore, we conclude that the structure of the gas phase lysozyme is quite different for the conventional ESI-MS experiments and the LEMS experiments.

The nonresonant fs laser pulse has sufficient intensity (10^{13} W/cm^2) to couple into pure protein (13), water and/or the metal substrate via a multiphoton excitation to enable the transfer of sample into the gas phase. The vaporization process resulting from the absorption of the laser pulse energy may proceed through several possible mechanisms. In one such mechanism, the condensed phase system can be excited into a repulsive adsorbate-substrate or a repulsive adsorbate-adsorbate (*e.g.,* protein-protein, protein-water) electronic state by either the direct absorption of photons or by collisions with hot electrons (1-10 eV) (*63-65*). This converts photon energy into potential energy which is subsequently transformed into translational kinetic energy due to electronic repulsion, enabling the transfer of molecules and clusters into the gas phase.

In addition, it is also possible that the electrons created at the metal surface can undergo cooling via collisions leading to the direct vibrational excitation of intramolecular bonds of the molecules (*66*). The excitation of the vibrational modes leads to expansion of the molecules against neighboring molecules, or the substrate, leading to

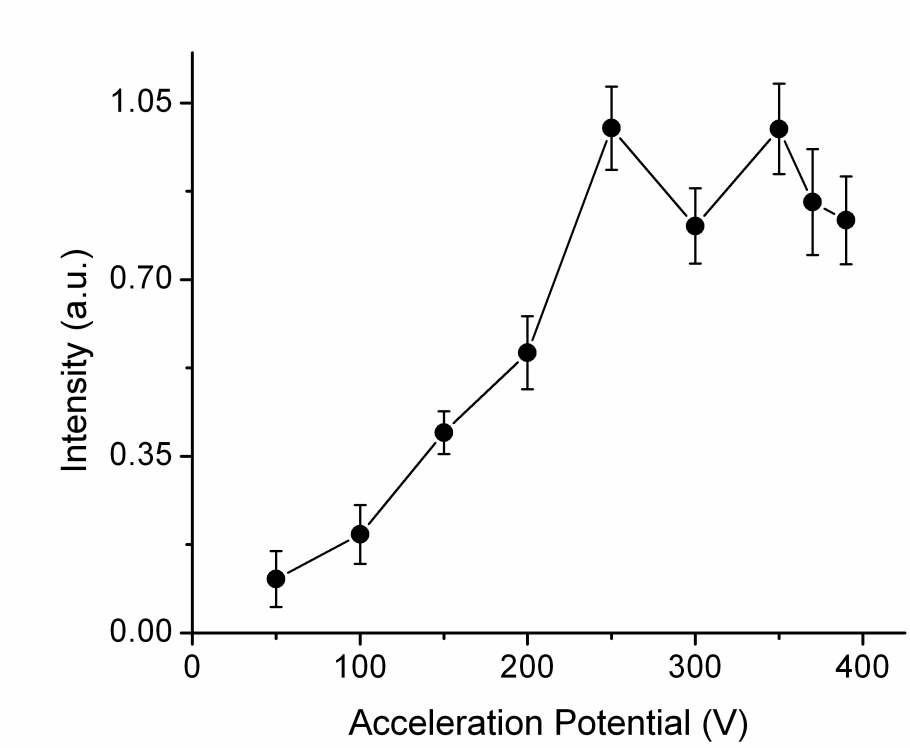

Figure 5.15. The integrated ion abundance of lysozyme as a function of acceleration potential using LEMS.

the creation of a pressure pulse ejecting molecules and clusters from the surface. The temperature of the vaporized material is equal to that of the local surface (*67*).

Once vaporized, the molecules or clusters undergo expansion into the gas phase where collisions with the background gas further decrease the internal energy, lowering the temperature and preventing molecular dissociation and unfolding of the protein (*68, 69*). We estimate that the final temperature of the molecules prior to capture in the electrospray plume is ~ 300 K. This allows the detection of intact protein, preserving condensed phase conformation, when nonresonant, fs laser vaporization is combined with post-electrospray ionization and time-of-flight mass analysis.

5.5 Conclusions

An intense, (10^{13} W/cm^2) nonresonant fs laser pulse can be used to vaporize macromolecules from their native environment into the gas phase for capture and ionization in an electrospray plume at atmospheric pressure. The discovery that intact vaporization of condensed phase protein can be induced using a nonresonant fs laser pulse (13, 30-34) was unanticipated since isolated protein in the gas phase under vacuum conditions will inevitably ionize and fragment (35, 36). The ability to analyze the molecular weight of proteins using LEMS was recently reported (13) and here we have shown that a protein's structural conformation is preserved upon intense, nonresonant fs laser vaporization. The ultrafast deposition of energy into the sample results in the nonthermal transfer of adsorbed protein into the gas phase preventing thermal denaturation (*i.e.,* alteration of protein's conformation). In addition to the nonthermal vaporization mechanism, the limited interaction time of the vaporized protein with the

denaturing solvent enables LEMS to be a softer vaporization/ionization method than conventional ESI-MS when using identical electrospray conditions. The ability to vaporize proteins while maintaining a folded conformation is an important step towards the measurement of noncovalent protein-protein and enzyme-substrate interactions. These measurements suggest that investigation of the *ex vivo* protein conformation analysis is now possible.

References

1. U. Mohideen *et al.*, High-intensity above-threshold ionization of He. *Phys. Rev. Lett.* **71**, 509 (1993).
2. R. R. Freeman *et al.*, Above-threshold ionization with subpicosecond laser-pulses. *Phys. Rev. Lett.* **59**, 1092 (1987).
3. T. Brabec, F. Krausz, Intense few-cycle laser fields: Frontiers of nonlinear optics. *Rev. Mod. Phys.* **72**, 545 (2000).
4. T. Popmintchev *et al.*, Phase matching of high harmonic generation in the soft and hard x-ray regions of the spectrum. *P. Natl. Acad. Sci. U.S.A.* **106**, 10516 (2009).
5. J. Mauritsson *et al.*, Attosecond pulse trains generated using two color laser fields. *Phys. Rev. Lett.* **97**, (2006).
6. K. Codling, L. J. Frasinski, Dissociative ionization of small molecules in intense laser fields. *J. Phys. B-At. Mol. Opt.* **26**, 783 (1993).
7. M. Lezius *et al.*, Nonadiabatic multielectron dynamics in strong field molecular ionization. *Phys. Rev. Lett.* **86**, 51 (2001).

8. A. N. Markevitch *et al.*, Nonadiabatic dynamics of polyatomic molecules and ions in strong laser fields. *Phys. Rev. A* **68**, (2003).

9. K. W. D. Ledingham, P. McKenna, R. P. Singhal, Applications for nuclear phenomena generated by ultra-intense lasers. *Science* **300**, 1107 (2003).

10. T. Ditmire *et al.*, Nuclear fusion from explosions of femtosecond laser-heated deuterium clusters. *Nature* **398**, 489 (1999).

11. H. J. Worner, H. Niikura, J. B. Bertrand, P. B. Corkum, D. M. Villeneuve, Observation of electronic structure minima in high-harmonic generation. *Phys. Rev. Lett.* **102**, (2009).

12. L. Nugent-Glandorf, M. Scheer, D. A. Samuels, V. Bierbaum, S. R. Leone, A laser-based instrument for the study of ultrafast chemical dynamics by soft x-ray-probe photoelectron spectroscopy. *Rev. Sci. Instrum.* **73**, 1875 (2002).

13. E. J. Judge, J. J. Brady, R. J. Levis, Mass analysis of biological macromolecules at atmospheric pressure using nonresonant femtosecond laser vaporization and electrospray ionization. *Anal. Chem.* **82**, 10203 (2010).

14. K. Palczewski *et al.*, Crystal structure of rhodopsin: A G protein-coupled receptor. *Science* **289**, 739 (2000).

15. N. Tjandra, A. Bax, Direct measurement of distances and angles in biomolecules by NMR in a dilute liquid crystalline medium. *Science* **278**, 1111 (1997).

16. T. D. Tullius, B. A. Dombroski, Hydroxyl radical "Footprinting": High-resolution information about DNA-protein contacts and application to lambda repressor and cro protein. *P. Natl. Acad. Sci. U.S.A.* **83**, 5469 (1986).

17. J. B. Fenn, M. Mann, C. K. Meng, S. F. Wong, C. M. Whitehouse, Electrospray ionization for mass-spectrometry of large biomolecules. *Science* **246**, 64 (1989).

18. R. Grandori, Origin of the conformation dependence of protein charge-state distributions in electrospray ionization mass spectrometry. *J. Mass Spectrom.* **38**, 11 (2003).

19. E. H. Seeley, S. R. Oppenheimer, D. Mi, P. Chaurand, R. M. Caprioli, Enhancement of protein sensitivity for MALDI imaging mass spectrometry after chemical treatment of tissue sections. *J. Am. Soc. Mass Spectrom.* **19**, 1069 (2008).

20. K. Dreisewerd, M. Schürenberg, M. Karas, F. Hillenkamp, Influence of the laser intensity and spot size on the desorption of molecules and ions in matrix-assisted laser desorption/ionization with a uniform beam profile. *Int. J. Mass Spectrom.* **141**, 127 (1995).

21. I. D. Figueroa, D. H. Russell, Matrix-assisted laser desorption ionization hydrogen/deuterium exchange studies to probe peptide conformational changes. *J. Am. Soc. Mass Spectrom.* **10**, 719 (1999).

22. J. Santrucek, M. Strohalm, V. Kadlcík, R. Hynek, M. Kodícek, Tyrosine residues modification studied by MALDI-TOF mass spectrometry. *Biochem. Bioph. Res. Co.* **323**, 1151 (2004).

23. T. E. Wales, J. R. Engen, Hydrogen exchange mass spectrometry for the analysis of protein dynamics. *Mass Spectrom. Rev.* **25**, 158 (2006).

24. P. Nemes, A. Vertes, Laser ablation electrospray ionization for atmospheric pressure, *in vivo*, and imaging mass spectrometry. *Anal. Chem.* **79**, 8098 (2007).

25. M.-Z. Huang, S.-S. Jhang, C.-N. Cheng, S.-C. Cheng, J. Shiea, Effects of matrix, electrospray solution, and laser light on the desorption and ionization mechanisms in electrospray-assisted laser desorption ionization mass spectrometry. *Analyst* **135**, 759 (2010).

26. J. S. Sampson, D. C. Muddiman, Atmospheric pressure infrared (10.6 μm) laser desorption electrospray ionization (IR-LDESI) coupled to a LTQ Fourier transform ion cyclotron resonance mass spectrometer. *Rapid Commun. Mass Spectrom.* **23**, 1989 (2009).

27. J. S. Sampson, K. K. Murray, D. C. Muddiman, Intact and top-down characterization of biomolecules and direct analysis using infrared matrix-assisted laser desorption electrospray ionization coupled to FT-ICR mass spectrometry. *J. Am. Soc. Mass Spectrom.* **20**, 667 (2009).

28. Y. H. Rezenom, J. Dong, K. K. Murray, Infrared laser-assisted desorption electrospray ionization mass spectrometry. *Analyst* **133**, 226 (2008).

29. H. E. Elsayed-Ali, T. B. Norris, M. A. Pessot, G. A. Mourou, Time-resolved observation of electron-phonon relaxation in copper. *Phys. Rev. Lett.* **58**, 1212 (1987).

30. J. J. Brady, E. J. Judge, R. J. Levis, Identification of explosives and explosive formulations using laser electrospray mass spectrometry. *Rapid Commun. Mass Spectrom.* **24**, 1659 (2010).

31. E. J. Judge, J. J. Brady, P. E. Barbano, R. J. Levis, Nonresonant femtosecond laser vaporization with electrospray post-ionization for *ex vivo* plant tissue typing using compressive linear classification. *Anal. Chem.* **83**, 2145 (2011).

32. J. J. Brady, E. J. Judge, R. J. Levis, Analysis of amphiphilic lipids and hydrophobic proteins using nonresonant femtosecond laser vaporization with electrospray post-ionization. *J. Am. Soc. Mass Spectrom.* **22**, 762 (2011).

33. E. J. Judge, J. J. Brady, D. R. Dalton, R. J. Levis, Mass analysis of pharmaceutical compounds from glass, cloth, steel and wood surfaces at atmospheric pressure using non-resonant femtosecond laser vaporization and electrospray ionization. *Anal. Chem.* **82**, 3231 (2010).

34. J. J. Brady, E. J. Judge, R. J. Levis, Mass spectrometry of intact neutral macromolecules using intense non-resonant femtosecond laser vaporization with electrospray post-ionization. *Rapid Commun. Mass Spectrom.* **23**, 3151 (2009).

35. R. J. Levis, M. J. DeWitt, Photoexcitation, ionization, and dissociation of molecules using intense near-infrared radiation of femtosecond duration. *J. Phys. Chem. A* **103**, 6493 (1999).

36. R. Weinkauf, P. Aicher, G. Wesley, J. Grotemeyer, E. W. Schlag, Femtosecond versus nanosecond multiphoton ionization and dissociation of large molecules. *J. Phys. Chem.* **98**, 8381 (1994).

37. T. A. Fligge, J. Kast, K. Bruns, M. Przybylski, Direct monitoring of protein-chemical reactions utilizing nanoelectrospray mass spectrometry. *J. Am. Soc. Mass Spectrom.* **10**, 112 (1999).

38. D. E. Clemmer, R. R. Hudgins, M. F. Jarrold, Naked protein conformations: Cytochrome C in the gas phase. *J. Am. Chem. Soc.* **117**, 10141 (1995).

39. Y. J. Lee *et al.*, Collision-induced dissociation of mobility-separated ions using an orifice-skimmer cone at the back of a drift tube. *Anal. Chem.* **73**, 3549 (2001).

40. S. J. Valentine, D. E. Clemmer, H/D exchange levels of shape-resolved cytochrome C conformers in the gas phase. *J. Am. Chem. Soc.* **119**, 3558 (1997).

41. H. R. Drew, R. E. Dickerson, The unfolding of the cytochromes C in methanol and acid. *J. Biol. Chem.* **253**, 8420 (1978).

42. L. Konermann, D. J. Douglas, Acid-induced unfolding of cytochrome C at different methanol concentrations: Electrospray ionization mass spectrometry specifically monitors changes in the tertiary structure. *Biochemistry* **36**, 12296 (1997).

43. P. Nemes, S. Goyal, A. Vertes, Conformational and noncovalent complexation changes in proteins during electrospray ionization. *Anal. Chem.* **80**, 387 (2007).

44. G. J. Van Berkel, F. Zhou, J. T. Aronson, Changes in bulk solution pH caused by the inherent controlled-current electrolytic process of an electrospray ion source. *Int. J. Mass Spectrom.* **162**, 55 (1997).

45. R. J. Levis, Laser desorption and ejection of biomolecules from the condensed phase into the gas phase. *Annu. Rev. Phys. Chem.* **45**, 483 (1994).

46. S. Williams *et al.*, Fast events in protein folding: Helix melting and formation in a small peptide. *Biochemistry* **35**, 691 (1996).

47. T. D. Wood *et al.*, Gas-phase folding and unfolding of cytochrome C cations. *P. Natl. Acad. Sci. U.S.A.* **92**, 2451 (1995).

48. A. Ikai, W. W. Fish, C. Tanford, Kinetics of unfolding and refolding of proteins: II. Results for cytochrome C. *J. Mol. Biol.* **73**, 165 (1973).

49. Z. Takats, J. M. Wiseman, B. Gologan, R. G. Cooks, Electrosonic spray ionization. A gentle technique for generating folded proteins and protein

complexes in the gas phase and for studying ion-molecule reactions at atmospheric pressure. *Anal. Chem.* **76**, 4050 (2004).

50. P. Yang, R. G. Cooks, Z. Ouyang, A. M. Hawkridge, D. C. Muddiman, Gentle protein ionization assisted by high-velocity gas flow. *Anal. Chem.* **77**, 6174 (2005).

51. I. X. Peng, R. R. O. Loo, J. Shiea, J. A. Loo, Reactive-electrospray-assisted laser desorption/ionization for characterization of peptides and proteins. *Anal. Chem.* **80**, 6995 (2008).

52. Q. Y. Wu, S. Vanorden, X. H. Cheng, R. Bakhtiar, R. D. Smith, Characterization of cytochrome C variants with high-resolution FTICR mass spectrometry-correlation of fragmentation and structure. *Anal. Chem.* **67**, 2498 (1995).

53. Z. Q. Zhang, J. Bordas-Nagy, Peptide conformation in gas phase probed by collision-induced dissociation and its correlation to conformation in condensed phases. *J. Am. Soc. Mass Spectrom.* **17**, 786 (2006).

54. T. J. D. Jørgensen, J. U. Andersen, P. Hvelplund, M. Sørensen, High-energy collisions of multiply charged lysozyme ions in gases. *Int. J. Mass Spectrom.* **207**, 31 (2001).

55. S. A. McLuckey, Principles of collisional activation in analytical mass spectrometry. *J. Am. Soc. Mass Spectrom.* **3**, 599 (1992).

56. M. F. Jarrold, Unfolding, refolding, and hydration of proteins in the gas phase. *Accounts Chem. Res.* **32**, 360 (1998).

57. D. M. Leitner, Energy flow in proteins. *Annu. Rev. Phys. Chem.* **59**, 233 (2008).

58. U. A. Mirza, S. L. Cohen, B. T. Chait, Heat-induced conformational changes in proteins studied by electrospray ionization mass spectrometry. *Anal. Chem.* **65**, 1 (1993).

59. D. A. Rogers, S. J. Ray, G. M. Hieftje, An electrospray/inductively coupled plasma dual-source time-of-flight mass spectrometer for rapid metallomic and speciation analysis part 1. Molecular channel characterization. *Metallomics* **2**, 271 (2010).

60. R. B. Cole, Some tenets pertaining to electrospray ionization mass spectrometry. *J. Mass Spectrom.* **35**, 763 (2000).

61. J. A. Loo, C. G. Edmonds, H. R. Udseth, R. D. Smith, Effect of reducing disulfide-containing proteins on electrospray ionization mass spectra. *Anal. Chem.* **62**, 693 (1990).

62. J. B. Fenn, Ion formation from charged droplets: Roles of geometry, energy, and time. *J. Am. Soc. Mass Spectrom.* **4**, 524 (1993).

63. H. Arnolds, C. E. M. Rehbein, G. Roberts, R. J. Levis, D. A. King, Femtosecond near-infrared laser desorption of multilayer benzene on Pt{111}: Spatial origin of hyperthermal desorption. *Chem. Phys. Lett.* **314**, 389 (1999).

64. H. Arnolds, R. J. Levis, D. A. King, Vibrationally assisted DIET through transient temperature rise: The case of benzene on Pt{111}. *Chem. Phys. Lett.* **380**, 444 (2003).

65. H. Arnolds, C. Rehbein, G. Roberts, R. J. Levis, D. A. King, Femtosecond near-infrared laser desorption of multilayer benzene on Pt{111}: A molecular newton's cradle? *J. Phys. Chem. B* **104**, 3375 (2000).

66. P. Williams, B. Sundqvist, Mechanism of sputtering of large biomolecular ions by impact of highly ionizing particles. *Phys. Rev. Lett.* **58**, 1031 (1987).

67. R. E. Johnson, B. U. R. Sundqvist, W. Ens, Laser-pulse ejection of organic molecules from a matrix: Lessons from fast-ion-induced ejection. *Rapid Commun. Mass Spectrom.* **5**, 574 (1991).

68. D. M. Schieltz *et al.*, Mass spectrometry of DNA mixtures by laser ablation from frozen aqueous solution. *Rapid Commun. Mass Spectrom.* **6**, 631 (1992).

69. R. W. Nelson, R. M. Thomas, P. Williams, Time-of-flight mass spectrometry of nucleic acids by laser ablation and ionization from a frozen aqueous matrix. *Rapid Commun. Mass Spectrom.* **4**, 348 (1990).

CHAPTER 6

SUMMARY AND OUTLOOK

This dissertation has detailed the design and implementation of a new laser-based mass spectrometric technique known as laser electrospray mass spectrometry. It has been shown that a femtosecond laser pulse can vaporize a wide range molecules, varying in polarity and size. The molecules are transferred into the gas phase intact and in the neutral state via a nonresonant, nonthermal mechanism. Electrospray post-ionization of the vaporized material (molecules and clusters) allows for mass spectral measurements to be made.

Methods to deliver non-volatile biological molecules intact into the gas phase, preferably maintaining solution phase structure, are of interest. We have reported that intense nonresonant laser pulses could be used to deliver proteins with molecular weight up to 16 kDa into the gas phase without fragmentation. To be of value for protein structural determination, the vaporization must ideally preserve the condensed phase primary, secondary and tertiary conformation. Another motivation for these investigations is the fact that the analysis of biological structure *in situ* presents a significant challenge. As a first step toward this goal, we have investigated the conformation of proteins vaporized from the solution phase, *in vitro,* using intense nonresonant femtosecond pulses. The proteins, cytochrome c and lysozyme, are vaporized from the condensed phase into the gas phase intact when exposed to an intense, nonresonant, ultrafast laser pulse. Electrospray post-ionization of the vaporized protein sample reveals that the protein maintains its solution-phase conformation through measurement of the charge state distribution and the collision-induced dissociation

channels produced. The measurements for cytochrome c and lysozyme indicate this remarkable result while conventional ESI-MS results in unfolding using identical electrospray conditions. These experiments reveal that nonresonant fs laser vaporization of aqueous protein is a softer vaporization/ionization method than conventional ESI-MS.

The ability to vaporize proteins while maintaining conformation is an important step towards the measurement of noncovalent protein-protein and enzyme-substrate interactions. These measurements suggest that investigation of the *ex vivo* protein conformation analysis is now possible.

REFERENCES CITED

Alexei, G., Michael, S., Jehuda, Y., Liquid chromatography/mass spectrometric analysis of explosives: RDX adduct ions. *Rapid Commun. Mass Spectrom.* **17**, 943 (2003).

Allwood, D. A., Dreyfus, R. W., Perera, I. K., Dyer, P. E., UV optical absorption of matrices used for matrix-assisted laser desorption/ionization. *Rapid Commun. Mass Spectrom.* **10**, 1575 (1996).

Allwood, D. A., Dreyfus, R. W., Perera, I. K., Dyer, P. E., Optical absorption of matrix compounds for laser-induced desorption and ionization (MALDI). *Appl. Surf. Sci.* **110**, 154 (1997).

Allwood, D. A., Dyer, P. E., Quantitative fluorescence measurements performed on typical matrix molecules in matrix-assisted laser desorption/ionization. *Chem. Phys.* **261**, 457 (2000).

Altelaar, A. F. M. *et al.*, Gold-enhanced biomolecular surface imaging of cells and tissue by SIMS and MALDI mass spectrometry. *Anal. Chem.* **78**, 734 (2006).

Apitz, I., Vogel, A., Material ejection in nanosecond Er:YAG laser ablation of water, liver, and skin. *Appl. Phys. A-Mater.* **81**, 329 (2005).

Arnolds, H., Levis, R. J., King, D. A., Vibrationally assisted DIET through transient temperature rise: The case of benzene on Pt{111}. *Chem. Phys. Lett.* **380**, 444 (2003).

Arnolds, H., Rehbein, C., Roberts, G., Levis, R. J., King, D. A., Femtosecond near-infrared laser desorption of multilayer benzene on Pt{111}: A molecular Newton's cradle? *J. Phys. Chem. B* **104**, 3375 (2000).

Arnolds, H., Rehbein, C. E. M., Roberts, G., Levis, R. J., King, D. A., Femtosecond near-infrared laser desorption of multilayer benzene on Pt{111}: Spatial origin of hyperthermal desorption. *Chem. Phys. Lett.* **314**, 389 (1999).

Backus, S., Durfee III, C. G., Murnane, M. M., Kapteyn, H. C., High power ultrafast lasers. *Rev. Sci. Instrum.* **69**, 1207 (1998).

Barber, M., Bordoli, R. S., Sedgwick, R. D., Tyler, A. N., Fast atom bombardment of solids (FAB) - A new ion-source for mass-spectrometry. *J. Chem. Soc., Chem. Commun.*, 325 (1981).

Bereman, M. S., Williams, T. I., Muddiman, D. C., Carbohydrate analysis by desorption electrospray ionization Fourier transform ion cyclotron resonance mass spectrometry. *Anal. Chem.* **79**, 8812 (2007).

Bourinbaiar, A. S., Coleman, C. F., The effect of gramicidin, a topical contraceptive and antimicrobial agent with anti-HIV activity, against herpes simplex viruses type 1 and 2 *in vitro*. *Arch. Virol.* **142**, 2225 (1997).

Brabec, T., Krausz, F., Intense few-cycle laser fields: Frontiers of nonlinear optics. *Rev. Mod. Phys.* **72**, 545 (2000).

Brady, J. J., Judge, E. J., Levis, R. J., Mass spectrometry of intact neutral macromolecules using intense non-resonant femtosecond laser vaporization with electrospray post-ionization. *Rapid Commun. Mass Spectrom.* **23**, 3151 (2009).

Brady, J. J., Judge, E. J., Levis, R. J., Identification of explosives and explosive formulations using laser electrospray mass spectrometry. *Rapid Commun. Mass Spectrom.* **24**, 1659 (2010).

Brady, J. J., Judge, E. J., Levis, R. J., Analysis of amphiphilic lipids and hydrophobic proteins using nonresonant femtosecond laser vaporization with electrospray post-ionization. *J. Am. Soc. Mass Spectrom.* **22**, 762 (2011).

Calvano, C. D., Palmisano, F., Zambonin, C. G., Laser desorption/ionization time-of-flight mass spectrometry of triacylglycerols in oils. *Rapid Commun. Mass Spectrom.* **19**, 1315 (2005).

Chen, Z., Vertes, A., Early plume expansion in atmospheric pressure midinfrared laser ablation of water-rich targets. *Phys. Rev. E* **77**, 036316 (2008).

Cheng, C. Y. *et al.*, Electrospray-assisted laser desorption/ionization mass spectrometry for continuously monitoring the states of ongoing chemical reactions in organic or aqueous solution under ambient conditions. *Anal. Chem.* **80**, 7699 (2008).

Cheng, J., Winograd, N., Depth profiling of peptide films with TOF-SIMS and a C-60 probe. *Anal. Chem.* **77**, 3651 (2005).

Cheng, S.-C., Cheng, T.-L., Chang, H.-C., Shiea, J., Using laser-induced acoustic desorption/electrospray ionization mass spectrometry to characterize small organic and large biological compounds in the solid state and in solution under ambient conditions. *Anal. Chem.* **81**, 868 (2009).

Chitta, R. K., Gross, M. L., Electrospray ionization-mass spectrometry and tandem mass spectrometry reveal self-association and metal-ion binding of hydrophobic peptides: A study of the gramicidin dimer. *Biophys. J.* **86**, 473 (2004).

Clemmer, D. E., Hudgins, R. R., Jarrold, M. F., Naked protein conformations: Cytochrome c in the gas phase. *J. Am. Chem. Soc.* **117**, 10141 (1995).

Codling, K., Frasinski, L. J., Dissociative ionization of small molecules in intense laser fields. *J. Phys. B* **26**, 783 (1993).

Cole, R. B., Some tenets pertaining to electrospray ionization mass spectrometry. *J. Mass Spectrom.* **35**, 763 (2000).

Cole, R. B., *Electrospray and MALDI mass spectrometry: Fundamentals, instrumentation, practicalities, and biological applications*. (John Wiley & Sons, 2009).

Cooks, R. G., Ouyang, Z., Takats, Z., Wiseman, J. M., Ambient mass spectrometry. *Science* **311**, 1566 (2006).

Coon, J. J., Harrison, W. W., Laser desorption-atmospheric pressure chemical ionization mass spectrometry for the analysis of peptides from aqueous solutions. *Anal. Chem.* **74**, 5600 (2002).

Coon, J. J., McHale, K. J., Harrison, W. W., Atmospheric pressure laser desorption/chemical ionization mass spectrometry: A new ionization method based on existing themes. *Rapid Commun. Mass Spectrom.* **16**, 681 (2002).

Cotte-Rodriguez, I., Hernandez-Soto, H., Chen, H., Cooks, R. G., *In situ* trace detection of peroxide explosives by desorption electrospray ionization and desorption atmospheric pressure chemical ionization. *Anal. Chem.* **80**, 1512 (2008).

Cotte-Rodriguez, I., Takats, Z., Talaty, N., Chen, H., Cooks, R. G., Desorption electrospray ionization of explosives on surfaces: Sensitivity and selectivity enhancement by reactive desorption electrospray ionization. *Anal. Chem.* **77**, 6755 (2005).

Cotter, R., *Time-of-Flight mass spectrometry: Instrumentation and applications in biological research.*, (ACS, Washington, D.C., 1997).

Dawson, J. H. J., Guilhaus, M., Orthogonal-acceleration time-of-flight mass spectrometer. *Rapid Commun. Mass Spectrom.* **3**, 155 (1989).

Dawson, P. H., Ed., *Quadrupole mass spectrometry and its applications.*, (Springer-Verlag New York, LLC, New York, 1997).

Delone, N. B., Krainov, V. P., *Mulitphoton processes in atoms*. (Springer-Verlag Berlin Heidelberg, ed. Second, 1999), pp. 314.

Demirev, P. *et al.*, Matrix-assisted laser desorption with ultra-short laser pulses. *Rapid Commun. Mass Spectrom.* **6**, 187 (1992).

Desmazieres, B., Buchmann, W., Terrier, P., Tortajada, J., APCI interface for LC- and SEC-MS analysis of synthetic polymers: Advantages and limits. *Anal. Chem.* **80**, 783 (2007).

Dewitt, M. J., Levis, R. J., Near-infrared femtosecond photoionization dissociation of cyclic aromatic-hydrocarbons. *J. Chem. Phys.* **102**, 8670 (1995).

Dikmelik, Y., McEnnis, C., Spicer, J. B., Femtosecond and nanosecond laser-induced breakdown spectroscopy of trinitrotoluene. *Opt. Express* **16**, 5332 (2008).

Ditmire, T. *et al.*, Nuclear fusion from explosions of femtosecond laser-heated deuterium clusters. *Nature* **398**, 489 (1999).

Dixon, R. B., Bereman, M. S., Muddiman, D. C., Hawkridge, A. M., Remote mass spectrometric sampling of electrospray- and desorption electrospray-generated ions using an air ejector. *J. Am. Soc. Mass Spectrom.* **18**, 1844 (2007).

Dixon, R. B., Sampson, J. S., Hawkridge, A. M., Muddiman, D. C., Ambient aerodynamic ionization source for remote analyte sampling and mass spectrometric analysis. *Anal. Chem.* **80**, 5266 (2008).

Dole, M. *et al.*, Molecular beams of macroions. *J. Chem. Phys.* **49**, 2240 (1968).

Douglas, D. J., French, J. B., Collisional focusing effects in radio frequency quadrupoles. *J. Am. Soc. Mass Spectrom.* **3**, 398 (1992).

Dreisewerd, K., Schürenberg, M., Karas, M., Hillenkamp, F., Influence of the laser intensity and spot size on the desorption of molecules and ions in matrix-assisted laser desorption/ionization with a uniform beam profile. *Int. J. Mass Spectrom.* **141**, 127 (1995).

Drew, H. R., Dickerson, R. E., The unfolding of the cytochromes c in methanol and acid. *J. Biol. Chem.* **253**, 8420 (1978).

Eide, I., Zahlsen, K., Chemical fingerprinting of biodiesel using electrospray mass spectrometry and chemometrics: Characterization, discrimination, identification, and quantification in petrodiesel. *Energ. Fuel* **21**, 3702 (2007).

Elsayed-Ali, H. E., Norris, T. B., Pessot, M. A., Mourou, G. A., Time-resolved observation of electron-phonon relaxation in copper. *Phys. Rev. Lett.* **58**, 1212 (1987).

Fenn, J. B., Ion formation from charged droplets: Roles of geometry, energy, and time. *J. Am. Soc. Mass Spectrom.* **4**, 524 (1993).

Fenn, J. B., Mann, M., Meng, C. K., Wong, S. F., Whitehouse, C. M., Electrospray ionization for mass-spectrometry of large biomolecules. *Science* **246**, 64 (1989).

Fenn, J. B., Mann, M., Meng, C. K., Wong, S. F., Whitehouse, C. M., Electrospray ionization - Principles and practice. *Mass Spectrom. Rev.* **9**, 37 (1990).

Figueroa, I. D., Russell, D. H., Matrix-assisted laser desorption ionization hydrogen/deuterium exchange studies to probe peptide conformational changes. *J. Am. Soc. Mass Spectrom.* **10**, 719 (1999).

Fligge, T. A., Kast, J., Bruns, K., Przybylski, M., Direct monitoring of protein-chemical reactions utilizing nanoelectrospray mass spectrometry. *J. Am. Soc. Mass Spectrom.* **10**, 112 (1999).

Freeman, R. R. *et al.*, Above-threshold ionization with subpicosecond laser-pulses. *Phys. Rev. Lett.* **59**, 1092 (1987).

Gabelica, V., Pauw, E. D., Internal energy and fragmentation of ions produced in electrospray sources. *Mass Spectrom. Rev.* **24**, 566 (2005).

Gottfried, J. L., De Lucia, F. C., Munson, C. A., Miziolek, A. W., Laser-induced breakdown spectroscopy for detection of explosives residues: A review of recent advances, challenges, and future prospects. *Anal. Bioanal. Chem.* **395**, 283 (2009).

Grandori, R., Origin of the conformation dependence of protein charge-state distributions in electrospray ionization mass spectrometry. *J. Mass Spectrom.* **38**, 11 (2003).

Guilhaus, M., Special feature: Tutorial. Principles and instrumentation in time-of-flight mass spectrometry. Physical and instrumental concepts. *J. Mass Spectrom.* **30**, 1519 (1995).

Harrision, A. G., *Chemical ionization mass spectrometry*. (CRC Press, Boca Raton, FL, 1983), pp. 156.

Hayes, J. M., Small, G. J., Supersonic jets, rotational cooling and analytical-chemistry. *Anal. Chem.* **55**, A565 (1983).

Hensel, R. R., King, R. C., Owens, K. G., Electrospray sample preparation for improved quantitation in matrix-assisted laser desorption/ionization time-of-flight mass spectrometry. *Rapid Commun. Mass Spectrom.* **11**, 1785 (1997).

Hicks, J. M., Urbach, L. E., Plummer, E. W., Dai, H.-L., Can pulsed laser excitation of surfaces be described by a thermal model? *Phys. Rev. Lett.* **61**, 2588 (1988).

Hillenkamp, F., Karas, M., Beavis, R. C., Chait, B. T., Matrix-assisted laser desorption ionization mass-spectrometry of biopolymers. *Anal. Chem.* **63**, A1193 (1991).

Hu, Q. *et al.*, The orbitrap: A new mass spectrometer. *J. Mass Spectrom.* **40**, 430 (2005).

Huang, M.-Z., Jhang, S.-S., Cheng, C.-N., Cheng, S.-C., Shiea, J., Effects of matrix, electrospray solution, and laser light on the desorption and ionization mechanisms in electrospray-assisted laser desorption ionization mass spectrometry. *Analyst* **135**, 759 (2010).

Huang, M. Z., Hsu, H. J., Lee, L. Y., Jeng, J. Y., Shiea, L. T., Direct protein detection from biological media through electrospray-assisted laser desorption ionization/mass spectrometry. *J. Proteome Res.* **5**, 1107 (2006).

Huang, M. Z. *et al.*, Characterization of the chemical components on the surface of different solids with electrospray-assisted laser desorption ionization mass spectrometry. *Rapid Commun. Mass Spectrom.* **21**, 1767 (2007).

Ikai, A., Fish, W. W., Tanford, C., Kinetics of unfolding and refolding of proteins: II. Results for cytochrome c. *J. Mol. Biol.* **73**, 165 (1973).

Iribarne, J. V., Thomson, B. A., On the evaporation of small ions from charged droplets. *J. Chem. Phys.* **64**, 2287 (1976).

James, B. S., Caroline, M., in *Laser applications to chemical, security and environmental analysis*. (Optical Society of America, 2008), pp. LThC2.

Jarrold, M. F., Unfolding, refolding, and hydration of proteins in the gas phase. *Accounts Chem. Res.* **32**, 360 (1998).

Jehuda, Y., Joseph, E. M., Richard, A. Y., Electrospray ionization tandem mass spectrometry collision-induced dissociation study of explosives in an ion trap mass spectrometer. *Rapid Commun. Mass Spectrom.* **11**, 1961 (1997).

Jia, L., Bo, Q., Hai, L., Fingerprinting of yogurt products by laser desorption spray post-ionization mass spectrometry. *Rapid Commun. Mass Spectrom.* **24**, 1365 (2010).

Johnson, R. E., Sundqvist, B. U. R., Ens, W., Laser-pulse ejection of organic molecules from a matrix: Lessons from fast-ion-induced ejection. *Rapid Commun. Mass Spectrom.* **5**, 574 (1991).

Jørgensen, T. J. D., Andersen, J. U., Hvelplund, P., Sørensen, M., High-energy collisions of multiply charged lysozyme ions in gases. *Int. J. Mass Spectrom.* **207**, 31 (2001).

Judge, E. J., Ph.D Thesis, Temple University (2011).

Judge, E. J., Brady, J. J., Barbano, P. E., Levis, R. J., Nonresonant femtosecond laser vaporization with electrospray post-ionization for *ex vivo* plant tissue typing using compressive linear classification. *Anal. Chem.* **83**, 2145 (2011).

Judge, E. J., Brady, J. J., Levis, R. J., Mass analysis of biological macromolecules at atmospheric pressure using nonresonant femtosecond laser vaporization and electrospray ionization. *Anal. Chem.* **82**, 10203 (2010).

Judge, E. J., Brady, J. J., Dalton, D. R., Levis, R. J., Mass analysis of pharmaceutical compounds from glass, cloth, steel and wood surfaces at atmospheric pressure using non-resonant femtosecond laser vaporization and electrospray ionization *Anal. Chem.* **82**, 3231 (2010).

Karas, M., Hillenkamp, F., Laser desorption ionization of proteins with molecular masses exceeding 10,000 Daltons. *Anal. Chem.* **60**, 2299 (1988).

Kebarle, P., Tang, L., From ions in solution to ions in the gas phase - the mechanism of electrospray mass spectrometry. *Anal. Chem.* **65**, 972A (1993).

Kinsel, G. R., Preston, L. M., Russell, D. H., Fragmentation of vitamin B12 during 337 nm matrix-assisted laser desorption ionization. *Biol. Mass Spectrom.* **23**, 205 (1994).

Knochenmuss, R., Ion formation mechanisms in UV-MALDI. *Analyst* **131**, 966 (2006).

Knochenmuss, R., Zhigilei, L. V., Molecular dynamics model of ultraviolet matrix-assisted laser desorption/ionization including ionization processes. *J. Phys. Chem. B* **109**, 22947 (2005).

Konermann, L., Douglas, D. J., Acid-induced unfolding of cytochrome c at different methanol concentrations: Electrospray ionization mass spectrometry specifically monitors changes in the tertiary structure. *Biochemistry-US* **36**, 12296 (1997).

Le, H. C., Zeitoun, D. E., Parisse, J. D., Sentis, M., Marine, W., Modeling of gas dynamics for a laser-generated plasma: Propagation into low-pressure gases. *Phys. Rev. E* **62**, 4152 (2000).

Ledingham, K. W. D., McKenna, P., Singhal, R. P., Applications for nuclear phenomena generated by ultra-intense lasers. *Science* **300**, 1107 (2003).

Ledingham, K. W. D. *et al.*, Multiply charged ions from aromatic molecules following irradiation in intense laser fields. *J. Phys. Chem. A* **103**, 2952 (1999).

Lee, Y. J. *et al.*, Collision-induced dissociation of mobility-separated ions using an orifice-skimmer cone at the back of a drift tube. *Anal. Chem.* **73**, 3549 (2001).

Leisner, A., Rohlfing, A., Berkenkamp, S., Hillenkamp, F., Dreisewerd, K., Infrared laser post-ionization of large biomolecules from an IR-MALD(I) plume. *J. Am. Soc. Mass Spectrom.* **15**, 934 (2004).

Leitner, D. M., Energy flow in proteins. *Annu. Rev. Phys. Chem.* **59**, 233 (2008).

Levis, R. J., Laser desorption and ejection of biomolecules from the condensed phase into the gas phase. *Annu. Rev. Phys. Chem.* **45**, 483 (1994).

Levis, R. J., DeWitt, M. J., Photoexcitation, ionization, and dissociation of molecules using intense near-infrared radiation of femtosecond duration. *J. Phys. Chem. A* **103**, 6493 (1999).

Lezius, M. *et al.*, Nonadiabatic multielectron dynamics in strong field molecular ionization. *Phys. Rev. Lett.* **86**, 51 (2001).

Li, L., Wang, A. P. L., Coulson, L. D., Continuous-flow matrix-assisted laser desorption ionization mass-spectrometry. *Anal. Chem.* **65**, 493 (1993).

Lin, S. Y., Huang, M. Z., Chang, H. C., Shiea, J., Using electrospray-assisted laser desorption/ionization mass spectrometry to characterize organic compounds separated on thin-layer chromatography plates. *Anal. Chem.* **79**, 8789 (2007).

Little, D. P., Speir, J. P., Senko, M. W., O'Connor, P. B., McLafferty, F. W., Infrared multiphoton dissociation of large multiply charged ions for biomolecule sequencing. *Anal. Chem.* **66**, 2809 (1994).

Loo, J. A., Edmonds, C. G., Udseth, H. R., Smith, R. D., Effect of reducing disulfide-containing proteins on electrospray ionization mass spectra. *Anal. Chem.* **62**, 693 (1990).

Markevitch, A. N. *et al.*, Nonadiabatic dynamics of polyatomic molecules and ions in strong laser fields. *Phys. Rev. A* **68**, (2003).

Mauritsson, J. *et al.*, Attosecond pulse trains generated using two color laser fields. *Phys. Rev. Lett.* **97**, (2006).

McLafferty, F. W., Turecek, F., *Interpretation of mass spectra*. (University Science Books, Sausalito, California, Fourth ed., 1993).

McLuckey, S. A., Principles of collisional activation in analytical mass spectrometry. *J. Am. Soc. Mass Spectrom.* **3**, 599 (1992).

Michael, E. S., Clark, C. D., Rebecca, F., Cherie, L. G., Christian, A. C., Analysis of triacetone triperoxide by gas chromatography/mass spectrometry and gas chromatography/tandem mass spectrometry by electron and chemical ionization. *Rapid Commun. Mass Spectrom.* **20**, 2851 (2006).

Miller, P. E., Denton, M. B., The quadruple mass filter: Basic operating concepts. *J. Chem. Educ.* **63**, 617 (1986).

Mirza, S. P., Halligan, B. D., Greene, A. S., Olivier, M., Improved method for the analysis of membrane proteins by mass spectrometry. *Physiol. Genomics* **30**, 89 (2007).

Mirza, U. A., Cohen, S. L., Chait, B. T., Heat-induced conformational changes in proteins studied by electrospray ionization mass spectrometry. *Anal. Chem.* **65**, 1 (1993).

Mohideen, U. *et al.*, High-intensity above-threshold ionization of He. *Phys. Rev. Lett.* **71**, 509 (1993).

Moore, D. S., Instrumentation for trace detection of high explosives. *Rev. Sci. Instrum.* **75**, 2499 (2004).

Mowry, C. D., Johnston, M. V., Simultaneous detection of ions and neutrals produced by matrix-assisted laser desorption. *Rapid Commun. Mass Spectrom.* **7**, 569 (1993).

Moyer, S. G., Cotter, R. J., Atmospheric pressure MALDI. *Anal. Chem.* **74**, 468A (2002).

Mullen, C., Huestis, D., Coggiola, M., Oser, H., Laser photoionization of triacetone triperoxide (TATP) by femtosecond and nanosecond laser pulses. *Int. J. Mass Spectrom.* **252**, 69 (2006).

Nelson, R. W., Thomas, R. M., Williams, P., Time-of-flight mass spectrometry of nucleic acids by laser ablation and ionization from a frozen aqueous matrix. *Rapid Commun. Mass Spectrom.* **4**, 348 (1990).

Nemes, P., Goyal, S., Vertes, A., Conformational and noncovalent complexation changes in proteins during electrospray ionization. *Anal. Chem.* **80**, 387 (2007).

Nemes, P., Vertes, A., Laser ablation electrospray ionization for atmospheric pressure, *in vivo*, and imaging mass spectrometry. *Anal. Chem.* **79**, 8098 (2007).

Nemes, P., Woods, A. S., Vertes, A., Simultaneous imaging of small metabolites and lipids in rat brain tissues at atmospheric pressure by laser ablation electrospray ionization mass spectrometry. *Anal. Chem.* **82**, 982 (2010).

Nordhoff, E. *et al.*, Matrix-assisted laser desorption ionization mass-spectrometry of nucleic-acids with wavelengths in the ultraviolet and infrared. *Rapid Commun. Mass Spectrom.* **6**, 771 (1992).

Nugent-Glandorf, L., Scheer, M., Samuels, D. A., Bierbaum, V., Leone, S. R., A laser-based instrument for the study of ultrafast chemical dynamics by soft x-ray-probe photoelectron spectroscopy. *Rev. Sci. Instrum.* **73**, 1875 (2002).

Ostrowski, S. G., Van Bell, C. T., Winograd, N., Ewing, A. G., Mass spectrometric imaging of highly curved membranes during *Tetrahymena* mating. *Science* **305**, 71 (2004).

Palczewski, K. *et al.*, Crystal structure of rhodopsin: A G protein-coupled receptor. *Science* **289**, 739 (2000).

Paul, W., Electromagnetic traps for charged and neutral particles. *Rev. Mod. Phys.* **62**, 531 (1990).

Peng, I. X., Loo, R. R. O., Shiea, J., Loo, J. A., Reactive-electrospray-assisted laser desorption/ionization for characterization of peptides and proteins. *Anal. Chem.* **80**, 6995 (2008).

Peng, I. X., Shiea, J., Loo, R. R. O., Loo, J. A., Electrospray-assisted laser desorption/ionization and tandem mass spectrometry of peptides and proteins. *Rapid Commun. Mass Spectrom.* **21**, 2541 (2007).

Pessot, M., Maine, P., Mourou, G., 1000 times expansion/compression of optical pulses for chirped pulse amplification. *Opt. Commun.* **62**, 419 (1987).

Peterlongo, A., Miotello, A., Kelly, R., Laser-pulse sputtering of aluminum - vaporization, boiling, superheating, and gas-dynamic effects. *Phys. Rev. E* **50**, 4716 (1994).

Piché, M., Salin, F., Self-mode locking of solid-state lasers without apertures. *Opt. Lett.* **18**, 1041 (1993).

Popmintchev, T. *et al.*, Phase matching of high harmonic generation in the soft and hard X-ray regions of the spectrum. *Proc. Nat. Acad. Sci. USA* **106**, 10516 (2009).

Popov, I. A., Chen, H., Kharybin, O. N., Nikolaev, E. N., Cooks, R. G., Detection of explosives on solid surfaces by thermal desorption and ambient ion/molecule reactions. *Chem. Commun.*, 1953 (2005).

Posthumus, J. H., The dynamics of small molecules in intense laser fields. *Rep. Prog. Phys.* **67**, 623 (2004).

Posthumus, M. A., Kistemaker, P. G., Meuzelaar, H. L. C., Ten Noever de Brauw, M. C., Laser desorption-mass spectrometry of polar nonvolatile bio-organic molecules. *Anal. Chem.* **50**, 985 (1978).

Van Breemen, R.B., M. Snow, Cotter, R. J., Time resolved laser desorption mass spectrometry, I. Desorption of preformed ions. *Int. J. Mass Spectrom. Ion Processes* **49**, 35 (1983).

Rezenom, Y. H., Dong, J., Murray, K. K., Infrared laser-assisted desorption electrospray ionization mass spectrometry. *Analyst* **133**, 226 (2008).

Roddy, T. P., Cannon, D. M., Meserole, C. A., Winograd, N., Ewing, A. G., Imaging of freeze-fractured cells with *in situ* fluorescence and time-of-flight secondary ion mass spectrometry. *Anal. Chem.* **74**, 4011 (2002).

Roddy, T. P., Cannon, D. M., Ostrowski, S. G., Ewing, A. G., Winograd, N., Proton transfer in time-of-flight secondary ion mass spectrometry studies of frozen-hydrated dipalmitoylphosphatidylcholine. *Anal. Chem.* **75**, 4087 (2003).

Rogers, D. A., Ray, S. J., Hieftje, G. M., An electrospray/inductively coupled plasma dual-source time-of-flight mass spectrometer for rapid metallomic and speciation analysis Part 1. Molecular channel characterization. *Metallomics* **2**, 271 (2010).

Rosinke, B. *et al.*, Matrix-assisted laser desorption/ionization mass-spectrometry (MALDI-MS) of membrane-proteins and noncovalent complexes. *J. Mass Spectrom.* **30**, 1462 (1995).

Sampson, J. S., Hawkridge, A. M., Muddiman, D. C., Generation and detection of multiply-charged peptides and proteins by matrix-assisted laser desorption electrospray ionization (MALDESI) Fourier transform ion cyclotron resonance mass spectrometry. *J. Am. Soc. Mass Spectrom.* **17**, 1712 (2006).

Sampson, J. S., Hawkridge, A. M., Muddiman, D. C., Direct characterization of intact polypeptides by matrix-assisted laser desorption electrospray ionization quadrupole Fourier transform ion cyclotron resonance mass spectrometry. *Rapid Commun. Mass Spectrom.* **21**, 1150 (2007).

Sampson, J. S., Hawkridge, A. M., Muddiman, D. C., Development and characterization of an ionization technique for analysis of biological macromolecules:

Liquid matrix-assisted laser desorption electrospray ionization. *Anal. Chem.* **80**, 6773 (2008).

Sampson, J. S., Muddiman, D. C., Atmospheric pressure infrared (10.6 μm) laser desorption electrospray ionization (IR-LDESI) coupled to a LTQ Fourier transform ion cyclotron resonance mass spectrometer. *Rapid Commun. Mass Spectrom.* **23**, 1989 (2009).

Sampson, J. S., Murray, K. K., Muddiman, D. C., Intact and top-down characterization of biomolecules and direct analysis using infrared matrix-assisted laser desorption electrospray ionization coupled to FT-ICR mass spectrometry. *J. Am. Soc. Mass Spectrom.* **20**, 667 (2009).

Santrucek, J., Strohalm, M., Kadlcík, V., Hynek, R., Kodícek, M., Tyrosine residues modification studied by MALDI-TOF mass spectrometry. *Biochem. Bioph. Res. Co.* **323**, 1151 (2004).

Sarges, R., Witkop, B., Gramicidin A. V. The structure of Valine- and Isoleucine-gramicidin A. *J. Am. Chem. Soc.* **87**, 2011 (1965).

Schieltz, D. M. *et al.*, Mass spectrometry of DNA mixtures by laser ablation from frozen aqueous solution. *Rapid Commun. Mass Spectrom.* **6**, 631 (1992).

Seeley, E. H., Oppenheimer, S. R., Mi, D., Chaurand, P., Caprioli, R. M., Enhancement of protein sensitivity for MALDI imaging mass spectrometry after chemical treatment of tissue sections. *J. Am. Soc. Mass Spectrom.* **19**, 1069 (2008).

Sethuraman, A., Vedantham, G., Imoto, T., Przybycien, T., Belfort, G., Protein unfolding at interfaces: Slow dynamics of α-helix to β-sheet transition. *Proteins* **56**, 669 (2004).

Shackleton, C. H. L., Falick, A. M., Green, B. N., Witkowska, H. E., Electrospray mass spectrometry in the clinical diagnosis of variant hemoglobins. *J. Chromatogr. B* **562**, 175 (1991).

Shibayama, N., Lomax, S. Q., Sutherland, K., Rie, E. R. d. l., Atmospheric pressure chemical ionization liquid chromatography mass spectrometry and its application to conservation: Analysis of triacylglycerols. *Stud. Conserv.* **44**, 253 (1999).

Shiea, J. *et al.*, Electrospray-assisted laser desorption/ionization mass spectrometry for direct ambient analysis of solids. *Rapid Commun. Mass Spectrom.* **19**, 3701 (2005).

Shiea, J. *et al.*, Detection of native protein ions in aqueous solution under ambient conditions by electrospray laser desorption/ionization mass spectrometry. *Anal. Chem.* **80**, 4845 (2008).

Shin, Y. S., Drolet, B., Mayer, R., Dolence, K., Basile, F., Desorption electrospray ionization-mass spectrometry of proteins. *Anal. Chem.* **79**, 3514 (2007).

Sigman, M. E., Ma, C.-Y., In-injection port thermal desorption for explosives trace evidence analysis. *Anal. Chem.* **71**, 4119 (1999).

Speir, J. P., Amster, I. J., Substrate-assisted laser desorption of neutral peptide molecules. *Anal. Chem.* **64**, 1041 (1992).

Speir, J. P., Gorman, G. S., Cornett, D. S., Amster, I. J., Controlling the dissociation of peptide ions using laser desorption chemical ionization Fourier-transform mass-spectrometry. *Anal. Chem.* **63**, 65 (1991).

Spickett, C. M., Pitt, A. R., Brown, A. J., Direct observation of lipid hydroperoxides in phospholipid vesicles by electrospray mass spectrometry. *Free Radical Bio. Med.* **25**, 613 (1998).

Strickland, D., Mourou, G., Compression of amplified chirped optical pulses. *Opt. Commun.* **56**, 219 (1985).

Takats, Z., Wiseman, J. M., Cooks, R. G., Ambient mass spectrometry using desorption electrospray ionization (DESI): Instrumentation, mechanisms and applications in forensics, chemistry, and biology. *J. Mass Spectrom.* **40**, 1261 (2005).

Takats, Z., Wiseman, J. M., Gologan, B., Cooks, R. G., Electrosonic spray ionization. A gentle technique for generating folded proteins and protein complexes in the gas phase and for studying ion-molecule reactions at atmospheric pressure. *Anal. Chem.* **76**, 4050 (2004).

Takats, Z., Wiseman, J. M., Gologan, B., Cooks, R. G., Mass spectrometry sampling under ambient conditions with desorption electrospray ionization. *Science* **306**, 471 (2004).

Tan, P. V., Laiko, V. V., Doroshenko, V. M., Atmospheric pressure MALDI with pulsed dynamic focusing for high-efficiency transmission of ions into a mass spectrometer. *Anal. Chem.* **76**, 2462 (2004).

Tanaka, K. *et al.*, Protein and polymer analyses up to *m/z* 100, 000 by laser ionization time-of-flight mass spectrometry. *Rapid Commun. Mass Spectrom.* **2**, 151 (1988).

Taylor, G., Disintegration of water drops in an electric field. *P. Roy. Soc. Lond. A Mat.* **280**, 383 (1964).

Tembreull, R., Lubman, D. M., Pulsed laser desorption of biological molecules in supersonic beam mass spectrometry with resonant two-photon ionization detection. *Anal. Chem.* **59**, 1082 (1987).

Tembreull, R., Lubman, D. M., Resonant two-photon ionization of small peptides using pulsed laser desorption in supersonic beam mass spectrometry. *Anal. Chem.* **59**, 1003 (1987).

Tjandra, N., Bax, A., Direct measurement of distances and angles in biomolecules by NMR in a dilute liquid crystalline medium. *Science* **278**, 1111 (1997).

Todd, P. J., Schaaff, T. G., Chaurand, P., Caprioli, R. M., Organic ion imaging of biological tissue with secondary ion mass spectrometry and matrix-assisted laser desorption/ionization. *J. Mass Spectrom.* **36**, 355 (2001).

Tullius, T. D., Dombroski, B. A., Hydroxyl radical "footprinting": High-resolution information about DNA-protein contacts and application to lambda repressor and *Cro* protein. *Proc. Nat. Acad. Sci. USA* **83**, 5469 (1986).

Valentine, S. J., Clemmer, D. E., H/D exchange levels of shape-resolved cytochrome c conformers in the gas phase. *J. Am. Chem. Soc.* **119**, 3558 (1997).

Van Berkel, G. J., Zhou, F., Aronson, J. T., Changes in bulk solution pH caused by the inherent controlled-current electrolytic process of an electrospray ion source. *Int. J. Mass Spectrom.* **162**, 55 (1997).

Verentchikov, A. N., Ens, W., Standing, K. G., Reflecting time-of-flight mass spectrometer with an electrospray ion source and orthogonal extraction. *Anal. Chem.* **66**, 126 (1994).

Visser, J., Mass spectrometric analysis of the sputter gas atmosphere without pressure reduction system. *J. Vac. Sci. Tech.* **10**, 464 (1973).

Waddell, R., Dale, D. E., Monagle, M., Smith, S. A., Determination of nitroaromatic and nitramine explosives from a PTFE wipe using thermal desorption-gas chromatography with electron-capture detection. *J. Chromatogr. A* **1062**, 125 (2005).

Wales, T. E., Engen, J. R., Hydrogen exchange mass spectrometry for the analysis of protein dynamics. *Mass Spectrom. Rev.* **25**, 158 (2006).

Weinkauf, R., Aicher, P., Wesley, G., Grotemeyer, J., Schlag, E. W., Femtosecond versus nanosecond multiphoton ionization and dissociation of large molecules. *J. Phys. Chem.* **98**, 8381 (1994).

Wichmann, J. M., Lupulescu, C., Wöste, L., Lindinger, A., Matrix-assisted laser desorption/ionization by using femtosecond laser pulses in the near-infrared wavelength regime. *Rapid Commun. Mass Spectrom.* **23**, 1105 (2009).

Williams, P., Sundqvist, B., Mechanism of sputtering of large biomolecular ions by impact of highly ionizing particles. *Phys. Rev. Lett.* **58**, 1031 (1987).

Williams, S. *et al.*, Fast events in protein folding: Helix melting and formation in a small peptide. *Biochemistry-US* **35**, 691 (1996).

Wood, T. D. *et al.*, Gas-phase folding and unfolding of cytochrome c cations. *Proc. Nat. Acad. Sci. USA* **92**, 2451 (1995).

Worner, H. J., Niikura, H., Bertrand, J. B., Corkum, P. B., Villeneuve, D. M., Observation of electronic structure minima in high-harmonic generation. *Phys. Rev. Lett.* **102**, (2009).

Wu, C. C., Yates, J. R., The application of mass spectrometry to membrane proteomics. *Nat. Biotechnol.* **21**, 262 (2003).

Wu, Q. Y., Vanorden, S., Cheng, X. H., Bakhtiar, R., Smith, R. D., Characterization of cytochrome c variants with high-resolution FTICR mass spectrometry- correlation of fragmentation and structure. *Anal. Chem.* **67**, 2498 (1995).

Wu, Z., Hendrickson, C. L., Rodgers, R. P., Marshall, A. G., Composition of explosives by electrospray ionization Fourier transform ion cyclotron resonance mass spectrometry. *Anal. Chem.* **74**, 1879 (2002).

Yang, J. J., Gobeli, D. A., El-Sayed, M. A., Change in the mechanism of laser multiphoton ionization-dissociation in benzaldehyde by changing the laser pulse width. *J. Phys. Chem.* **89**, 3426 (1985).

Yang, P., Cooks, R. G., Ouyang, Z., Hawkridge, A. M., Muddiman, D. C., Gentle protein ionization assisted by high-velocity gas flow. *Anal. Chem.* **77**, 6174 (2005).

Yinon, J., Harvan, D. J., Hass, J. R., Mass spectral fragmentation pathways in RDX and HMX. A mass analyzed ion kinetic energy spectrometric/collisional induced dissociation study. *Org. Mass Spectrom.* **17**, 321 (1982).

Yoo, J. H., Jeong, S. H., Greif, R., Russo, R. E., Explosive change in crater properties during high power nanosecond laser ablation of silicon. *J. Appl. Phys.* **88**, 1638 (2000).

Zenobi, R., Knochenmuss, R., Ion formation in MALDI mass spectrometry. *Mass Spectrom. Rev.* **17**, 337 (1998).

Zhang, M. *et al.*, Using molecular recognition of β–cyclodextrin to determine molecular weights of low-molecular-weight explosives by MALDI-TOF mass spectrometry. *J. Am. Soc. Mass Spectrom.* **17**, 189 (2006).

Zhang, Z. Q., Bordas-Nagy, J., Peptide conformation in gas phase probed by collision-induced dissociation and its correlation to conformation in condensed phases. *J. Am. Soc. Mass Spectrom.* **17**, 786 (2006).

Zhu, L., Gamez, G., Chen, H., Chingin, K., Zenobi, R., Rapid detection of melamine in untreated milk and wheat gluten by ultrasound-assisted extractive electrospray ionization mass spectrometry (EESI-MS) *Chem. Commun.*, 559 (2009).